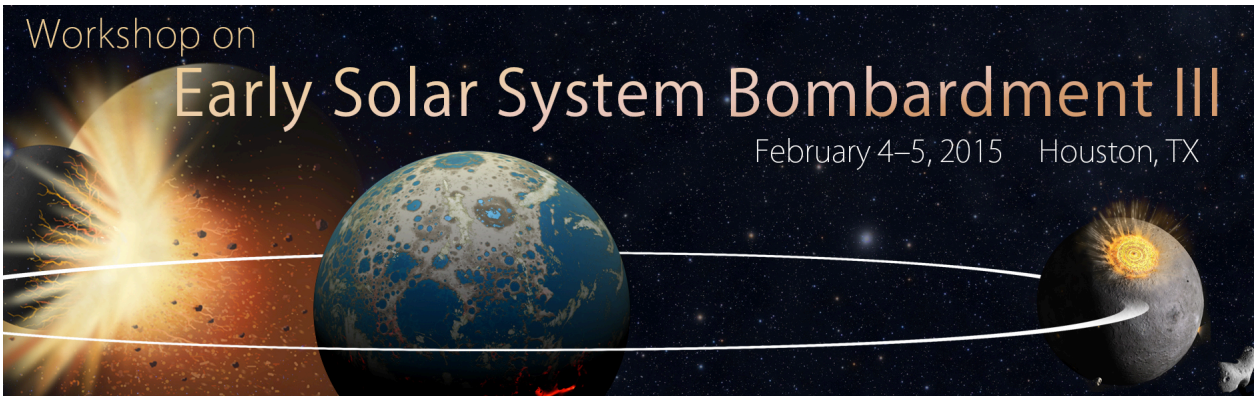

Program and Abstract Volume

LPI Contribution No. 1826

LUNAR AND PLANETARY INSTITUTE

USRA

Workshop on
Early Solar System Impact Bombardment III

February 4–5, 2015 • Houston, Texas

Institutional Support

Universities Space Research Association

Lunar and Planetary Institute

National Aeronautics and Space Administration

NASA Solar System Exploration Research Virtual Institute (SSERVI)

Conveners

Dr. David Kring
Lunar and Planetary Institute

Dr. Robin Canup
Southwest Research Institute

Scientific Organizing Committee

Simone Marchi
Southwest Research Institute

Kaveh Pahlevan
Nice Observatory

Ross Potter
Lunar and Planetary Institute/Brown University

Timothy Swindle
University of Arizona

Richard Walker
University of Maryland

Lunar and Planetary Institute 3600 Bay Area Boulevard Houston TX 77058-1113

LPI Contribution No. 1826

Compiled in 2015 by

Meeting and Publication Services
Lunar and Planetary Institute
USRA Houston
3600 Bay Area Boulevard, Houston TX 77058-1113

This material is based upon work supported by NASA under Award No. NNX08AC28A. Any opinions, findings, and conclusions or recommendations expressed in this volume are those of the author(s) and do not necessarily reflect the views of the National Aeronautics and Space Administration.

The Lunar and Planetary Institute is operated by the Universities Space Research Association under a cooperative agreement with the Science Mission Directorate of the National Aeronautics and Space Administration.

Abstracts in this volume may be cited as

Author A. B. (2014) Title of abstract. In *Workshop on Early Solar System Impact Bombardment III,* p. XX. LPI Contribution No. 1826, Lunar and Planetary Institute, Houston.

ISSN No. 0161-5297

Preface

This volume contains abstracts that have been accepted for presentation at the Workshop on Early Solar System Impact Bombardment III, February 4–5, 2015, Houston, Texas.

Administration and publications support for this meeting were provided by the staff of the Meeting and Publication Services Department at the Lunar and Planetary Institute.

Technical Guide to Sessions

Wednesday, February 4, 2015

8:15 a.m.	Lecture Hall	Big Impacts and Their Chemical Consequences
1:15 p.m.	Lecture Hall	Chronology of Impacts
5:30 p.m.	Great Room	Poster Session: Early Solar System Bombardment

Thursday, February 5, 2015

8:15 a.m.	Lecture Hall	Bombardment: Early and Late
1:30 p.m.	Lecture Hall	Consequences of Bombardment

Contents

Program

Wednesday, February 4, 2015
BIG IMPACTS AND THEIR CHEMICAL CONSEQUENCES
8:15 a.m. Lecture Hall

Discussions on the giant impact hypothesis and other early accretional issues

Chairs: **Robin Canup**
Kevin Righter

8:15 a.m. Kring D. * and Canup R. *
Introductory Remarks

8:30 a.m. Canup R. *
The Development and Evolution of the Giant Impact Hypothesis

8:50 a.m. Jacobson S. A. * Young E. D. Rubie D. C. Morbidelli A.
Compositions of the Terrestrial Planets in the Grand Tack Model **[#3034]**
We constrain the isotopic composition of the proto-lunar impactor in the Grand Tack model.

9:10 a.m. Quarles B. * Lissauer J. J.
Theian Orbital Evolution Amidst the Planetary Leftovers **[#3039]**
We evaluate the evolution of planetesimals assuming a five terrestrial planet solar system. The distributions are randomized in semimajor axis and excited in eccentricity. These results will be used in a larger work to model late giant impacts.

9:30 a.m. Charnoz S. * Michaut C.
Evolution of the Protolunar Disk: Dynamics, Cooling Timescale and Implantation of Volatiles into the Earth **[#3002]**
We present a dynamical simulation of the protolunar disk evolution coupling dynamics and thermodynamics. We find that the disk accumulates in a liquid torus <1.7 Re that cools in $<10^5$ years. If the vapor is viscous then volatiles may be lost to earth.

9:50 a.m. Pahlevan K. * Morbidelli A.
The Lunar Inclination as a Monitor of Late Stage Terrestrial Accretion **[#3041]**
We have identified a mechanism that can naturally reproduce the lunar orbital excitation and sets direct constraints on the number and mass of remnant bodies in the terrestrial planet region at the time of the Moon-forming giant impact.

10:10 a.m. COFFEE BREAK

10:25 a.m. Touboul M. T. Puchtel I. S. Walker R. J. *
The Tungsten Isotope Composition of the Moon: New Constraints on the Giant Impact **[#3040]**
The implications of tungsten isotopes for the giant impact hypothesis and the concept of disproportional accretion are discussed.

10:45 a.m. Righter K. *
Re-Evaluation of HSE Data in Light of High P-T Partitioning Data: Late Chondritic Addition to Inner Solar System Bodies not Always Required for HSE **[#3023]**
Evaluation of new data reveals evidence for late chondritic additions is lacking in Moon and Mars, and HSEs have other explanation in Vesta and angrites.

11:05 a.m. Boujibar A. * Andrault D. Bolfan-Casanova N. Bouhifd M. A.
Cosmochemical Fractionation by Collisional Erosion During the Earth's Accretion **[#3011]**
We propose a fractionation mechanism associated to the accretion of the Earth starting from enstatite chondrites. It involves proto-crust erosion by planetary impacts and fractional re-condensation of the ejecta on the planetary surface.

11:25 a.m. Potter R. W. K. * Kring D. A.
Testing the Collisional Erosion Hypothesis for the Hadean Earth **[#3010]**
Analytical methods are used to assess removal of Earth's crustal material from the time of the proposed Moon-forming impact through the end of the Late Heavy Bombardment.

11:45 a.m. LUNCH

Wednesday, February 4, 2015
CHRONOLOGY OF IMPACTS
1:15 p.m. Lecture Hall

Discussions on the ages of early solar system impact events

Chairs: **Timothy Swindle**
Richard Walker

1:15 p.m. Swindle T. D. * Kring D. A.
Was There a Concentration of Lunar and Asteroidal Impacts at ~4000 Ma? **[#3030]**
Although the extreme version of a "lunar cataclysm" envisioned by G. Ryder is clearly not accurate, geochronological evidence from both the Moon and meteorites suggests that there was an increase in the number of impact resetting events at ~4000 Ma.

1:35 p.m. Norman M. D. *
The Nature of the 4.2 Ga Impact Episode on the Moon: Evidence from North Ray Crater Breccias, Apollo 16 **[#3014]**
The range of Ar ages obtained from clasts in the North Ray breccias may reflect variable resetting of ejecta from a 4.2 Ga basin that occurred in the PKT and was subsequently transported to the Apollo 16 site by Imbrium deposits.

1:55 p.m. Cohen B. A. HRH * Petro N. E. Esq. Lawrence S. J. Hon.
What do Nectaris Basin Impact Melt Rocks Look Like and Where can We find Them? **[#3019]**
We are revisiting the effort to identify Nectaris basin impact-melt rocks at the Apollo 16 site, to model their emplacement, and to examine other sites where Nectaris impact melt is more abundant and/or more recognizable for potential further study.

2:15 p.m. Hurwitz D. * Kring D. A.
Identifying the Geologic Context of Apollo 17 Aphanitic and Poikilitic Impact Melt Breccias **[#3037]**
High resolution image and topography data are used to identify sources of Apollo 17 aphanitic and poikilitic impact melt breccias. Observations indicate both sample classes originated in massif outcrops that were not contaminated by younger material.

2:35 p.m. Zellner N. E. B. * Delano J. W.
Relationships Among Chemical Composition, Size, and Shape when Evaluating $^{40}Ar/^{39}Ar$ Ages of Lunar Impact Glasses **[#3018]**
Studies of size, shape, chemical composition and $^{40}Ar/^{39}Ar$ age suggest that feldspathic lunar impact glasses are not likely to provide much information about very old episodes of lunar bombardment.

2:55 p.m. Boehnke P. * Heizler M. T. Harrison T. M. Lovera O. M. Warren P. H.
Lunar $^{40}Ar/^{39}Ar$ Step-Heating Data and the Late Heavy Bombardment **[#3029]**
A thermochronologic interpretation of Apollo $^{40}Ar/^{39}Ar$ data suggests significant bias in existing "plateau" age based interpretations.

3:15 p.m. COFFEE BREAK

3:30 p.m. Crow C. A. * McKeegan K. D. Moser D. E.
Lunar Zircons: What's the Big Picture? **[#3020]**
An extensive U-Pb, REE, and microstructural survey of Apollo zircons from which we can draw constraints regarding the duration of KREEP magmatism, zircon formation mechanisms, and possibly the early impact history of the Moon.

3:50 p.m. Wielicki M. M. * Harrison T. M.
Zircon Formation in Impact Melts: Complications for Deciphering Planetary Impact Histories **[#3024]**
We explore the formation conditions and inheritance probability of zircon in impact melts and the implications of using zircon geochronology to investigate planetary impact histories.

4:10 p.m. Moser D. E. *
Zirconium Minerals from Mars, Moon and Earth Indicate Crustal 'Refugia' on Early Bombardment Surfaces **[#3038]**
A comparison of the shock microstructural and U-Pb histories of zirconium minerals from the bombardment epoch of Mars, Moon and Earth points to perseverance of early planetary crustal domains throughout the large impactor flux.

4:30 p.m. Marchi S. Bottke W. F. * Elkins-Tanton L. T. Wuennemann K. Morbidelli A. Kring D. A.
The Bombardment of the Earth During the Hadean and Early Archean Eras **[#3008]**
I will present a recent model of asteroid bombardment on the early Earth and discuss implication for the early habitability.

4:50 p.m. Lowe D. R. * Byerly G. R.
The Terrestrial Record of an Extended Late Heavy Bombardment **[#3015]**
Terrestrial ejecta layers 3.2–3.5 billion years old record the frequency and effects of large asteroid impacts during late Late Heavy Bombardment. They indicate that the Earth's surface continued to be battered by large impacts as late as 3.2 Ga.

5:10 p.m. Koeberl C. * Schulz T. Özdemir S. Mohr-Westheide T. Reimold W. U. Hofmann A.
Remnants of Early Archean Impact Events on Earth: New Studies on Spherule Layers from the Barberton Mountain Land, South Africa **[#3017]**
New geochemical and isotopic data on the 3.4 Ga spherule layers from the Barberton Mountain Belt in South Africa help to constrain the early impact record on Earth.

Wednesday, February 4, 2015
POSTER SESSION: EARLY SOLAR SYSTEM BOMBARDMENT
5:30 p.m. Great Room

Schmedemann N. Kneissl T. Neesemann A. Michael G. Hiesinger H. Jaumann R.
Raymond C. A. Russell C. T.
The Age of the Rheasilvia Basin — How the two Geological Interpretations and Chronology Systems Differ **[#3006]**
We review and analyze the major disagreements in the formation age of the Rheasilvia basin on Vesta that were published recently.

Davis C. L. Moser D. E.
U-Pb Composition and Shock Microstructures of In-Situ *Accessory Phases Across the Vredefort Impact Structure, South Africa: A Terrestrial Analogue for Dating the Lunar Surface and Other Planetary Bodies* **[#3028]**
Accessory phases (i.e. zircon, monazite) co-exist within individual samples of the Vredefort dome, with a dichotomy of U-Pb ages and microstructural evolution. Vredefort is a terrestrial analogue for complex craters on other planetary bodies.

Righter K. Cosca M. A.
$^{40}Ar/^{39}Ar$ Age of Hornblende-Bearing R Chondrite LAP 04840 **[#3022]**
This unusual meteorite yields an Ar-Ar age of 4.29 Ga — evidence for post shock annealing in the R chondrite parent body.

Thursday, February 5, 2015
BOMBARDMENT: EARLY AND LATE
8:15 a.m. Lecture Hall

Discussions on the size distributions and projectile sources of impact events

Chairs: **David Kring**
Ross Potter

8:15 a.m. Bottke W. F. * Vokrouhlicky D. Marchi S. Jackson A. Levison H. Swindle T.
The Earliest Lunar Bombardment Produced by Moon-Forming Impact Ejecta **[#3012]**
The giant impact that formed the Moon ejected several percent of an Earth mass out of cis-lunar space in the form of small debris. Using collisional and dynamical models, we show its return can reproduce the Moon's pre-Nectarian impact record.

8:35 a.m. Jackson A. P. * Asphaug E. Elkins-Tanton L. T. Minton D. A.
Stop Hitting Yourself: Did most Terrestrial Impactors Originate from the Terrestrial Planets? **[#3036]**
In addition to building planets giant impacts also release large quantities of debris. The ultimate fate of this is largely re-accretion, and this debris population could be the dominant source of impactors in the early solar system.

8:55 a.m. Frey H. V. *
Evidence Supporting an Early as Well as Late Heavy Bombardment of the Moon **[#3007]**
Evidence supporting an intense early bombardment on the Moon in addition to the traditional Late Heavy Bombardment includes decreasing contrasts in basin topographic relief and Bouguer gravity with increasing crater retention age.

9:15 a.m. Hartmann W. K. *
Reviewing "Terminal Cataclysm": What Does it Mean? **[#3003]**
The author reviews papers related to terminal cataclysm since 1966. Recent papers by Marchi et al. and others are discussed. New curves of flux vs. time calculated by Marchi et al. resemble early data from the 1970s and 1980s.

9:35 a.m. Schultz P. H. * **CANCELED**
Sizes of Asteroids Responsible for Large Impact Basins on the Moon During the Late Heavy Bombardment **[#3031]**
An independent method for determining the sizes of asteroids responsible large lunar basins indicate that the proposed E-belt of asteroids was once populated by large (250 km diameter) proto-planets before contributing to the LHB.

9:55 a.m. COFFEE BREAK

10:10 a.m. Mazrouei S. * Ghent R. R. Bottke W. F.
Application of a new Method for Exploring the Copernican Cratering Record **[#3032]**
Here we investigate the Copernican-era lunar impact flux using a new method for determining crater ages. Changes in the impact flux rate can possibly tell us about asteroid disruption events and fragment evolution in the asteroid belt.

10:30 a.m. Minton D. A. * Jackson A. P. Asphaug E. Fassett C. I. Richardson J. E. Jr.
Debris from Borealis Basin Formation as the Primary Impactor Population of Late Heavy Bombardment **[#3033]**
Here we investigate a novel Giant Impact Debris (GID) hypothesis to explain a number of observations regarding the LHB. In the GID hypothesis, the formation of the crustal dichotomy on Mars (Borealis Basin) generates LHB impactors.

10:50 a.m. Movshovitz N. * Nimmo F. Korycansky D. G. Asphaug E. Owen J. M.
Destruction and Re-Accretion of Outer Solar System Satellites During the Late Heavy Bombardment **[#3013]**
Using a Monte-Carlo approach we calculate, for 11 mid-sized satellites of Saturn and Uranus, the probability of experiencing at least one catastrophic collision during a hypothetical LHB.

11:10 a.m. Schmedemann N. * Wagner R. J. Michael G. Denk T. Kneissl T.
The Crater Production Functions for Mimas **[#3021]**
We present crater data from Mimas and compare the measured crater size-frequency distribution with previously published crater production functions derived from the cometary size-distribution and a lunar-like version.

11:30 a.m. Walker R. J. * James O. B. Kring D. A. Liu J. Sharp M. G. Puchtel I. S.
Highly Siderophile Element Characteristics of Lunar Impact Melt Rocks: A Picture Begins to Emerge **[#3016]**
Lunar impact melt rocks from multiple sites have highly siderophile element characteristics suggestive of two component mixing. This may indicate that the HSE present in all of the rocks were present in the crust at the times of basin formation.

11:50 a.m. Hurwitz D. * Kring D. A.
Potential Sample Sites for South Pole — Aitken Basin Impact Melt within the Schrodinger Basin **[#3035]**
Observed and petrologically modeled FeO contents are used to estimate how much SPA impact melt is currently in SPA and Schrödinger, key targets for science and exploration. Results indicate SPA melt can be sampled in the southern wall of Schrödinger.

12:10 p.m. LUNCH

Thursday, February 5, 2015
CONSEQUENCES OF BOMBARDMENT
1:30 p.m. Lecture Hall

Discussions on the consequences of impact events

Chair: **Barbara Cohen**

1:30 p.m. Kring D. A. * McGovern P. J. Potter R. W. K. Collins G. S. Grange M. L. Nemchin A. A.
Was an Epoch of Lunar Magmatism Triggered by the South Pole-Aitken Basin Impact? **[#3009]**
We investigate a new impact hypothesis to explain a spike in lunar zircon ages between 4.36 and 4.30 billion years ago.

1:50 p.m. McGovern P. J. * Potter R. W. K. Collins G. S. Kring D. A. Grange M. L. Nemchin A. A.
Pulses of Magma Movement Triggered by the South Pole-Aitken Impact **[#3027]**
The South Pole-Aitken impact produced enormous pressure waves throughout the Moon. Here we explore the mechanical effects that such waves would exert on magma pathways in the lunar crust, linking hydrocode model results to magma ascent theory.

2:10 p.m. Kiefer W. S. * Macke R. J. Britt D. T. Irving A. J. Consolmagno G. J.
The Density and Porosity of Lunar Impact Breccias and Impact Melt Rocks and Implications for Gravity Modeling of Impact Basin Structure **[#3004]**
Measured bulk densities of lunar impact breccias and melt rocks increase the basin melt sheet thickness inferred with GRAIL gravity data. The grain densities of these rocks are consistent with an origin from a mixture of crust and mantle material.

2:30 p.m. Stickle A. M. * Buczkowski D. L. Iyer K. A.
Damage Due to Giant Impacts into Differentiated Bodies: A Mechanism for Large-Scale Trough Formation on Vesta **[#3026]**
Experiments show discrete subsurface failure planes are a result of impact into spherical targets. CTH simulations provide insight into the processes controlling the failure, while large-scale models explain large-scale troughs on Vesta's surface.

2:50 p.m. de Niem D. * Kührt E.
Impact Craters on Comets from a Granular Material Perspective **[#3025]**
The contribution applies an algorithm for finite-deformation elasticity and plasticity to demonstrate new results for the behaviour of granular materials during impact crater formation in a low-gravity environment.

3:10 p.m. WORKSHOP ADJOURNS

Lunar $^{40}Ar/^{39}Ar$ step-heating data and the Late Heavy Bombardment. P. Boehnke[1], M. T. Heizler[2], T. M. Harrison[1], O. M. Lovera[1] and, P. H. Warren[1] [1]Department of Earth, Planetary, and Space Sciences, UCLA, Los Angeles, CA (pboehnke@gmail.com), [2]New Mexico Bureau of Geology & Mineral Resources, Socorro, NM.

Introduction: Much of the evidence for the timing of the Late Heavy Bombardment [1] comes from interpreting disturbed $^{40}Ar/^{39}Ar$ step-heating data in terms of "apparent" plateau ages. However, the basis of these interpretations is often flawed in both theory and practice. Here we both critically review published interpretations of lunar $^{40}Ar/^{39}Ar$ analyses and show how robust, thermochronological data can be extracted from Apollo 16 samples and used to place quantitative constraints on reheating histories.

The concept of the plateau age is limited to those release spectra that show essentially closed system behavior. The vast majority of Apollo samples fail to meet this criterion and therefore cannot be assessed in this fashion. Causes for open system behavior include mixing of different aged clasts, recoil during irradiation, and, most importantly, diffusive loss during later impact/heating events. While both mixing and recoil effectively prevent recovery of impact ages, they can provide minimum estimates. However, diffusive loss of ^{40}Ar can be effectively modeled using data recovered during step-heating and modeled with a multiphase, multi-diffusion domain model [2].

Unfortunately, the vast majority of whole-rock lunar step-heated $^{40}Ar/^{39}Ar$ measurements utilized a simple, monotonic heating schedules [c.f., 3] which does not allow for unique recovery of sample specific Arrhenius parameters. This analytical deficiency precludes reconstructing the time and temperature of the reheating event from the vast archive of previous data. This limitation is transcended by use of temperature cycling and isothermal duplicates [4] in the laboratory heating schedule. Our results suggest that the majority of Apollo 16 samples are amenable to this form of multi-diffusion-domain (MDD) modeling.

We have systematically assessed the previous literature for both the minimum ages of the last complete resetting (or rock forming event) and the ages of later ^{40}Ar loss. A plot of minimum ages (Fig. 1) shows a consistent decline from an apparent peak at ~3.7 Ga. If interpreted as the timing of reheating due to impact, this broad bombardment history appears inconsistent with a discrete LHB type event at ~3.85 Ga [1] but instead supports a continual decline in impact frequency [5].

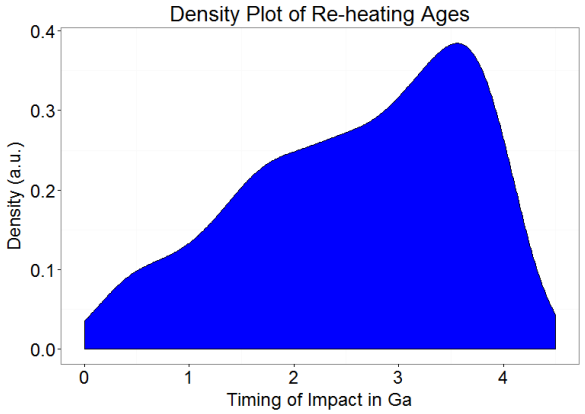

Figure 1 A compilation of initial minimum ages of Apollo $^{40}Ar/^{39}Ar$ step-heating analyses shows a broad distribution from a ca. 3.7 Ga peak.

While there is an apparent decline in frequency above ~3.7 Ga, this is likely due to both the nature of the early heating steps which represent the least retentive ^{40}Ar and is thus easily reset, coupled with impact saturation.

Alternatively, using the maximum ages of each sample, rather than assigning an arbitrary "plateau" age, we find that the peak ages for Apollo 16 samples using our data and combined with previous works [6,7] shows a peak at ≥4 Ga (Fig. 2) and a distinct lack of one at 3.85 Ga.

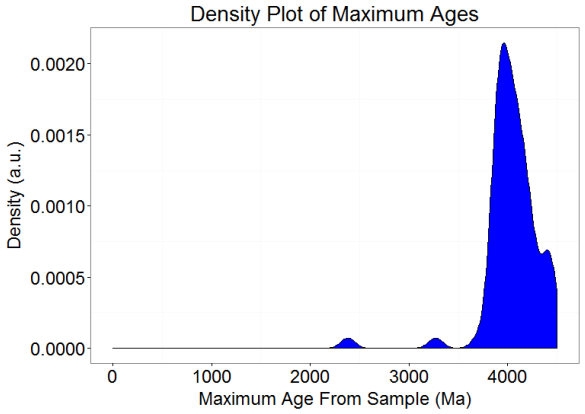

Figure 2 Maximum apparent ages for Apollo 16 samples. Note the peak is at ≥4 Ga and there is a gradual decline to ~3.5 Ga.

Our analysis contradicts the conclusion of most earlier studies [e.g., 8,9], again underscoring the subjective nature of assigned "plateau" ages in disturbed samples. To illustrate our point we used a random sampling of data from Apollo samples where the "plat-

eau" ages are compared with the maximum age from individual heating steps. Our results indicate that 50 to 70% of samples have a significant difference between the claimed "plateau" age and the maximum age. These discrepancies define a distribution with a maximum in this case of ~550 Ma (Fig. 3).

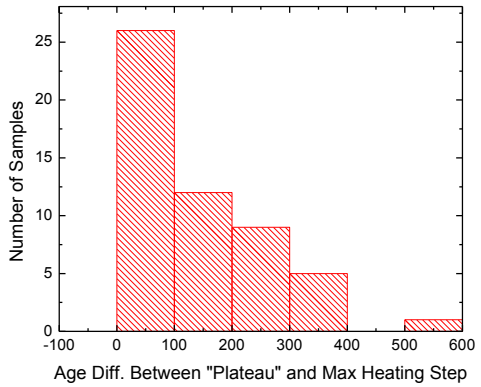

Figure 3 The difference between the "plateau" age and maximum age of any heating step. Note the one sided nature of the bias, the plateau ages are always younger.

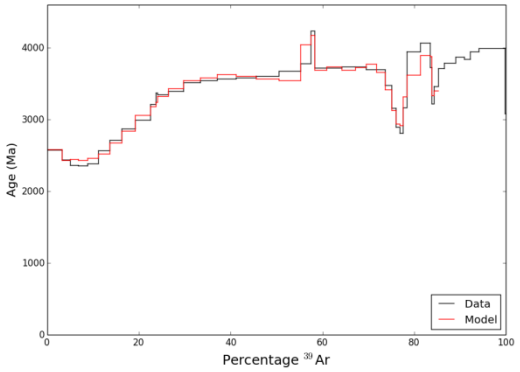

Figure 4 Age spectra for Apollo sample 67514,43. Note the dip in age which is evidence of multi-*E* behavior.

Our thermochronologic investigations have shown that the majority of Apollo samples we have analyzed show clear evidence for multi-*E* behavior. For example, the age spectrum for intensely brecciated ferroan anorthosite 67514,43 (Fig. 4) shows a dip in age at a ^{39}Ar fraction release of ~75% which, coupled with the kinetic data is diagnostic of the presence of multiple activation energies. A unique fit is obtained for a heating of ~3,800 K for 2 µsec, interpreted to represent a shock heating event [10]. This age spectrum required a re-heating event at ~2.1 Ga and an age of last complete resetting at >4 Ga to achieve an appropriate model fit. In a "plateau" interpretation, an age of ~3.5 Ga would have been assigned. This sample highlights the importance of diffusion modeling for proper interpretation of lunar ^{40}Ar/^{39}Ar ages. The accompanying Arrhenius plot is well fit by two *E's* of ~39 and 95 kcal/mol, similar to that found for plagioclase and pyroxene (Fig. 5). However, with multiple *E's* the age spectrum is a function of the lab heating schedule [11]. Therefore the apparent "plateau" ages are analytical artifacts rather than a reflection of events in the sample's history.

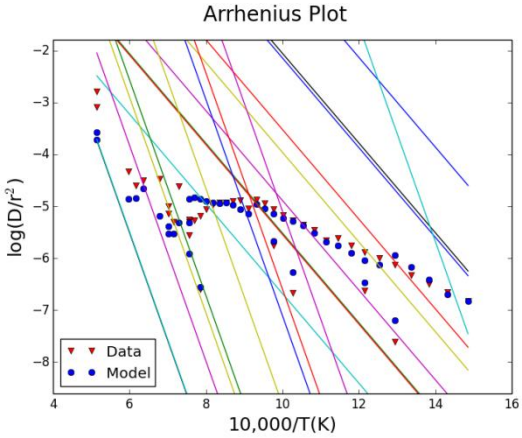

Figure 5 Arrhenius plot and model fit for sample 67514,43. The model needs two activation energies for a good fit.

Evaluating the Apollo ^{40}Ar/^{39}Ar data within a quantitative thermochronological framework does not support a single bombardment spike at ca. 3.85 Ga. Indeed, the basis of this interpretation (i.e., arbitrarily assigned "plateau" ages) is shown to yield highly biased results. Instead, we argue that the data supports a protracted impact history.

References:

[1] Tera F. et al. (1974) *EPSL*, 22, 1-21. [2] Boehnke P. et al. (2014) LPSC 45, 2545. [3] Shuster D.L. et al. (2010) *EPSL*, 155-165. [4] Lovera O.M. et al. (1991). *JGR*, 96, 2057-2069. [5] Culler T. S. et al. (2000) Science, 1785-1788. [6] Norman M. D. et al. (2006) GCA, 6032-6049. [7] Norman M. D. et al. (2010) GCA, 763-783. [8] Dalrymple G. B. and Ryder G. (1996) JGR, 101, 26069-26084. [9] Chapman C. R. et al. (2007) Icarus, 233-245. [10] Boehnke P. et al. (2014) 14th Int. Conf. Thermochron., S2-1. [11] Harrison T. M. et al. (1991) GCA, 1435-1448.

THE EARLIEST LUNAR BOMBARDMENT PRODUCED BY MOON-FORMING IMPACT EJECTA. W.F. Bottke[1], D. Vokrouhlicky[2], S. Marchi[1], A. Jackson[3], H. Levison[1], T. Swindle[4]. [1]Southwest Research Institute and NASA SSERVI-ISET team, Boulder, CO, USA (bottke@boulder.swri.edu) [2]Institute of Astronomy, Charles University, V Holesovickach 2, CZ-18000, Prague 8, Czech Republic Univ., Czech Republic. [3]Arizona State U., Phoenix, AZ, USA. [4]Lunar and Planetary Laboratory, U. Arizona, Tucson, AZ, USA.

Introduction. The Moon likely formed in a collision between a large protoplanet and the proto-Earth [e.g., 1,2]. This giant impact (GI) occurred during the late stages of Earth's accretion; the abundance of highly siderophile elements in Earth's mantle indicate the Earth only accreted ~0.5% of its mass from broadly chondritic projectiles after this time [e.g., 3]. This makes the GI one of the youngest largest collisions to take place in the terrestrial planet region.

Recently, we used this inference to argue that GI ejecta dominated the population of km-sized bodies in the terrestrial planet region during the late stages of planet formation [4]. As evidence, consider that GI simulations, capable of reproducing Earth-Moon system constraints, often eject several percent of an Earth mass out of cis-lunar space [1-2]. If a considerable fraction of this mass were solid debris, as described by many GI simulations, and the GI ejecta size frequency distribution (SFD) had a steep slope, which we infer from modeling work and data [4], km-sized bodies could plausibly have struck main belt asteroids at velocities $V > 10$ km/s. This is enough to heat and degas target rock; models show such impacts produce ~1,000 times more highly heated material by volume than typical main belt collisions at ~5 km/s [5]. By tracking the temporal evolution of GI ejecta, we predicted a "signature" of the GI was left behind in the ^{40}Ar-^{39}Ar shock degassing ages of asteroid meteorites, and that they show the Moon formed ~4.48 Ga [4].

If GI ejecta blasted the asteroid belt, a large fraction should have also returned to hit the Moon. Here we examined whether the most ancient lunar craters and basins could plausibly come from these projectiles.

Dynamical Model of GI Ejecta. To explore the evolution of GI ejecta, we tracked 30,000 test bodies for 600 My using the numerical integrator SWIFT-RMVS3. The planets Venus-Neptune were included in the integrations with starting orbits described in [6]. For their initial orbits, the bodies were assigned a random isotropic trajectory away from Earth's center, were placed along Earth's Hill sphere, and were given an initial ejection velocity "at infinity" of 1, 3, 5, 7, or 9 km/s, respectively. The results were combined by weighing the outcomes using an initial velocity distribution corresponding to GI hydrocode simulations; 14%, 27%, 26%, 18%, and 15% of the objects were ejected at 1, 3, 5, 7, 9 km/s [7].

Using [8], we estimated that ~1% of our GI test bodies should have struck the Moon ~0.01-400 My after the GI. The timing and impact velocities V of the test bodies are shown in **Fig. 1**. We find that 30% and 65% hit within 1 and 10 My of the GI, respectively. Their median V was < 10 km/s. The last 35% hit between 10-400 My. Their median V was >10 km/s. Velocities increase as the test bodies are perturbed by the terrestrial planets.

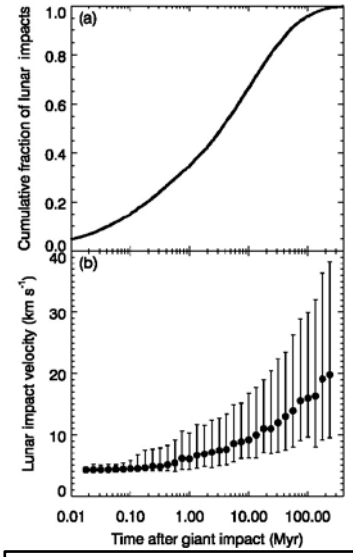

Fig. 1. GI ejecta hits the Moon

Collisional Evolution of GI Ejecta. A key uncertainty here is the nature of the GI ejecta SFD. We infer its properties in part from the ancient lunar impact record. The Moon has ~25 Pre-Nectarian (pN) lunar basins made by the impact of $D > 20$ km diameter projectiles [9]. Assuming 1% lunar accretion, the GI ejecta SFD only had a few thousand $D > 20$ km bodies. Mass balance therefore requires the majority of GI ejecta to be in a steep SFD dominated by $D < 20$ km bodies. Tests suggest that ~10^{10} km-sized projectiles were thrown out of cis-lunar space (**Fig. 2**) [4].

Support for such steep SFDs can be found in nature (e.g., Rheasilvia basin on (4) Vesta produced frag-

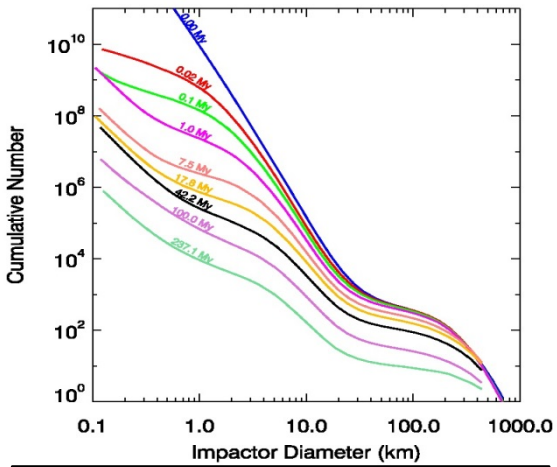

Fig. 2. Collisional evolution of GI ejecta over time.

ments with a steep cumulative power law SFD; exponents of -3.7 and -8 for diameter $D > 3$ km and > 5 km bodies, respectively) [10].

A consequence of a steep GI SFD is that the fragments should undergo vigorous collisional evolution with themselves (**Fig. 2**). Collision evolution codes indicate $D < 1$ km bodies undergo rapid demolition, enough to reduce the population by several orders of magnitude in mass within 0.1-1 My of the GI [11]. The surviving fragments develop a bump near $D \sim 2$ km that eventually evolves to 5-6 km as the SFD settles into a collisional steady state. At late times, most mass loss is produced by dynamical processes.

Comparing Model Results to Data. Combining results from Figs. 1 and 2, we can predict the SFD of GI projectiles that created pN craters and basins (**Fig. 3**). The blue and red curves show cumulative impacts 7.5 and 15 My after the GI, respectively (Fig. 3a). By converting these populations into craters, we find we can reproduce the oldest crater SFDs found on pN (green) and SPA (grey) terrains (Fig. 3b) [12].

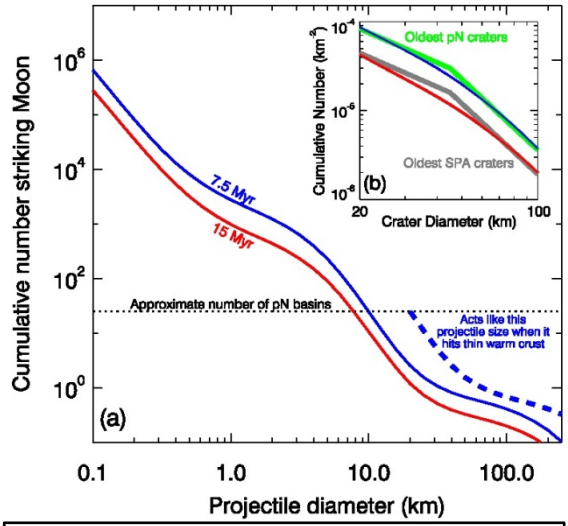

Fig. 3. (a) GI projectiles hitting Moon over 7.5 and 15 My; (b) pN craters compared to model results.

Here the bump in Fig. 3a near 3-4 km diameter projectiles corresponds to a bump observed in Fig. 3b for 40-50 km craters [12]. We predict these terrains formed 7.5 and 15 My after the GI, respectively. To account for pN basins, we assumed the early pN crust was thin and had high temperatures, low viscosities, and rheological properties broadly comparable to those that existed on the lunar nearside when Imbrium basin formed [13]. This may allow $D > 10$ km projectiles to act like larger projectiles (blue dashed line) and match the observed number of pN basins (black dashed line). This would also explain the absence of 120 km < D < 300 km craters on ancient Pre-Nectarian terrains [12].

Implications. There are several interesting implications that come from this scenario:

1. Considerable GI ejecta hit the Moon prior to the oldest pN terrains when the crust was thin, hot, and mushy. The consequences of such impact events are unknown, but we suspect they would leave behind features similar to *palimpsests,* the flat basins found on Callisto. Such outcomes could explain why several prominent pN basins (e.g., Tranquillitatis, Fecunditatis, Australe, perhaps Procellarum) lack the topographic and gravity signatures of younger basins [e.g., 14].

2. Numerous impacts breaching the early crust might allow the upper mantle to cool rapidly. This might explain why the ancient SPA basin managed to create a large topographic signature [e.g., 9].

3. Projectiles derived from the crust/mantle of the GI bodies may be lacking in FeNi. Impact melt pools created by these impactors will be missing the key material that can record a magnetic signature from the putative lunar dynamo [15]. This may explain why few pN basins have magnetic anomalies [16].

4. The SPA impact required 4×10^{26} J [17]. Assuming 100% accretion, an SPA projectile ~220 km in diameter striking at ~7 km/s could provide the Moon's HSE abundances [3]. Interestingly, this velocity is a good match to Fig. 1 and not so much to leftover planetesimals [18]. *Did SPA come from GI ejecta?*

5. If GI ejecta dominate early lunar bombardment, few major impacts occur on the terrestrial planets between ~4.45 and 4.1-4.2 Ga, the time of the Late Heavy Bombardment (LHB) [6]. The renewal of major impacts after a ~0.2-0.3 Gy "lull" might help to explain (i) why Mercury was resurfaced at the start of the LHB [19], (ii) why Earth's zircon record peaks at 4.1-4.2 Ga [20], and (iii) why few obvious Martian basins have been found to be older than Hellas [21].

References: [1] Cuk, M., & Stewart, S.T. (2012) Science, 338, 1047. [2] Canup, R.M. (2012) Science, 338, 1052 [3] Bottke, W.F. et al. (2010) Science 330, 1527. [4] Bottke, W. F. et al. (2014) Science, submitted. [5] Marchi, S., et al. (2013) Nature Geo. 6, 303. [6] Bottke, W.F., et al. (2012) Nature 485, 78. [7] Jackson, A.P., & Wyatt, M.C. (2012) MNRAS, 425, 657. [8] Bandermann, L.W. & S. F. Singer. (1973) Icarus 19, 108. [9] Wilhelms, D. E. (1987) USGS Prof. Paper 1348. [10] Nesvorný, D. (2012) HCM Asteroid Families V2.0. NASA Planetary Data System. [11] Morbidelli, A., et al. (2009), Icarus, 204, 558. [12] Marchi, S., et al. (2012). EPSL 325-326, 27. [13] Miljkovic, K. et al. (2013) Science 342, 724. [14] Zuber, M. et al. (2013) 339, 668. [15] Wieczorek, M. et al. (2012) Science 335, 1212. [16] Hood L. L. et al. (2014) LPSC XLV, #1482. [17] Potter, R. W. K. et al. (2012) Icarus 220, 730. [18] Bottke, W.F., et al. (2007) Icarus, 190, 203. [19] Marchi, S., et al. (2013) Nature 499, 59-61. [20] Marchi, S., et al. (2014) Nature 511, 578. [21] Robbins, S. J., et al. (2013). Icarus 225, 173-184.

Cosmochemical fractionation by collisional erosion during the Earth's accretion. A. Boujibar[1,2], D. Andrault[1], N. Bolfan-Casanova[1] and M. A. Bouhifd[1], [1]Laboratoire Magmas et Volcans, Université Blaise Pascal, CNRS UMR-6524, 5 rue Kessler, 63000 Clermont-Ferrand, France, [2]Now at NASA Johnson Space Center, 2101 Nasa Parkway, Houston, TX 77058, USA.

Introduction: Numerical models have shown that colliding objects do not simply merge. Catastrophic disruption inducing collisional stripping of the embryos' mantles and excavation of the planetary surfaces have commonly occurred during planetary accretion [1]. On the other hand, planetary bodies with a radius >200 km formed ~1.5 Ma after the CAIs formation are likely composed of a differentiated interior [2]. It is still unclear how chemical fractionation occur on mantles of planetary bodies. This could have been caused by small-scale melting [3], or by the presence of a magma ocean [4]. Since planetary embryos could have differentiated early in the history of the Solar System, their partial destruction have produced heterogeneous bodies. The aim of this study is to investigate how collisional erosion processes [5] can modify the chemical composition of planetary bodies.

The chemical composition of the building blocks that accreted to form the Earth remain uncertain. However, enstatite chondrites (EC) and especially those of EH-type show remarkable similarities in isotopic compositions (for Ca, N, Mo, Ru, Os, Cr, Ni, and Ti). Therefore, these meteorites likely formed in the same region of the solar nebula than Earth. However EC and Earth present important chemical differences, such as (i) the absence of FeO in the chondrites in contrast to the 8 wt% FeO present in Earth's mantle, (ii) a low Mg/Si ratio (~0.63) relative to the terrestrial value (~1.1) together with (iii) low abundances in refractory lithophile elements and high concentrations of moderately volatile elements in EC in comparison to Earth's mantle. While several internal processes have been proposed to explain the difference in FeO content in Earth and EC [6], all the other issues remained unsolved until now. In the present study, we tested how much the chemical divergence between the bulk Earth and EC can be unravelled by the processes of early crust collisional erosion.

Experimental methods: We investigated experimentally the composition of melts produced by low degrees of partial melting of EC at the pressure conditions expected for melt segregation in partially molten planetary embryos. High pressure experiments were conducted using multi anvil press apparatus at pressures ranging 5 to 25 GPa and temperatures close to the solidus in order to extract the chemical compositions of the first melts. Mass balance calculations allowed us the estimation of the degree of melting in our charges.

Melting results:

Our experiments provide the chemical compositions of the pseudo-eutectic melts at 5, 10, 20 and 25 GPa. The change of these compositions with pressure are in very good agreement with a previous experimental study of partial melting of enstatite chondrites at 1 bar [7]. These first melts are all characterized by high concentrations of SiO_2 (up to 75 wt%), Al_2O_3 and alkali elements (Na_2O and K_2O) and low concentrations of MgO. The most striking features are the increase of MgO and decrease of SiO_2 and Al_2O_3 contents with increasing pressure. Their compositions are equivalent to that of rhyolites at 1 bar and become progressively trachy-basaltic as the pressure increases (Fig. 1).

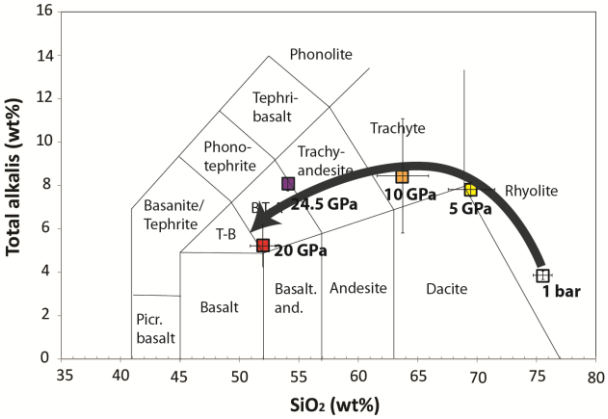

Figure 1: *TAS diagram (total alkali (Na_2O+K_2O) versus SiO_2 concentrations) showing the evolution of the composition of the pseudo-eutectic melts with pressure, obtained in the present study (5 to 25 GPa) and in a previous study at 1 bar [7].*

In partially molten planetesimals, the ascent of such melts towards the planetary surface could occur relatively easily due to their low melt densities, even for low degrees of partial melting [3].

Evolution of the chemical composition of the Earth:

These experimental results are then used to evaluate how the collisional erosion of planetary surfaces can change the chemical composition of differentiated EH-type planetary embryos. We calculate the evolution of the Mg/Si ratio of the planetary body, after the ascent then impact erosion of pseudo-eutectic melts equilibrated at different pressures. This ratio is then

compared to the terrestrial value (~0.9). As the pseudo-eutectic melts have high SiO_2-content, the Mg/Si ratio of the differentiated planetary body increases with increasing the amount of crustal erosion and evolves toward the present day BE (Bulk Earth) ratio (Fig. 2). With low pressures of melt-solid equilibration, less extensive crustal erosion is needed due to higher SiO_2-contents in the melts. The BE Mg/Si ratio can be achieved from an EH-type precursor, by erosion of a crust of 15 to 18% the planetary mass for solid-melt equilibrium pressures lower than 10 GPa.

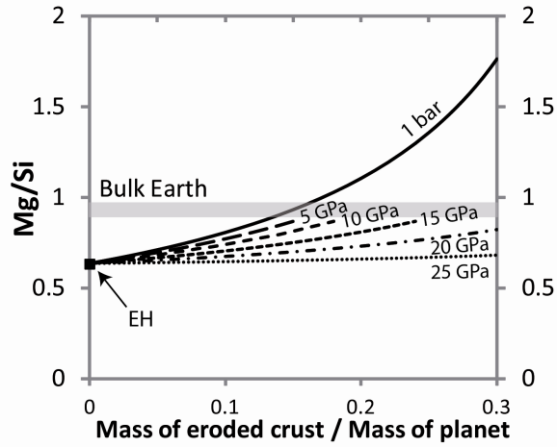

Figure 2: *Change of the planetary Mg/Si ratio after an erosion of a crust with a composition equivalent to that of pseudo-eutectic melts generated at pressures comprised between 1 bar and 25 GPa. The black square and the grey area represent the values of the EH chondrites and the Bulk Earth respectively.*

The formation of such SiO_2-rich crusts necessitates low degree of partial melting. Therefore removing proto-crust to a level of 15-18 wt% of the planetary mass calls for repeated processes of proto-crust formation and collisional erosion.

These differentiation processes affect also the concentrations of the other major elements. The obtained concentrations of Na, Ca and Al are different from that of the present Earth and their misfits are correlated with the temperature of condensation of the considered elements. These misfits could therefore be resolved if the processes of crustal erosion are associated to a re-condensation of elements that lead to a chemical fractionation: with a larger loss of the most volatile elements and a preferential condensation of the most refractory elements. A number of models of collisional erosion/re-condensation of elements can yield the terrestrial composition. The model with the lowest amount of surface erosion necessitates a re-condensation of 100% the refractory elements while an additional erosion of a fraction of the planetary mantle requires less fractionation of the elements (Fig. 3). The dual processes of collisional erosion and re-condensation of refractory elements can also solve the previously reported dramatic consequences on the thermal history of Earth that could have the loss of incompatible and refractory heat-producing elements, such as U and Th [5, 8].

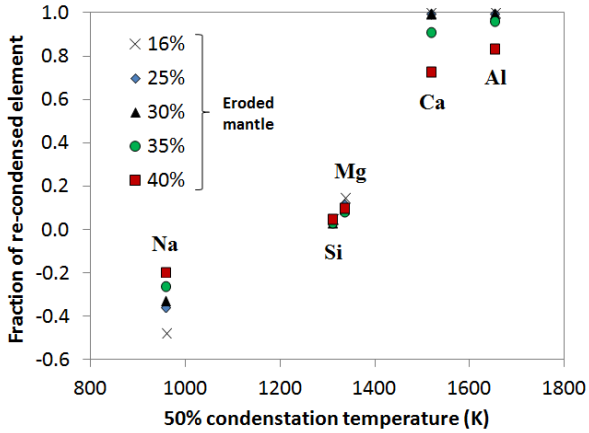

Figure 3: *Degree of chemical fractionation required by our model, for different amount of collisional erosion. 15% of the planetary mass required to match the terrestrial Mg/Si ratio is considered in addition to the eroded mantle. For example, with a total erosion of 15 to 45% the planetary mass, 100% of Ca and Al, 10% of Mg and 5% of Si have to re-condense to reach the present-day composition of the Earth.*

Possible interactions with nebular material

Furthermore if collisional erosion occurred early in the history of the Solar System, it would affect both planetary bodies and the nebular material. Due to their higher surface/volume ratio, the chondritic material that was left over from the accretion may have preferentially reacted with the gas enriched in SiO_2 and volatile lithophile elements produced with the vaporization of the eroded crust. This could explain the enrichments in Na, S and Si observed at the edges of chondrules [9] and the contrasted behaviours of the lithophile and non-lithophile volatile elements in the non-carbonaceous chondrites [10].

References: [1] Asphaug E. (2010) *Chem. der Erde, 70,* 199–219. [2] Elkins-Tanton L. T. et al. (2011) *E. & Planet. Sci. Lett., 305,* 1-10. [3] Wilson, L., Keil, K. (2012) *Chem. der Erd*e, *72,* 289-321. [4] Greenwood R. C. et al. (2005) *Nature, 435,* 916-918. [5] O'Neill H. S. C. & Palme H. (2008) *Phil. Trans. R. Soc. A, 366,* 4205-4238. [6] Javoy M. et al. (2010) *E. & Planet. Sci. Lett., 293,* 259-268. [7] McCoy T. J. et al. (1999) *Meteoritics & Planet. Sci., 34,* 735-746. [8] Jackson M. G. & Jellinek A. M. (2013) *G^3, 14,* 2954-2976. [9] Marrocchi Y. & Libourel G. (2013) *GCA, 119,*117-136.[10] Krot A. N. et al. (2003) Treat. on Geoch, vol. 1.

Evolution of the protolunar disk: dynamics, cooling timescale and implantation of volatiles into the Earth

Sébastien CHARNOZ[1], Chloé MICHAUT[2] ; (1) Laboratoire AIM / IPGP (1 rue Jussieu 75005 Paris France) charnoz@cea.fr, (2) IPGP (1 rue Jussieu 75005 Paris France)

It is thought that the Moon accreted from the protolunar disk that resulted from the last giant impact on Earth. The protolunar disk is one of the least known structure of planetary sciences and the present we present the first numerical exploration of its evolution.

Due to its high temperature, the protolunar disk may act as a thermochemical reactor in which the material is processed before being incorporated into the Moon, if the disk survives long enough. Volatile escape as well as isotopic diffusion inside the disk might explain the geochemical composition of the Moon and its similar isotopic composition with the Earth. However the disk lifetime dynamics and thermodynamics are mostly unknown

Here, we numerically explore the long term viscous evolution of the protolunar disk using a one dimensional model where the different phases (vapor and condensed) are vertically stratified and at thermodynamical equilibrium. We account for viscous heating, radiative cooling, phase transitions and gravitational instability. The viscosity of the gas, liquid and solid phases dictates the disk evolution.

We find that (1) the disk's vapor condenses rapidly into liquid in about 10 years (2) most of the disk mass flows inward rapidly into a hot and compact liquid disk between 1 and 1.7 Earth's radii, a region where the liquid is gravitationally stable (3) this liquid disk survives 10^3 to 10^4 years above 2000K depending on the vapor effective viscosity (4) when solidification proceeds, the disk experiences a series of brief and intense heat bursts due to viscous instabilities that lengthen the disk cooling time (5) the disk finally becomes solid in 10^4 to 10^5 years. Viscous heating is never balanced by radiative cooling.

A very promising aspects concerns the viscous evolution of volatiles : if the vapor phase is abnormally viscous, due to magneto-rotational instability for instance, the volatiles mostly accrete on Earth leaving a disk enriched in refractory elements. This opens a way to form a volatile-depleted Moon and would suggest that the missing Moon's volatiles are buried today into the Earth. This would also probably imply the presence of an early magnetic field on the proto-Earth. The disk cooling timescale may be long enough to allow for planet/disk isotopic equilibration.

WHAT DO NECTARIS BASIN IMPACT MELT ROCKS LOOK LIKE AND WHERE CAN WE FIND THEM? B. A. Cohen[1], N. E. Petro[2], and S. J. Lawrence[3]; [1]NASA Marshall Space Flight Center, Huntsville AL 35812 (Barbara.A.Cohen@nasa.gov), [2]NASA Goddard Space Flight Center, Greenbelt MD 20771; [3]School of Earth and Space Exploration, Arizona State University, Tempe AZ 85281.

Introduction: The formation of the Nectaris basin is a key event defining the stratigraphy of the Moon. Its absolute age, therefore, is a linchpin for lunar bombardment history. Fernandes et al. [1] gave a thorough account of the history of different samples thought to originate in Nectaris, with the upshot being there is little agreement on what samples represent Nectaris, if any. We are revisiting the effort to identify Nectaris basin impact-melt rocks at the Apollo 16 site, to model their emplacement, and to use these parameters to examine other sites where Nectaris impact melt is more abundant and/or more recognizable for potential further study.

Nectaris melt in Apollo 16 soil? A compendium of all the rocks so far dated (only a fraction of all possible samples) from the Apollo 16 collection is shown in Fig. 1. Though it reflects our known bias as a community toward dating radiogenic-rich, mafic impact-melt rocks, it does show several important features: a clear time of crystallization of lunar crustal rocks, represented by the abundant (though undersampled) ferroan anorthosites; a small group of ~4.1-4.2 Ga samples as noted by [1]; two distinct groups of impact-melt samples clustered ~3.95 and ~3.85 Ga; a tail off of assorted impact-melt compositions similar to the lunar meteorite ages [2]; and a handful of glassy materials spanning time until present.

At the Apollo 16 site, the formation of the Imbrium basin was undoubtedly the last major modification to the surface, forming the Cayley plains and possibly also the Descartes formation [3]. However, as the largest, it would also have the greatest depth of mixing, dredging up and mixing with material deposited by all previous impacts. We are using an updated regolith ejecta and melt model [4-6] to better constrain the amount of impact-melted material in the ejecta from successive basins contributing to the Apollo 16 regolith. Our preliminary results are shown in Fig. 2 (top), where Imbrium and Serenitatis ejecta make up the majority of the basin impact melt at the Apollo 16 surface, but a significant amount of Nectaris melt should also be present. However, since each ejecta emplacement event mixes and dilutes previous material, we are also trying to understand mixing and dilution with each successive ejecta blanket (Fig. 2 bottom). We will take this work further, constraining it with observations that mafic impact melt-breccias make up about ~29% of the Apollo 16 impact samples [7].

The Nectaris impact exhumed material from up to 45 km depth [8], which is probably not deep enough to excavate a KREEP layer, if it existed at the time of Nectaris basin formation., but may be enough to incorporate a noritic lower crustal component [9], along with a significant anorthositic component from the upper crust. Given that there is no PKT-compositional "halo" around Nectaris, we can infer that Nectaris basin impact melt is very likely not KREEPY, and instead should be quite aluminous and possibly iron-rich.

Aluminous Group 3 samples [7] are among the youngest group based on their Ar-Ar ages [10], not predating the KREEP-rich poikilitic impact melts which are taken as Imbrium melt. Group 4 samples (low KREEP) are a logical alternative. These anorthositic impact-melt breccias have older Ar ages. [11], but a variety of textures including some described as "fragment laden," which may have old ages due to incomplete

Figure 1: All ages for Apollo 16 samples.

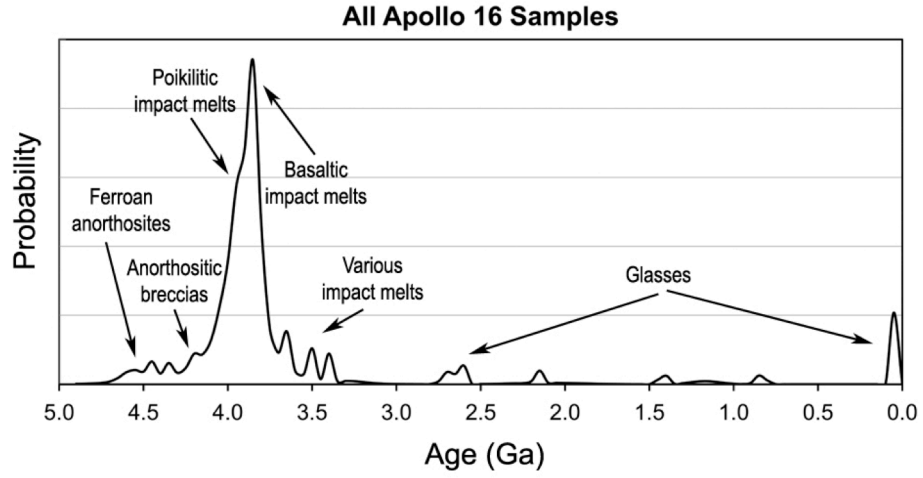

outgassing. More work can be done to correlate these samples with their isotopic information compiled in Fig. 1.

Nectaris melt in situ? Although the Nectaris basin itself has experienced both basaltic infill and impact erosion, its original morphology is still recognizable. Small plains near inner basin ring massifs and inter-massif "draped" deposits were identified as remnants of the Nectaris basin impact melt sheet [12]. Using Clementine spectral data, Spudis [13] determined that the mean iron content of these impact-melt units is higher than Orientale (FeO=5.6 vs 4.6 wt.%), which suggests more mafic target material underlying Nectaris, as both basins are comparable in size and should have excavated to similar depths. However, the range of FeO within the Nectaris units is broad, suggesting regolith development over these units that has introduced non-melt components. No changes were observed near small craters that would suggest compositional variability with depth in these units.

We are revisiting these interesting exposures with other remote-sensing datasets. Comparisons of the composition of this unit with other known sample sites help constrain the Nectaris melt characteristic even further. It is hoped that through these combined approaches, we will be able to better recognize Nectaris impact melt and target it for detailed geochronology.

References: [1] Fernandes, V. A., et al. (2013) *MAPS*, 48, 241-269. [2] Cohen, B. A., et al. (2000) *Science*, 290, 1754-1756. [3] Norman, M. D., et al. (2010) *GCA*, 74, 763-783. [4] Petro, N. E. and C. M. Pieters (2006) *JGR*, 111, DOI: 10.1029/2005JE002559. [5] Fassett, C. I., et al. (2012) *Journal of Geophysical Research: Planets*, 117, E00H06. [6] Cohen, B. A. and R. F. Coker (2010) #2475. [7] Korotev, R. L. (1997) *Meteoritics*, 32, 447-478. [8] Wieczorek, M. A. and R. J. Phillips (1999) *Icarus*, 139, 246-259. [9] Wieczorek, M. A. and M. T. Zuber (2001) *GRL*, 28, 4023-4026. [10] Norman, M. D., et al. (2006) *GCA*, 70, 6032-6049. [11] Stöffler, D. A., et al. (1985) *PLPSC*, 15, 449-506. [12] Spudis, P. D. and M. C. Smith (2013) 1483. [13] Spudis, P. D. (2013) EPSC2013–758.

Figure 2: Contributions from (top) ejecta and (bottom) impact melt of major basins to the Apollo 16 regolith.

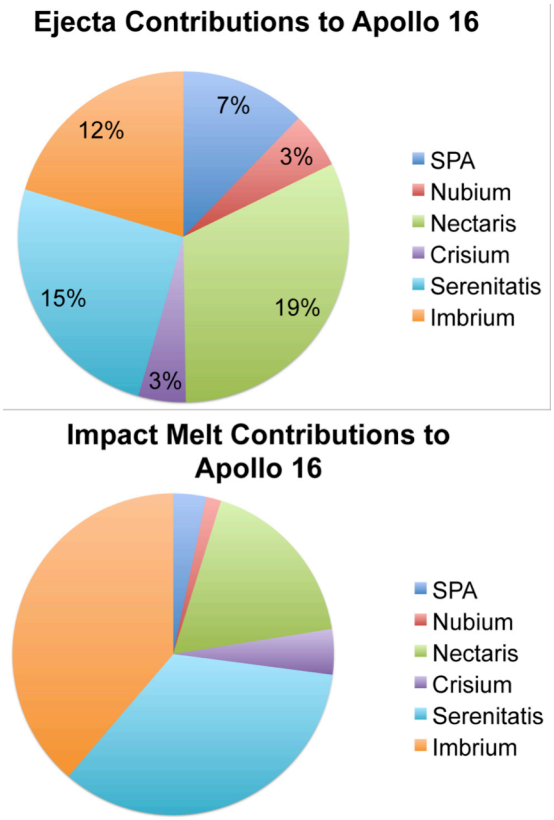

LUNAR ZIRCONS: WHAT'S THE BIG PICTURE? C. A. Crow[1], K. D. McKeegan[1], and D. E. Moser[2], [1]University of California, Los Angeles (595 Charles Young Drive E, Box 951567, Los Aneles, CA 90095; ccrow@ucla.edu), [2]University of Western Ontario (Biological & Geological Sciences Building, 1151 Richmond Street N, London, Ontario, Canada, N6A 5B7).

Introduction: Zircon is a late stage accessory mineral that incorporates radiogenic parents such as uranium and thorium, while preferentially excluding their daughter product lead, allowing for precise U-Pb and Pb-Pb ages to be determined for individual grains [1]. Zircons also incorporate other trace elements such as the rare earth elements (REEs) and titanium, which can reflect the composition and temperature of the parent magma [2]. Microstructural studies of terrestrial and lunar impact zircons found that some types of shock deformation may result in increased Pb mobility, but the extent to which these microstructures affect radiogenic ages and/or trace element compositions in lunar grains is still unclear (e.g. [3-6]).

The lunar zircons analyzed to date have Pb-Pb ages that range from 3.9 to 4.4 Ga (e.g. [6-8]). These relatively old ages, predating the hypothesized late heavy bombardment (LHB) [REF], and the ability of these grains to retain primary crystallization ages and signatures of secondary impact processes, make them suitable for investigating the early magmatic and impact history of the Moon. We have conducted an extensive U-Pb, REE, and microstructural survey of Apollo zircons that, in combination with previous studies, represents a robust lunar zircon dataset from which we can draw constraints regarding the duration of KREEP magmatism, zircon formation mechanisms, and possibly the early impact history of the Moon.

Methods: Zircons were separated from Apollo 14, 15, and 17 samples by crushing and heavy liquid density separation. We sampled six breccias (14304, 14305, 14321, 15405, 15455, 72275), one saw cutting (14163), and two soils (14259, 15311). All grains were imaged by scanning electron microscopy (SEM) to search for cracks, inclusions, and regions of cathodoluminescence (CL) variation. After preliminary characterization, U-Pb and Pb-Pb ages for 155 zircons and trace elements of 89 zircons were collected with the UCLA Cameca IMS-1270. A selection of 30 grains were then searched for the presence of crystallographically-controlled shock microstructures at the University of Western Ontario, Zircon and Accessory Phase Lab (ZAP Lab) by using a combination of secondary electron (SE), low kV backscatter electron (BSE), CL, and electron backscatter diffraction (EBSD) mapping.

Results:

Microstructures. The 30 zircons survied for shock microstructures were from breccias 14305, 14321, and soils 14259, 15311. Of these zircons only one grain exhibited granular texture and none have crystal-plastic deformation greater than 8°, which are features thought to result from recrystallization during shock metamorphism and strain during crater relaxation respectively. Both are thought to cause significant Pb-loss in impact zircons [5]. Shock microtwins have also been suggested to be a pathway of Pb-loss [5]. Three of the grains contained shock microtwins, but all have concordant ages >4.24 Ga. Only a small fraction of the grains exhibit microstructures that afford disturbance of the pre-shock U-Pb ratios.

Trace elements: Increased resolution of SEM imaging allowed us to identify impact melt inclusions down to the submicron scale. After removing REE analyses where SIMS spots overlapped inclusions or cracks, and analyses with >600ppm Fe, the lunar zircons can be characterized by one REE pattern with varying total REE concentration. The trace elements also exhibit trends indicative of formation by fractional crystallization, which is consistent with, but not uniquely indicative of, crystallization in a KREEP like magma [9].

Ages. The vast majority of the lunar zircons have U-Pb ages that are concordant within error (typically 4%). The distributions of the corresponding Pb-Pb ages in our study are not homogeneous amongst the Apollo landing sites. This is in agreement with previously published Apollo 14 and 17 zircon ages [REF]. Our Apollo 15 and 17 samples only contain zircons that are older than 4.1 Ga, while Apollo 14 also samples a younger population of grains that have ages ranging to as young as ~3.9 Ga. Only 10% of the zircons are in this younger population, and they are typically smaller grains (<50 microns) or show evidence of Pb loss or impact crystallization textures. As an ensemble, the crystallization ages and REE patterns suggest a widespread, extended period of KREEP magmatism spanning from ~4.4 to ~4.1 Ga but that only Apollo 14 zircons have a significant younger population that may represent extension of magmatism for another ~200 Ma or that this population was reset by LHB era impacts. Regardless, Apollo 15 and 17 zircon Pb-Pb ages are not largely affected by LHB era basin forming impact events.

References: [1] Compston W. W. et al. 1984 *J. Geophys. Res.* 89, B525-B534. [2] Hoskin P. W. O. and Schaltegger U. 2003. *Rev. Min. Geochem*. 53, 27-62. [3] Krogh T.E. et al., 1996. *Geophys. Mono.* 95,

343-353. [4] Moser D. E. 1997. *Geology* 25 7-10. [5] Moser D. E. et al. 2011. *Can. J. Earth Sci.* 48, 117-139. [6] Grange M. L. et al. 2013. *Geochim. Cosmochim. Acta* 101:112-132. [7] Taylor D. J. et al. 2009. *Earth Planet. Sci. Lett.* 279, 157-164. [8] Nemchin A. A. et al. 2010. *Am. Min.* 95, 273-283. [9] Clairborne et al. 2010. *Cont. Min. Pet.* 160, 511-531.

U-Pb COMPOSITION AND SHOCK MICROSTRUCTURES OF *IN-SITU* ACCESSORY PHASES ACROSS THE VREDEFORT IMPACT STRUCTURE, SOUTH AFRICA: A TERRESTRIAL ANALOGUE FOR DATING THE LUNAR SURFACE AND OTHER PLANETARY BODIES. C.L. Davis[1] and D.E. Moser[1], [1]Department of Earth Sciences, Western University, London, ON, CAN, N6K 367, cdavis59@uwo.ca.

Introduction: Highly refractory micro-minerals such as zircon, monazite and baddeleyite can survive and record intense shock metamorphism, and occasionally recrystallize to date impact events. Their micro-scale records have the potential to be used to deduce the timing and magnitude of large impacts in *ex-situ* solar system samples (i.e. meteorites, crystal clasts in breccias) provided we have a more complete understanding of mineral and isotopic response and variability to a large impact event. Terrestrial analogue sites, such as the Vredefort impact structure of South Africa, represent a rare opportunity to characterize the effects of complex and large (~300 km on Earth) impact events and impact-related melting on micro-minerals *in-situ* across a known pressure and temperature gradient.

The U and Pb composition (and therefore U-Pb isotopic dates) of shocked accessory phases respond to the passage and after-effects of a shockwave in a variety of ways, ranging from complete to zero U-Pb age-resetting [1]. On a regional scale, this dichotomy is attributed to radial distance from the crater center and the magnitude and duration of post-shock heating, broadly defining the so-called "hot-shock" and "cold-shock" zones, respectively [1]. On a microscopic scale, however, the mechanisms underlying the variation of Pb-loss among zircons within a single sample are poorly understood. The range of Pb-loss and age-resetting can occur within a single zircon population and occasionally within a single zircon. Previous studies have considered the Vredefort dome as an analogue for the lunar surface and other similiar rocky bodies, based primarily on the similarity of some impact-induced textures and microstructures [2]. The recent report of glassy inclusions along planar features in zircon derived from shock melting of the host rock [1], and similar inclusions in lunar zircons [3,4] also raises the possibility of linking shock environments to crater floor composition of potential application to lunar impact chronology. Here we present progress using a combination of analytical techniques to elucidate the heterogeneous processes of an impact-related shockwave on minerals at the micro-scale, as well as the variable resilience of these phases despite severe shock heating.

Methods: Selected samples from across the shock metamorphic gradient and rock types of the Vredefort dome (near-center, intermediate, and collar locations) were analyzed. These samples were prepared as thin sections to allow for the *in-situ* analysis of accessory phases within the context of the surrounding mineralogy. Location mapping and analysis of microminerals was accomplished with a Hitachi SU6600 field emission scanning electron microscope at the Western Zircon Accessory Phase Laboratory using backscatter electron (BSE) imaging, secondary electron (SE) imaging, cathodoluminescence (CL, colour plus UV) imaging, and electron backscatter diffraction (EBSD).

Results: Rocks collected and analyzed thus far include samples of Archean granodioritic gneiss (Inland-see Leucogranofels) from the core, charnockitic felsic orthogneiss and mafic granulite from an intermediate location (Vredefort discontinuity) and foliated granitoid (Outer Granite Gneiss) from the collar regions. Multiple (U-Pb) dateable accessory phases (i.e. zircon, monazite) coexist within the majority of these rocks. At extreme shock levels in the core region, zircon and monazite exhibit microstructures ranging from crystallographically controlled planar features to entirely recrystallized and polycrystalline (granular) pseudomorphs. Inclusions of shock melt may play a role in nucleating the recrystallization of domains that date the impact event. Inclusions are also common in lower grade shock metamorphic regions (Fig. 1). Similar melt inclusions are reported in zircon from lunar impact breccias from Apollo sample returns, and the

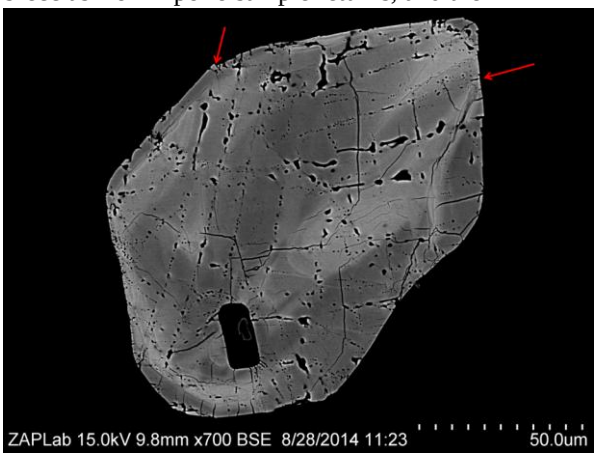

Figure 1: Zircon F3655 from sample V2-1 charnockitic gneiss showing at least two orientations (red arrows) of shock-generated inclusions of melt of the host rock distributed along the traces of planar microstructures.

plagioclase-rich charnockitic gneiss samples provide a valuable link to similiarly plagioclase-rich lunar sam-

ples. Chemical and microstructural characterization of the inclusions and immediate grain environment are in progress. The inclusion chemistry, distribution, and spatially correlated U-Pb compositions will be measured in different grain settings in adjacent rock types across the shock metamorphic gradient at Vredefort. The results will hopefully resolve the mechanisms underlying the dichotomy between reset and non-reset U-Pb ages of accessory phases, and ultimately improve the accuracy of bombardment chronologies based on *ex-situ*, extraterrestrial U-bearing microminerals.

References: [1] Moser, D.E. et al. (2011) *CGES, 48,* 117–139. [2] Gibson, R.L. et al. (2002) *Geology, 30(5), 475-478.* [3] Spicuzza, M.J. et al. (2012) *LPSC XLIV,* Abstract #2878. [4] Crow, C.A. et al. (2014) *77th Meteoritical Society Meeting,* Abstract #5366.

Impact craters on comets from a granular material perspective

Detlef de Niem[1], Ekkehard Kührt[1], [1]DLR Institute of Planetary Research, Rutherford Str.2, D-12489 Berlin, Germany (detlef.deniem@dlr.de),

On small solar-system bodies or on the lunar surface, under conditions of vanishing atmosphere a porous regolith or ice-dust layer is present. These dry, porous surface conditions are quite different from those of geomaterials in the Earth' crust, where natural gas and pore fluids additionally modify the wave speeds [2]. Landing on a comet rather than on an asteroid is a challenging endeavour in itself but only in this way one may learn something about the mechanical properties of these small building blocks of larger bodies in the outer solar system. Meanwhile high-resolution images of the surface of comet 67P/Churyumov-Gerassimenko, the target of ESA's Rosetta Mission obtained by the OSIRIS instrument and with the help of the ROLIS camera [3] aboard the lander Philae have revealed crater-like features at all scales resolvable by the instruments. It is not clear yet which of these features have an impact origin or were formed by activity but there are impact crater candidates. The unintentional jumps of the lander and the data of Philae experiments like SESAME, MUPUS and SD2 also give some hints concerning mechanical properties of the surface. While the role of porosity for impact crater formation has been emphasized previously and modeled, for example in connection with the Deep Impact cratering experiment [4], using the P-alpha model [5],[6], additional insight may come by regarding properties of contact forces between small grains. These forces cannot be characterized with the help of porosity alone. An unusual feature of Hertz' contact forces [1] is that the bulk and shear moduli of the effective medium approach zero at vanishing volumetric strain [7],[8]. Although this largely is the consequence of ignoring adhesion, for macroscopic grains and rough surfaces the non-linearity remains; at least the Deep Impact experiment provided indirect evidence that adhesive forces between grains on a cometary surface play a minor role. Granular materials behave highly non-linear even under small strain [7],[8],[9]. This presents a difficulty for treatment of the shear stress within the traditional, linearized hypo-elastic formulation. Here a finite strain algorithm [12] has been adapted to include the pressure and shear stress arising from an ensemble of grains in an effective-medium approximation, furthermore two additional ordinary materials such as fluids and gases can be modeled due to the multi-material capability inherited from a previous hydrocode [11]. The deviatoric stress of the granular target material is similar in form to that recently proposed by [10] but additionally Coulomb friction limits the shear stress in proportion to the effective-medium pressure. In this way a dissipative loss mechanism is present but there is no adjustable strength parameter. This algorithm can simulate cratering in granular-material targets at small and moderately large velocities such as have been characteristic during the formation of small solar-system bodies and still occur in the outer solar system. Even on the lunar surface, granular material properties may dominate the late stage of crater formation, although a unified description including hypervelocity phenomena is not yet available with the present method. Fig.1 shows a simulation example where a porous D=12.8 meters spherical impactor strikes a 60% porous half-space vertically at 100 m/s under low gravity $g = 2.5 \times 10^{-4}$ m/s^2, simulated in cylindrical coordinates. The properties of the matrix material are chosen to resemble H_2O ice: a solid density of 0.917 g cm^{-3}, Poisson ratio of 0.31 and bulk modulus of the grains of 9.47 GPa. The effective-medium pressure is proportional to the solid material volume fraction Φ_s, to the coordination number, and varies with Hertz' deformation parameter $\propto \xi^{3/2}$ [9], the effective shear modulus is $\propto \xi^{1/2}$ [8]. In Hertz' contact mechanics ξ measures the relative approach of two spherical grains. In finite deformation elasticity ξ is related to the average density ratio by $(1-\xi)^3 = (\Phi_{s0}\rho_{s0})/(\Phi_s\rho_s)$, here subscripts $s0$ denote quantities in the initial, non-deformed state. A low-density gas with P=10^{-2} Pa and a density of 10^{-10} g cm^{-3} fills the space above the free surface but largely is without consequences for the ballistic motion of ejecta. The kinetic energy of the impactor of about 2.01×10^9 J is approximately one order of magnitude lower than that used in the Deep Impact experiment. Despite the lower kinetic energy and linear momentum (in the hypothesis of Schmidt and Holsapple [13] for scaling of crater dimensions, the coupling parameter is a quantity in between kinetic energy and momentum), the transient cavity size at a simulated time of 10 seconds, lowermost frame in Fig.1, already reaches a value close to the upper limit suggested for the crater created during Deep Impact experiment after flyby images had been obtained at 9P/Tempel 1 6 years later by the Stardust-NExt mission[14]. Although the simulation time still is much lower than that required for a gravity-dominated crater to form, the early stage already allows to estimate the mass accreted by the target body at such 'moderate' velocities. An interesting feature also is that the ejecta curtain always remains quite narrow, initially emerges at a low angle and then gradually steepens up.

References

[1] H. Hertz, *Journal für die reine und angewandte Mathematik (Crelle)* **92**, 156-171 (1881).

[2] I. Y. Belyaeva, L. A. Ostrovsky, V. Y. Zaitsev, *J. Acoust. Soc. Am.* **99 (3)**, 1360-1365 (1996).

[3] S. Mottola, G. Arnold, H.-G. Grothues, H. Hirsch, R. Jaumann, J. Michaelis, G. Neukum, R. Wäsch, J.-P. Bibring, In: *ESA Special Publication on the ROSETTA Mission* **ESA-SP1165**, (2002).

[4] K. Wünnemann, G.S. Collins, H.J. Melosh, *Icarus* **180**, 514-527 (2006).

[5] W. Hermann, *J. Appl. Phys.* **40 (1968)**, 2490-2499.

[6] R. Menikoff, E. Kober, *Proceedings APS topical conf. shock compression in condensed matter,* **LA-UR-99-2364**, (1999).

[7] R. D. Mindlin, *Trans. ASME* **71**, A-259 (1949).

[8] Walton, K., *J. Mech. Phys. Solids* **35 (2)**, 213-226 (1987).

[9] A. N. Norris, D. L., Johnson, *J. Appl. Mechanics* **64**, 39-49 (1997).

[10] Y. Jiang, M. Liu, *Phys. Rev. Lett. A* **91 (14)**, 144301-1-144301-4 (2003).

[11] D. de Niem, E. Kührt, U. Motschmann, *Computer Phys. Comm.* **176**, 170-190 (2007)

[12] D. de Niem, 11th Int. Conf. Num. Anal. Appl. Math. 2013, *AIP Conf. Proc. 1558, 2402-2405 (2013); doi: 10.1063/1.4826025.*

[13] R. M. Schmidt, K. A. Holsapple, *Geol. Soc. Am. Spec. Pap.* **190**, 93-162 (1982)

[14] J.E. Richardson, H.J. Melosh, *Icarus* **222**, 492-501 (2013).

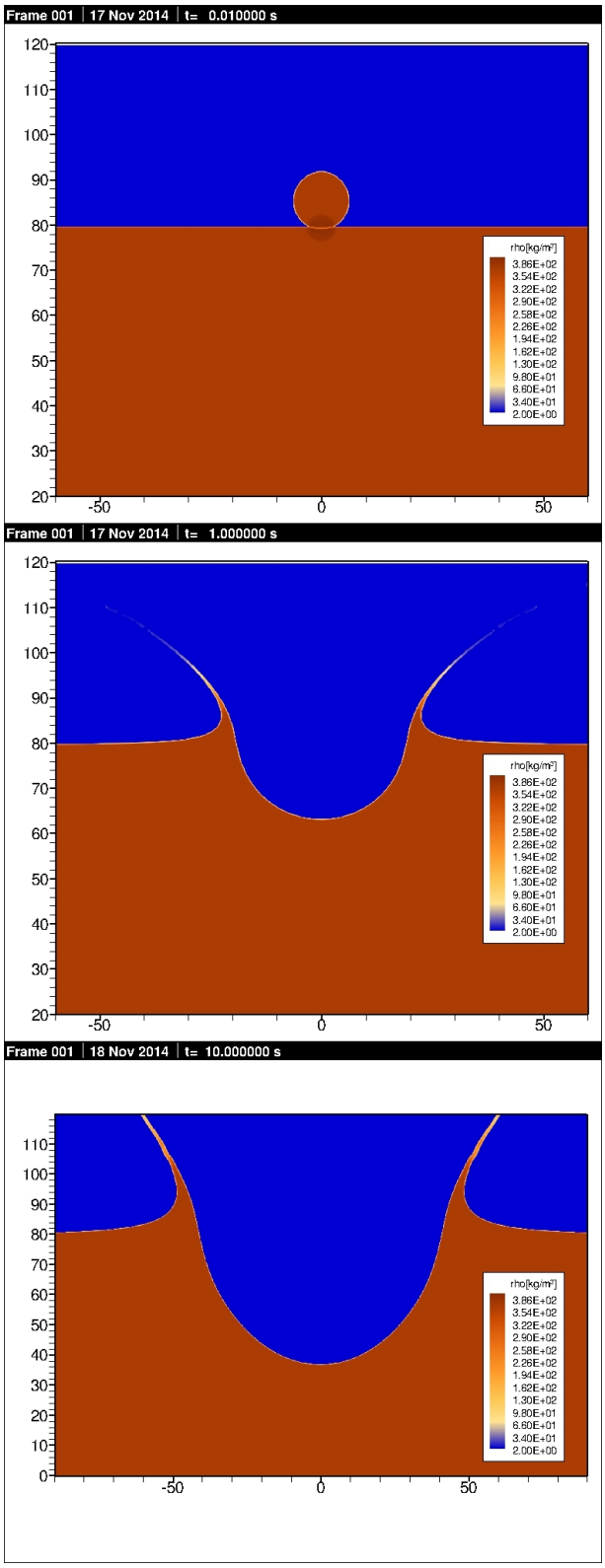

Figure 1: Snapshots from simulation of 100 m/s impact, kinetic energy of 2.01×10^9 J, into 60% porous granular target. Matrix material with properties of H_2O ice, surface gravity of 2.5×10^{-4} m s^{-2}. Note quite slow shock propagation into granular materials 10 milliseconds after contact, visible as slightly more dark colour in uppermost frame. Last frame at 10 seconds. Axis units: meters.

EVIDENCE SUPPORTING AN EARLY AS WELL AS LATE HEAVY BOMBARDMENT ON THE MOON H.V. Frey, Planetary Geodynamics Lab, Goddard Space Flight Center, Greenbelt, MD 20771, Herbert.V.Frey@nasa.gov .

Summary: Evidence supporting an intense early bombardment on the Moon in addition to the traditional Late Heavy Bombardment at ~ 4 BY ago include the distribution of N(50) Crater Retention Ages (CRAs) for candidate basins, a variety of absolute age scenarios for both a "young" and an "old" Nectaris age, and the decreasing contrasts in both topographic relief and Bouguer gravity with increasing CRA.

Crater Retention Ages: N(50) Crater Retention Ages (CRAs) for an expanded inventory of large lunar basins [1-3] based on Quasi-Circular Depressions (QCDs) in LOLA data [2,3] and Circular Thin Areas (CTAs) from model crustal thickness [4,5] show two peaks, even when weaker candidates are eliminated [6] (Figure 1). The break between older and younger impact basins is pre-Nectarian [6], as others suggested based on a smaller number of basins [7], shown in Figure 2. This two peak distribution suggests the possibility of both an Early Heavy Bombardment [6] as well as the generally recognized Late Heavy Bombardment [8-10].

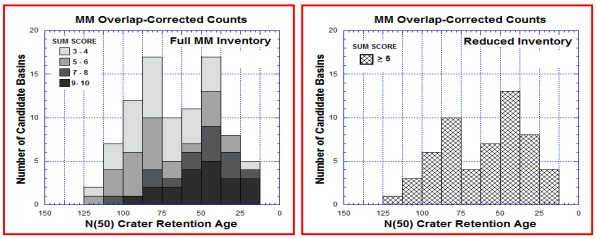

Figure 1. Distribution of Overlap-Corrected N(50) CRAs for an inventory of 90 candidate basins [11] (left), and for a much reduced inventory of 56 basins (right). Full inventory also shows distribution of summary scores (sum of topographic expression and crustal thickness expression scores) in grayscale. Weaker candidates shown in lighter shades. Reduced inventory eliminates new candidates [11] and all candidates with summary scores <5 out of a possible 10. Both inventories show an obvious two-peak distribution.

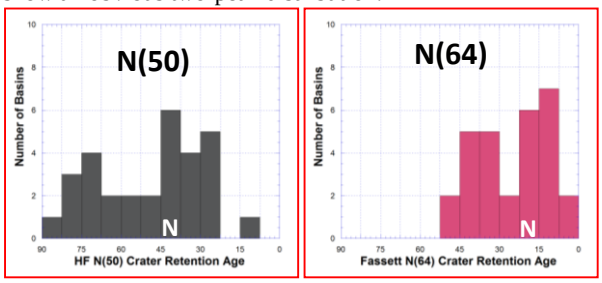

Figure 2. Distribution of N(50) CRAs (left) from Frey [1] (83 candidate basins) and N(64) CRAs (right) from Fassett et al. [7] (30 basins). Histograms have the same scale and bin size. Both show two peaks. The break between them is pre-Nectaris, the CRA for which is shown by the white N. This may suggest an Early as well as a Late Heavy Bombardment.

Absolute Age Scenarios: Absolute ages for most large lunar basin candidates are not known. Frey and McBride [12] presented scenarios for Model Absolute Ages (MAAs) using the few "known" absolute ages based on returned Apollo samples [13, references therein]. It was necessary to assume an age for the oldest inter-basin crust, several small areas of which were found to have N(50)~155, substantially older than the basin CRAs (Figure 1). An Assumed Oldest Age (AOA) of 4.5 BY was initially assumed, though cases with 4.4 BY were also considered. Results for full and reduced inventories were generally similar, but the MAAs depend greatly on the assumed age for Nectaris. If Nectaris is young (3.9 BY), the AA vs CRA relationship is a simple straight line and the two-peak distribution found in Overlap-Corrected N(50) CRAs is preserved, with peaks at ~3.9 BY and ~4.1 BY.

If Nectaris is 4.2 BY old, i.e. the source of the Apollo 16 impact breccia described by [14], the situation is more complex (Figure 3). The 4 basin points and the AOA point cannot be fit by a single straight line. A variety of scenarios were considered as shown in Figure 3. Results are shown in Figure 4.

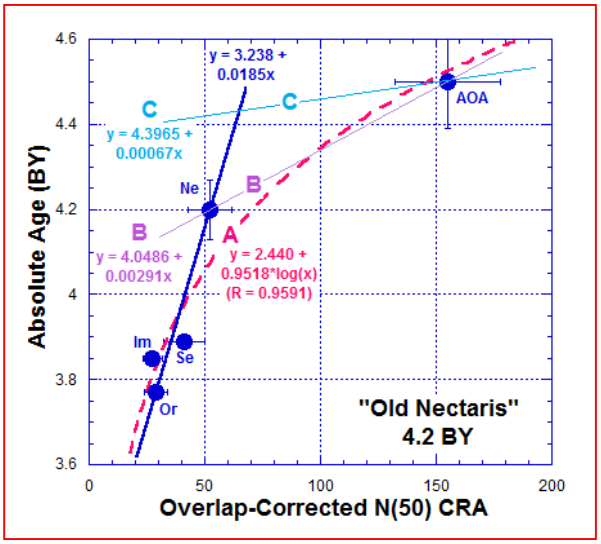

Figure 3. AA vs N(50) CRAs for Nectaris = 4.2 BY old. A = log(x) type fit to the 4 basins with known AAs and the Assumed Oldest Age (AOA) of 4.5 BY. B = two branch linear fit through Nectaris. C = two branch linear fit through the AA value on the younger branch at N(50) = 65 (the trough in the two-peak distribution of CRAs in Figure 1).

The **Case A** log(x) fit produces a most prominent peak at ~4.25 +/- 0.15 BY which is stronger than the secondary peak at 4.0 +/- 0.1 BY (Figure 4A). The **Case B** two branch, straightline fits through Nectaris push more basins to older ages (Figure 4B). A peak occurs at ~4.3 BY but is much more prominent than in A (the vertical scale is the same for all plots in Figure 4). There is a very much weaker peak at ~4.0 to 4.1 and a peak half this high at ~3.7 BY. The **Case C** two branch straightline fit through the AA on the younger branch at N(50) = 65 (the trough in the distribution of CRAs in Figure 1) results in a very large number of candidate basins with MAAs of 4.4-4.5 BY. The younger portion of the distribution is the same as in Case B, because the curve used over this CRA range is the same. Case C emphasizes the likely two population nature of the N(50) CRAs, but, like Case A and B, does NOT have a prominent and narrow peak at 3.9 BY. In all cases the older peak is more prominent.

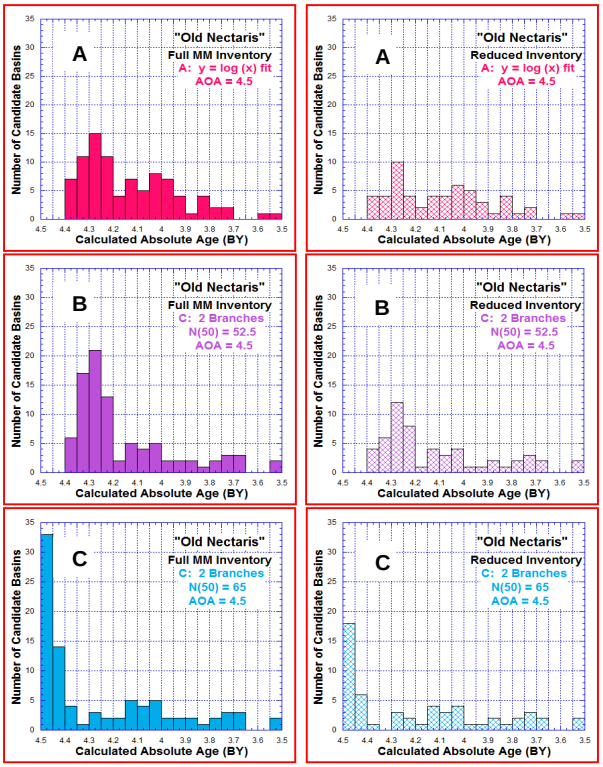

Figure 4. MAA distributions for the full inventory (left) and the reduced inventory (right) for the three "Old Nectaris" scenarios shown in Figure 3. See text for details. All three scenarios make the oldest peak the most prominent, and spread out the ages of basins younger than the 4.2 age for Nectaris into two weak peaks at ~ 4.1 and 3.7 BY.

Geophysical Contrasts. Contrasts in topographic relief and Bouguer gravity were derived from profiles through the candidate basins. Contrasts plotted versus Overlap-Corrected N(50) CRAs are shown in Figure 5. In both cases there is a general increase in contrast with decreasing CRA, as might be expected if earlier basins formed during a time when compensatsion of impact topography happened more easily.

There are reasons to eliminate points in the two plots. Figure 5A makes no correction for basins with significant mare fill or which occur in mare regions, where true basin relief may be underestimated. Figure 5B includes basins formed in extremely thin crust (e.g., SPA) and also unusually thick crust (Korolev, Dirichlet-Jackson, Hertzsprung, Fitzgerald-Jackson). Bouguer contrasts for these are are likely anomalous, as is that for SPA. Bouguer contrasts for the smallest basins (D<400 km) have low values and show no trend with age, suggesting they may have been too small to produce much contrast when formed. Both plots include cases where finding values from profiles is difficult and compromised by basin overlap. These are shown by smaller interior symbols in both plots. Removing these (and SPA, anomalous in both plots) produces the stronger trends in Figures 5C and 5D. Note some of the low contrast values at young ages in 5C are relatively weak candidates, so the actual trend in topographic relief may be even stronger than shown.

The older population has overall weaker contrasts than the younger population, consistent with the older basins forming early in lunar history when compensation of basin topography happened more quickly and thoroughly.

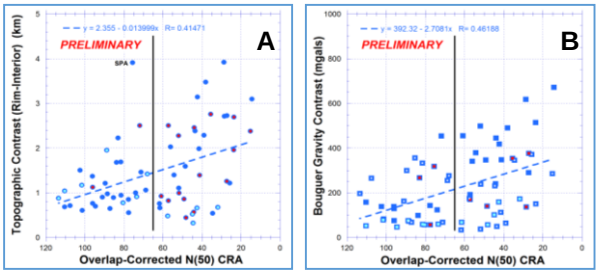

Figure 5. Above: Topographic (rim minus interior) contrast (A) and Bouguer gravity contrast (B) vs Overlap-Corrected N(50) CRA. Black vertical line shows separation between an older and younger population of large candidate impact basins, defined by the trough in Figure 1 and occurring at N(50) ~ 65. Linear fits to all the points shown; in both cases R ~ 0.4. Many of the points can be reasonably eliminated: these are marked with the interior symbols. Below: Without these likely anomalous points the trend toward increasing contrast with decreasing age is much stronger, with R ~ 0.6 for Topographic Relief (C) and ~0.8 for Bouguer Gravity (D).

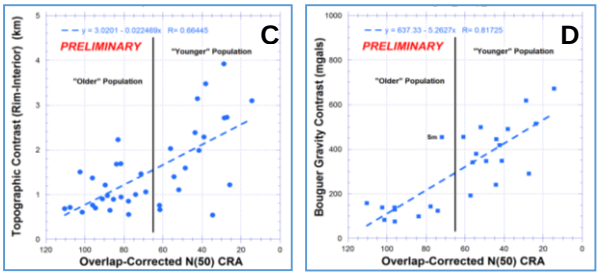

Summary: The distribution of N(50) Crater Retention Ages (CRAs) for candidate basins, a variety of absolute age scenarios for both a "young" and an "old" Nectaris age, and the decreasing contrasts in both topographic relief and Bouguer gravity with increasing CRA are all consistent with an Early as well as a Late Heavy Bombardment, perhaps by two different populations of large diameter impactors.

References. [1] Frey, H.V. (2012) LPSC 43, abstract #1852. [2] Romine, G. and H. Frey (2011) LPSC 42, abstract #1188. [3]] Frey, H. V., H. M. Meyer and G. C. Romine (2012a) *Early Solar System Impact Bombardment II*, Abstract #4005. [4]] Wieczorek, M.A. (private communication). [5] Meyer, H.M. and H.V. Frey (2012) LPSC 43, abstreact #1936. [6] Frey, H.V. and E.E. Burgess (2013) LPSC 44 abstract #1606. [7] Fassett, C.I. et al., JGR (Planets) LRO special issue. [8] Tera, F. et al. (1974) Earth Planet. Sci. Lett. 22, 1-22. [9] Ryder, G. et al. (2002) in R.M. Canup and K. Righter (eds) Origin of the Earth and Moon, 475-492, Un. AZ Press, Tucson. [10] Ryder, G. (2002) JGR 107, 5022, doi: 10.1029/2001JE001583. [11] McBride, M.J. and H.V. Frey (2014) LPSC 45, abstract # 2150. [12] Frey, H.V. and McBride, M.J., LPSC 45, abstract # 1101. [13] Stoffler, D. et al. (2006) Chapter 5 in New views of the Moon, Rev. Mineralogy and Geochem., vol. 60. [14] Norman, M.D. and A.A. Nemchin (2104) Earth. Planet. Sci. Lett. 388, 387-398.

REVIEWING "TERMINAL CATACLYSM:" WHAT DOES IT MEAN? William K. Hartmann, Planetary Science Institute, 1700 E. Ft. Lowell Road, Suite 106, Tucson AZ 85719; hartmann@psi.edu

Introduction: The idea of an early intense bombardment of the moon can be traced back at least to the 1960s [1], and the more specific concept of a terminal cataclysm dates from ca. 1973 [2,3]. Since then, the term "terminal cataclysm" (or an equivalent term) has been used in many papers as if it were a well-defined, empirically confirmed phenomenon. The meanings attached to this concept, however, range all over the map, from a global metamorphic event, or a 150 Ma-long spike in cratering centered at ~3.92 Ga ago, to still other concepts, such as few impacts before 3.9 Ga ago. Here, we argue that this semantic imprecision has hurt our understanding of the solar system.

History of Concepts*:* Various concepts have been discussed.

** In 1966, Hartmann [1] showed that the average cratering rate before ~3.6 Ga (evidenced in the lunar highlands) had to average ~150-200 times the average rate since then.

** Tera et al. in 1973-4 [2,3] based on Apollo rock samples, proposed a global "terminal cataclysm" metamorphic event at ~3.9 Ga ago, to explain paucity of earlier rocks. They suggested it might involve either the Imbrium basin impact around 3.9 Ga ago, or a clustering of many impact basins around that time.

** Hartmann, in 1975 [4], argued that a unique cataclysmic event at 3.9 Ga might be a "misconception" and that absence of early samples might involve more uniformitarian cratering, but so intense before ~ 4.0 Ga that earlier rocks were reset in age or lost by pulverization.

** The concept of "late heavy bombardment," ("LHB") at 3.9 Ga gained wide acceptance in 1990 when Ryder [5] showed that a huge spike in Apollo impact melt ages centered around 3.85-4.0 Ga ago. He also argued, importantly, that relative lack of impact melts from ~4.4 to 4.0 Ga indicated lack of impacts in that period.

** Circa 1998, Haskin, Korotev, and co-workers [6] argued that prevalence of ~3.9 Ga dates involved KREEP-rich ejecta from the Imbrium impact at that time, present at several Apollo sites. This was controversial, but echoed one of the proposals of Tera et al. in 1974.

** In 2000, Cohen, Swindle, and Kring [7] began reporting dates of impact melt clasts in KREEP-poor lunar meteorites. Their data show no Ryder-like spike at 3.9 Ga. Nonetheless they inferred "Support for the Lunar Cataclysm Hypothesis" (from their title), citing Ryder's rule, that lack of impact melts = lack of impacts, so that impacts must have started with a burst around 4.0.

** In 2001, Stöffler and Ryder [8, Table VI) estimated impact ages (at least 2 values each) for 5 basins. Here I add their 1σ error bar to their high value and subtract it from their lowest value, and list the average resulting value in brackets. Expressed in Ga, they give: Orientale 3.72-3.85 [3.785]; Imbrium 3.75-3.87 [3.81]; Crisium 3.80-3.91 [3.855]; Serenitatis 3.84-3.90 [3.87]; Nectaris 3.80-3.95 [3.875]. Thus they pack major basins with a wide range of crater density into an interval ~ 90 Ma, and no more than 230 Ma at 1-sigma levels. This work encouraged the idea that radiometric data had proven the existence of a terminal cataclysm.

** In 2003, Hartmann [9] argued that the Cohen data plus asteroidal meteorite data conflicted with the concept of a global lunar terminal impact cataclysm at 3.85-4.0, since their data show no sharp spike of impacts at that time.

** Around 2005 dynamicists introduced the "Nice model," in which outer solar system resonance effects scattered a wave of planetesimals into the inner solar system [10]. By assuming that this happened at 3.9 Ga, they argued that the dynamical model explained the LHB. These models showed few impacts during 4.4 to 4.0 Ga, supporting Ryder's rule. The title of [10] directly linked "Origin of the cataclysmic Late Heavy Bombardment period" to the Nice model. This work encouraged the idea that the Nice model had confirmed the LHB concept.

** By 2011, Norman and Nemchin [11] and others reported increasing numbers of pre-4.0 Ga impact melt dates, e.g. ~4.2 and ~4.33, from upland breccias. This refuted Ryder's rule that no large impacts happened before 4.0 Ga ago.

**After ~2011, dynamical models responded by moving away from a sharp spike at 3.9 Ga, for example introducing sawtooth spikes before 4.1 Ga, and a drawn out decline after 3.8. The latter decline was supported by earlier cratering data from Hartmann and Neukum [12]. In 2014, Marchi, and co-authors including Bottke, Morbidelli, and Kring [13, Fig. 1], presented new calculations of impact rates from scattered asteroids, showing a smooth decline in cratering from 4.4 to 4.0 Ga, which matched (unmentioned) curves based on cratering data, published as early as 1970. However they still proposed that an LHB could be added to their curve.

Current Status of Terminal Cataclysm. Today, growing indications that the putative massive scattering of outer solar system objects into the inner solar system 3.85-4.0 Ga ago never happened, since no Ryder-like spikes are observed in asteroidal or lunar meteorite data. Similarly, the concentration of basin scale impacts at 3.78-3.88 Ga ago is dubious, not only because 4 out of the 5 "dated" basins have inadequate samples from rim structures or ejecta, but also because we now have impact melt concentrations at ~4.2 Ga and earlier.

Thus, the terms "terminal cataclysm," "late heavy bombardment", "LHB," etc., though still commonly and casually used by scientists and journalists, have evaporated into nothing that has a clear, verifiable meaning. Perhaps it is time to end the use of these terms unless clear definitions and better evidence are provided. As stated in [11], "The strong version of the late cataclysm hypothesis in which all of the lunar basins formed between 3.8 and 4.0Ga (Ryder, 2002; Gomes et al., 2005; Abramov and Mojzsis, 2009) appears untenable."

Hypothesis for Explaining the Age Distribution of Lunar and Asteroidal Sample: As reviewed by Neukum et al [12], reconstructions of the curve of cratering rate vs. time, based on Apollo and Luna samples, even as far back as 1970 [14], show that the impact rate 3.8-3.9 Ga ago was of order 150-200 times the present rate, but declining rapidly. As shown in [9, 15], this was sufficient to cause much more rapid growth of regolith (and mega-regolith) than in the last 3.6 Ga. The general idea [4, 9, 15] is that around 3.8 to 4.0 Ga ago, an interval as short as 50-100 Ma was adequate to create many 10s of meters of pulverized material. This alone shows that samples earlier than 4.0 Ga should be hard to find, as observed in the early 70s by Tera et al. [2,3].

But a more subtle, profound, and under-appreciated effect is involved (9,15), involving the size-frequency distribution (SFD) of craters. If we slightly extrapolate the published impact rate-vs time backwards to the 4.0-4.1 Ga era along the curves published by Hartmann [14], Neukum [cf. 12], and most recently by Marchi et al. [13], we find that around 4.0-4.1 Ga ago, new surfaces became saturated with all craters in the diameter range of 2 to 100 km simultaneously, within ~100 Ma after their formation. Therefore, the period from 3.9 to 4.1 Ga ago (and probably before) marks a critical era, in which megaregolith ate into the lunar crust to depths of kilometers in short intervals of order 100 Ma or less. If we accept any steeply declining curve of impact flux vs. time, with a shape of form shown by in published curves from 1970 [14] to 2014 [13], then we can say that rocks older than 3.9 to 4.1 Ga would be hard to find, as per [2,3].

A still more subtle effect explains why pre-4.1 impact melts are more scarce than pre-4.1 igneous rocks. The largest volume of impact melts was contained in a modest number of localized impact melt lenses, with different ages, in the upper kilometers of the largest basin floors. Intact samples of the magma ocean igneous crust, however, exist below the megaregolith everywhere on the moon. Thus, if the megaregolith in the first 600 Ma rapidly reached depths of a few km, then the impact melt lenses may have been mostly converted to small clasts in upland breccias, and few impact melts older than 3.9 Gy are broadcast upon the lunar surface in recent time by "Tycho- or Copernicus-scale impacts" --- but those same sized impacts can tap into sub-megaregolith igneous crust.

As discussed in [9], this model is consistent not only with lunar observations, but also with asteroidal meteorite data.

References:

[1] Hartmann W.K. 1966. *Icarus* **5,** 406-418.
[2] Tera F. et al. 1973. LPSC abstract, p. 723.
[3] Tera F. et al. 1974. *EPSK* **22,** 1 21.
[4] Hartmann W. K. 1975. *Icarus* **24,** 181-187.
[5] Ryder G. 1990. *EOS* **71,** 313.
[6] Haskin L. A. et al. 1998. *MAPS* **33,** 959-975.
[7] Cohen B., Swindle T., Kring D. 2000. *Science* **290,** 1754-1756.
[8] Stöffler D. and Ryder G. 2001. In *Chronology and Evolution of Mars*, Eds. R. Kallenbach, J. Geiss, and W. K. Hartmann. Kluwer Academic Publishers, Netherlands (also *Space Sci. Rev.* **96,** 105-164).
[9] Hartmann W. K. 2003. *MAPS* **38,** 579-593.
[10] Morbidelli A., Bottke W. 2006. 1st International Conference on Impact Cratering in the Solar System (Noordwijk: ESTEC), abstract.
[11] Norman M., Nemchin A. 2012. Early Solar System Impact Bombardment II Conference, Abstract 4013.
[12] Marchi S. et al. 2014. *Nature* **511,** 578-582.
[13] Neukum G., Ivanov B. A., Hartmann W. K. 2001. In *Chronology and Evolution of Mars*, Eds. R. Kallenbach, J. Geiss, and W. K. Hartmann. Kluwer Academic Publishers, Netherlands (also *Space Sci. Rev.* **96**, 55-86).
[14] Hartmann W. K. 1970. *Icarus* **12**, 131-133; and *Icarus* **13,** 209-301.
[15] Hartmann W. K. 1980. In *Proc. Conf. Lunar Highlands Crust,* Eds. J. Papike and R. Merrill. Pergamon Press, New York. pp. 155-171.

IDENTIFYING THE GEOLOGIC CONTEXT OF APOLLO 17 APHANITIC AND POIKILITIC IMPACT MELT BRECCIAS. Debra Hurwitz[1] and David A. Kring[1]; [1]Center for Lunar Science and Exploration, NASA Solar System Exploration Research Virtual Institute, Lunar and Planetary Institute, 3600 Bay Area Blvd., Houston, TX, 77058, (hurwitz@lpi.usra.edu)

Introduction: The identification of the impact events that produced melt samples collected during the Apollo 17 mission to the Taurus Littrow valley remain controversial four decades later. Specifically, no consensus has yet been reached whether collected aphanitic and poikilitic samples were produced as a result of the Serenitatis impact [1-3], the Imbrium impact [4], a combination of both impact events [5], and/or as a result of another pre- or post-Serenitatis impact event [e.g., 6]. The uncertainty behind the source of collected samples engenders uncertainty in the implications of the measured sample ages and compositions. The current study uses high-resolution Lunar Reconnaissance Orbiter Narrow Angle Camera (LROC NAC) imagery and Lunar Orbiter Laser Altimetry (LOLA) topography data to investigate the geologic context and, thus, source(s) of aphanitic and poikilitic impact melt breccias.

Geology of Taurus Littrow valley: The Taurus Littrow valley is a graben oriented radially to the Serenitatis basin. The graben is bounded to the north and south by massifs, steep (~25°), relatively cohesive structures that rise to heights of 2000 and 2300 m, respectively, above the valley floor (Fig. 1). Astronauts Cernan and Schmitt observed "source-crops" of boulders on the upper one-half to two-thirds of both massifs and boulder tracks that connect these source-crops to boulders near the base of each massif [7]. The Sculptured Hills, as described by the astronauts on the surface, form a darker grey, hummocky unit that has been pockmarked with small craters and typically has more gradual though undulatory slopes (10°–30°). This unit lies atop the massifs or, in the vicinity of Station 8, drapes over the valley floor.

In some locations, both atop the massifs and on the valley floor, the terrain is covered with clusters of fresh superposed craters that are interpreted to have been emplaced ~100 Myr ago during the Tycho impact event [8]. Additional geologic units identified within the Taurus Littrow valley include mare basalts that cover the valley floor, a bright deposit that appears to have slumped from the South Massif, the Lincoln Scarp that crosses the valley, and Wessex Cleft, a saddle with darker deposits that lies between the North Massif and the Sculptured Hills unit to the east.

Impact melt samples were often collected from boulders at the base of massifs. As an example of their sources, we illustrate (dotted lines in Fig. 1b) the boulder tracks that lead to samples at Station 2 at the base of the South Massif (SM) and Station 6 at the base of the North Massif (NM).

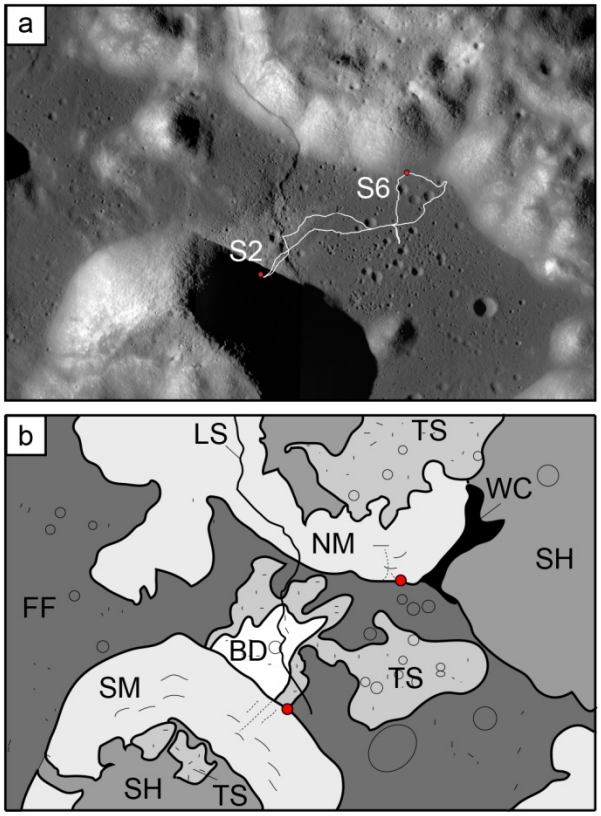

Fig. 1: Taurus Littrow valley shown in (a) LROC NAC images with the Apollo 17 traverse tracks noted, and (b) a preliminary geologic sketch map. Units include the North and South Massifs (NM, SM), the Sculptured Hills (SH), Tycho secondary crater clusters (TS), floor fill (FF), bright deposits (BD), the Lincoln Scarp (LS), and the Wessex Cleft (WC). Red dots note stations 2 (S2) and 6 (S6) where relevant samples were collected, and dotted lines above the red dots trace boulder tracks that lead to source outcrops on the massif walls. The scene is ~30 km across.

Relevant samples from Station 6: Multiple boulders can be traced to their uphill sources (Fig. 2). One of those boulders appears to have fragmented, producing a five-boulder cluster (red dot). Two representative samples are 76295, a blue-grey, nonvesicular impact melt breccia with an aphanitic matrix from Boulder 1, and sample 76315, a micropoikilitic impact melt breccia sampled from the "transitional zone" of Boulder 2. Sample 76295 contains a marbled texture of the tan and blue-grey breccias, while sample 76315 is a dark grey breccia with several lighter grey clasts. Both samples have

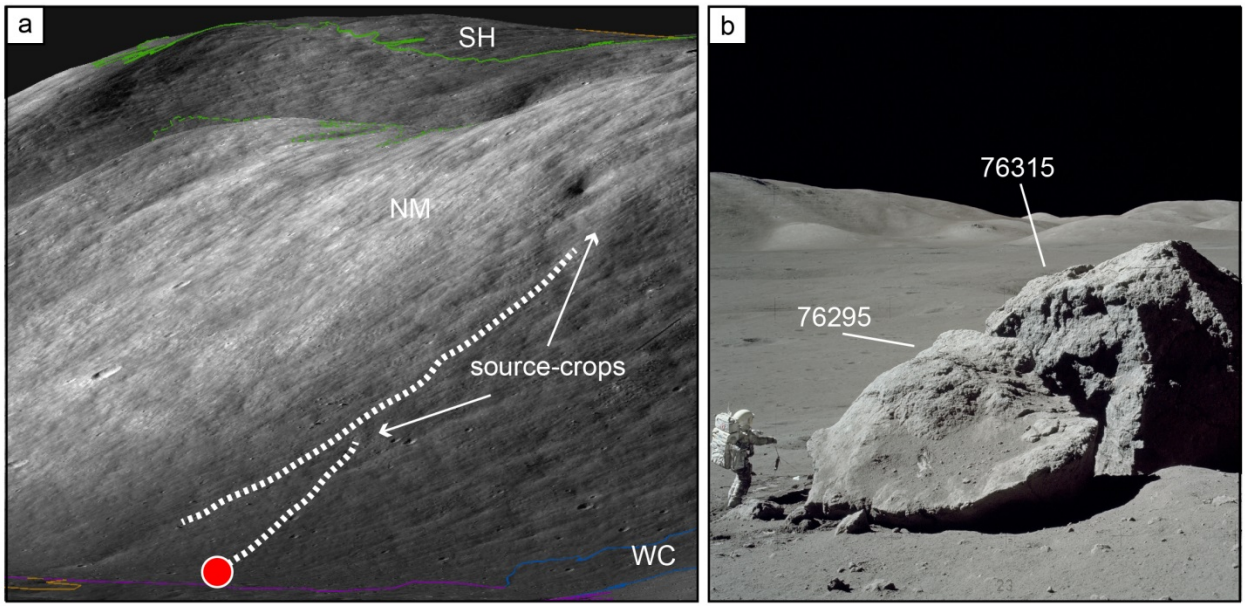

Fig. 2: (a) Perspective view of Station 6 using LROC NAC images overlain on Lunar Orbiter Laser Altimetry (LOLA) data. Samples were collected at the base of the North Massif (NM, red dot) from a boulder with a clear track from a "source-crop" about a third of the way up the massif (dashed line). The source outcrop is clearly within the NM unit and is not contaminated by Sculptured Hills (SH) or Wessex Cleft (WC) material. (b) Boulders 1 (left) and 2 (right) sampled by astronauts Cernan and Schmitt (shown, NASA photo AS17-140-21496). These boulders are interpreted to be fragments of a single boulder that rolled down the massif. Relevant samples for this study include 76295 (aphanitic melt breccia, Boulder 1) and 76315 (micropoikilitic melt breccia, Boulder 2).

similar petrography, with 50% plagioclase, 40% pyroxene (mostly low-Ca), and minor amounts of olivine, ilmenite, and other minerals [8,9]. The tan matrix of sample 76295 yielded an Ar-Ar age of 3.95 ± 0.04 Ga, and the blue-grey matrix of sample 76295 yielded an Ar-Ar age of 3.96 ± 0.04 Ga [10]. Similarly, sample 76315 yielded an Ar-Ar age of 3.900 ± 0.016 Ga [11]. The similarities in composition and age across the transitional zone suggests that both aphanitic and poikilitic breccias have the same source.

Results: A perspective view of Station 6 (Fig. 2) allows the boulders to be traced to their uphill sources that lie within the massif, not in the overlying Sculptured Hills formation. The source outcrop is not contaminated by either the darker Wessex Cleft (WC) material to the east or debris from the Sculptured Hills (SH) atop the North Massif (NM). Furthermore, there is no evidence of a fresh crater in the Sculptured Hills that could have redistributed SH material onto the slope of the NM. These high-resolution and topographically-draped images ease concerns [4] that the melts may be derived from the Sculptured Hills formation and, thus, potentially from the Imbrium basin.

Conclusions: The boulders sampled during the Apollo 17 mission originated from outcrops within massifs generally thought to have formed as a result of the Serenitatis impact event and blanketed by Serenitatis melt [e.g., 1]. If those samples were indeed produced by the Serenitatis impact event, then Serenitatis formed ~3.89 Ga in the midst of the lunar cataclysm. Three basins formed after Serenitatis and before Imbrium, which formed between 3.77 or 3.85 Ga [12], and eight basins formed prior to Serenitatis during the earlier part of the Nectarian. If, however, Serenitatis is stratigraphically older than Nectaris as has recently been suggested [4], then as many as 25 basins may have formed between Serenitatis and Imbrium, implying a much more intense basin-forming epoch than is currently recognized.

References: [1] Head J.W. (1974) *Moon*, *9*, 355–395. [2] Head J.W. (1979) *Moon Planets*, *21*, 439–462. [3] Wolfe E.W., et al. (1981) *USGS Prof. Pap. 1080*, 280 pp. [4] Spudis P.D., et al. (2011) *JGR*, *116*(E00H03). [5] Spudis P.D. and Ryder G. (1981) *Multi-ring Basins*, p. 133–148. [6] Morgan J.W., et al. (1975) *Moon*, *14*, 373–383. [7] Schmitt H.H. and Cernan E.A. (1972) *Apollo 17 Prelim. Sci. Rep.*, 5-1–5-21. [8] Lucchitta B.K. (1977) *Icarus*, *30*, 80–96. [9] Heiken G.H., et al. (1973), *NASA TMX-58116*, 56 pp. [10] Cadogan P.H. and Turner G. (1976) *LSC VII*, 2267–2285. [11] Dalrymple G. B. and Ryder G. (1996) *JGR*, *101*(E11), 26,069–26,084. [12] Stöffler D. and Ryder G. (2001) *Space Sci. Rev.*, *96*, 9–54. [

POTENTIAL SAMPLE SITES FOR SOUTH POLE–AITKEN BASIN IMPACT MELT WITHIN THE SCHRÖDINGER BASIN. Debra Hurwitz[1] and David A. Kring[1]; [1]Center for Lunar Science and Exploration, NASA Solar System Exploration Research Virtual Institute, Lunar and Planetary Institute, 3600 Bay Area Blvd., Houston, TX, 77058, (hurwitz@lpi.usra.edu)

Introduction: The intensity of impact activity during the earliest history of the Solar System is poorly constrained, because the record has been largely erased from the Earth and, thus far, we have very few samples from ancient terrains preserved on other planetary surfaces. The South Pole–Aitken (SPA) basin is the oldest basin identified on the Moon based on stratigraphic superposition and, thus, represents a key target for characterizing this earliest impact record [1,2]. To determine the absolute age of SPA, rocks that formed as a result of the impact, such as impact melt, must be identified, collected, and analyzed. In this paper, we use high-resolution images obtained by the Lunar Reconnaissance Orbiter Narrow Angle Camera (LROC NAC) to explore locations that are enriched in FeO, a signature interpreted to be SPA impact melt. One particular region of interest is southeastern Schrödinger basin (Fig. 1), which lies within the FeO anomaly associated with SPA and may provide an optimal location to address several key science priorities.

Identifying SPA Impact Melt: Petrological modeling suggests the melt sheet generated in the central transient crater during the SPA impact event would have differentiated, forming a shallow layer of FeO-enriched (~29 wt% FeO) low-Ca pyroxene (pyx) + plagioclase (plag)-bearing material beneath a layer of quenched melt [3,4]. This quenched melt would have the same bulk composition as both the initial melt within the melt sheet and the melt ejected from the transient cavity. Modeling suggests this initial melt composition contained ~15 wt% FeO and, when crystallized, would have been dominated by low- and high-Ca pyx with plag [4].

SPA Melt Preserved in SPA Interior: The iron content within SPA is currently observed to be 10-15 wt% in the basin center and 7-10 wt% in the modification zone where Schrödinger is located [5]. In the surrounding highlands, FeO content is 3-5 wt% [6,7]. The discrepancy between the modeled FeO contents in the differentiated (29 wt% FeO) or quenched (15 wt% FeO) impact melt and observed FeO contents can be resolved if SPA material was diluted by FeO-depleted impact ejecta from outside SPA. Previous estimates of the proportion of SPA-generated materials residing within the basin vary greatly from ~40% [8] to 50–80% [9] based on the volume of material balistically emplaced in SPA from younger impact events.

Using previous petrological model results with observed FeO contents, we independently estimate the amount of SPA impact melt that currently resides in the SPA interior (Fig. 2). It should be noted that ~14% of central SPA has been resurfaced by mare (~17–20 wt% FeO), material that contributes to the observed FeO signature. This contaminating material slightly decreases the apparent FeO content in central SPA to 27 wt%.

The observed FeO content of ~15 wt% in central SPA requires ~50–55 wt% contamination by FeO-depleted

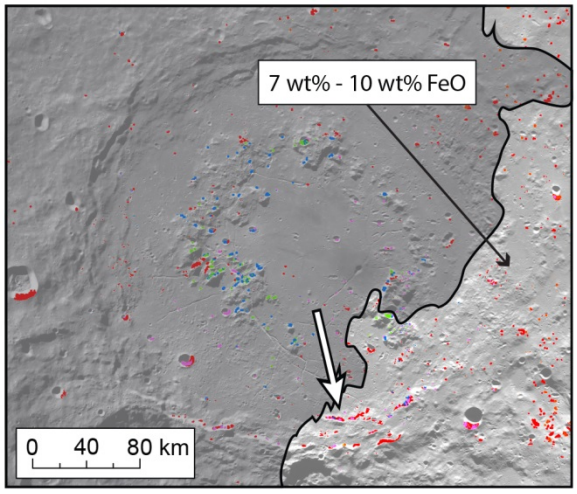

Fig. 1: Schrödinger lies in southwestern SPA. The FeO anomaly that coincides with the SPA interioris exposed in the eastern and southeastern portion of this basin. This FeO-enriched signature is interpreted to represent SPA-derived material, and samples collected within this region may be analyzed to determine the age of the oldest basin preserved on the Moon. Red and pink pixels indicate the presence of pyroxene and plagioclase [10], a signature that is consistent with quenched SPA impact melt [4].

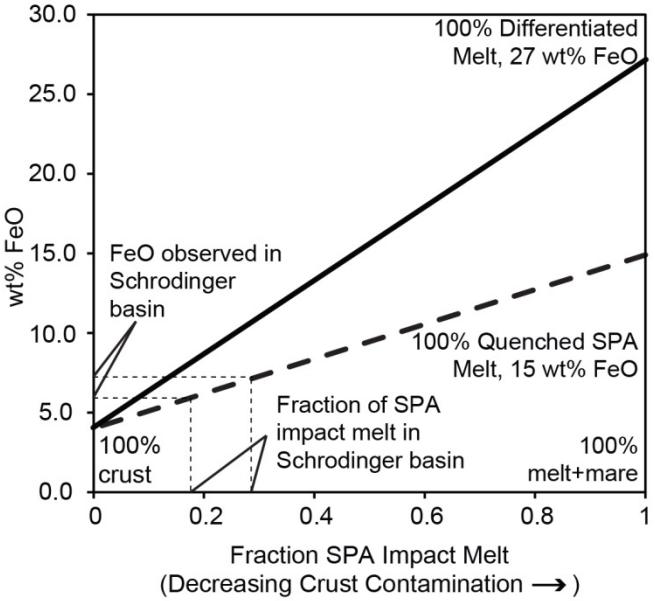

Fig. 2: Fraction of SPA impact melt as a function of FeO content. As FeO-depleted material outside SPA is redistributed within SPA in the form of ejecta of younger craters, the apparent FeO content decreases. This approach allows us to estimate the amount of SPA-derived material preserved at the surface.

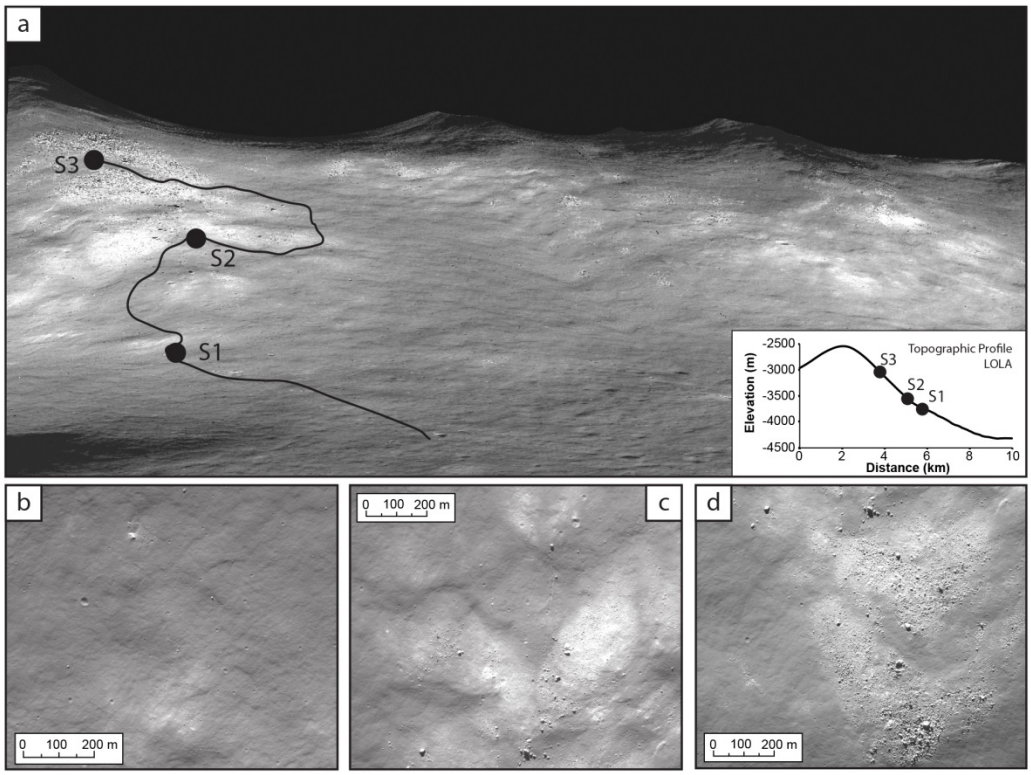

Fig. 3: (a) Perspective view of the pyx- and plag-bearing outcrop observed in a southern wall terrace of Schrödinger (white arrow in Fig. 1). White patches indicate exposed outcrop and speckled terrains indicate the presence of boulders. A ~5 km traverse (avg. slope 10^{o}) is plotted with three stations where SPA impact melt might be sampled. (b) Station 1, 600 m above the surrounding plains (see topo inset in a) has small rocks and boulders, (c) Station 2, 900 m above the plains, has more substantial outcrops and boulders with tracks, and (d) Station 3, 1500 m above the plains, contains large boulders that could be sampled to complete a cross sectional analysis of the terrace. LROC NAC images.

materials, indicating that ~45–50 wt% of the regolith is currently composed of predominantly differentiated SPA impact melt with some (14%) mare materials. The observed FeO content within southeast Schrödinger basin (~7 wt%) is consistent with ~20–30 wt% quenched SPA impact melt remaining in the local regolith (dashed lines in Fig. 2). These percentages represent a mimimum estimate for how much SPA-derived material is preserved within Schrödinger as determined by FeO content. Based on these results, regolith and, potentially, pyx- and plag-bearing outcrops within the FeO-enriched regions of Schrödinger basin contain SPA impact melt.

Analyses: Using LROC NAC images, we investigated the terrace in the south wall of Schrödinger (Fig. 1) to identify possible sources of the observed FeO-enriched, pyx- and plag-bearing signatures. Analyses indicate that outcrops and boulders contribute to these signatures and, thus, we have designed a traverse to sample those potential SPA-derived materials (Fig. 3).

The suggested 5 km traverse (Fig. 3a) directs a rover from a landing site on level, smooth plains on the basin floor to outcrops of rocks likely to contain the chemical and mineralogical signature of SPA impact melt. Three prospective stations represent locations where sampling and additional geologic investigations could be performed. Station 1 is located at an elevation ~600 m up a slope of ~9° from the adjacent plains (Fig. 3b). This site is characterized by a small outcrop and nearby boulders that appear to have slumped from the adjacent terrace. Station 2 is located ~1.2 km up a slope of ~15° from Station 1 (Fig. 3c). This site contains a much larger group of outcrops with boulders that left tracks in the loose regolith. Station 3 is located ~2 km up a slope of ~11° from Station 2 (Fig. 3d). This site is characterized by large boulders (diameter ~50 m) atop expansive outcrops. Samples collected at these stations would generate a stratigraphic sequence of the terrace, comparing rocks near the top of the terrace with those at the base. Additionally, targeted analyses of the rocks collected at all sites can provide insight into the age and composition not only of SPA but also of Schrödinger, effectively bracketing the epoch of large basin formation on the Moon.

Concluding Remarks: Rocks identified in this study represent material exposed during the Schrödinger-forming impact event, an event that likely penetrated into and redistributed material formed during the SPA-forming impact event. Sampling SPA material within Schrödinger is attractive for other reasons too. Because it is a relatively young basin with spectacular rock exposures, missions to Schrödinger can also recover samples that address a broad range of lunar science and exploration objectives (e.g., [1,2,11]).

References: [1] NRC (2007); [2] NRC (2010); [3] Vaughan W.M. et al. (2013) *Icarus*, *223*(2), 749; [4] Hurwitz D.M. and Kring D.A. (2014) *JGRP*, *119*(6) 1110; [5] Lucey P.G., et al. (1998) *JGR*, *103*(E2), 3701. [6] Korotev R.L. et al. (2003) *GCA*, *67*(24), 4895. [7] Gillis J.J. et al. (2004) *GCA*, *68*(18), 3791. [8] Cohen B.A. and Coker R.F. (2010) *NLSI 2*. [9] Petro N.E. and Pieters C.M. (2004) *JGR*, *109*(E06004). [10] Kramer G.Y. et al. (2012) *Icarus*, *223*, 131; [11] Kring D.A. (2014) *Sci. Challenges Lunar Sample Return Workshop, ESA-ESTEC*.

Stop hitting yourself: Did most terrestrial impactors originate from the terrestrial planets? Alan P. Jackson[1], Erik Asphaug[1], Linda T. Elkins-Tanton[1], David A. Minton[2], [1]School of Earth and Space Exploration, Arizona State University, Tempe, AZ 85287, [2]Department of Earth, Atmospheric & Planetary Sciences, Purdue University, West Lafayette, IN 47907

Introduction: Giant impacts are a key component of planet formation. In our own inner solar system giant impacts have been proposed to explain Mercury's large core fraction [1], the formation of the Moon [2], and the Martian hemispheric dichotomy (MHD)/Borealis basin impact [3].

Giant impacts release substantial quantities of debris. Formation of a planet like Earth results in the release of ~0.15M_E [4] – a mass greater than Mars. By comparison the Asteroid belt, including possible ancient extensions, is unlikely to have exceeded 0.01M_E since the dissipation of the solar nebula [5].

Once released into the solar system this debris will interact with the planets, primarily through re-accretion, and from the masses alone it is clear that the effects of this on the forming planets will not be insignificant.

Cratering: A principal role of giant impact debris is as a source of impactors onto the terrestrial planets. On worlds with old surfaces, such as the Moon, Mars and Mercury, this can leave populations of impact craters that will still be visible today. Indeed in light of the quantities of debris released giant impact debris may have been the dominant source of impactors in the early solar system.

Magma oceans: A consideration for re-impacting giant impact debris is that a body that has recently undergone a giant impact will be at least partially covered by a magma ocean. Debris re-impacts will only be recorded if they strike a solid surface, so if we want to investigate cratering records we must account for the magma ocean solidification time on the progenitor body. Impacts can also influence the solidification process, both through the input of accretion energy as an additional heat source, and on smaller bodies like the Moon and Mercury, by disrupting the forming crust allowing the magma ocean to cool faster.

Moon-formation and the MHD impact: The two most well constrained giant impacts in the inner solar system are the formation of the Moon and the MHD/Borealis impact. A wide range of evidence suggests that Moon-formation occurred relatively late, around 50-150Myr after the first solids [e.g. 6, 7], such that we can expect other bodies to have had solid surfaces at this time. The timing of the MHD impact is less certain, however it only melted the northern hemisphere [3], and the hemispheric dichotomy would have been erased if Mars suffered another giant impact later.

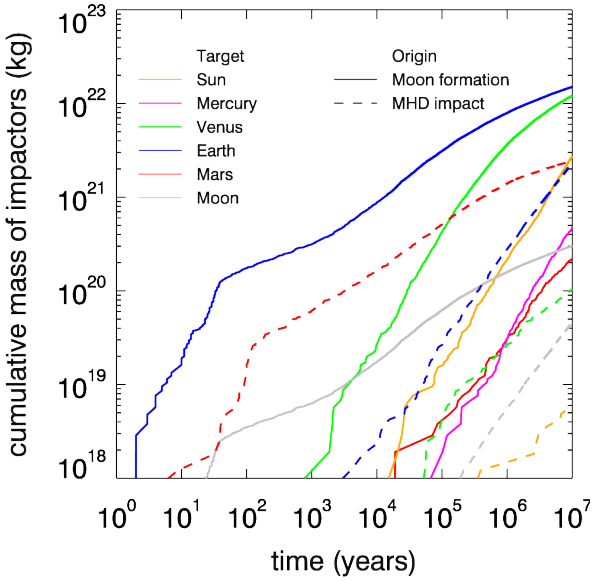

Fig. 1: Cumulative mass of impactors received from the Moon-forming and MHD impacts. Moon-formation releases 10^{23} kg of debris while the MHD impact release 2.2×10^{22} kg. A simple size distribution with $n(D)\propto D^{-3.5}$ and maximum size 500km is assumed. The Earth-Moon accretion ratio is set to be 50 for illustrative purposes.

We thus focus on these two impacts as the best candidates to have left cratering signatures in the inner solar system that can be seen today, particularly on the Moon and Mars. We suggest that many of the earliest craters on these two bodies may be the result of re-impacting debris from their respective giant impacts. Fig. 1 shows the masses of impactors received by various solar system bodies from the Moon-forming and MHD impacts as a function of time after the initial impact. Collisional evolution of the debris is neglected here.

References: [1] Benz W., et al (2007) *Space Sci. Rev.*, *132*, 189–202. [2] Canup R.M. (2004) *ARA&A*, *42*, 441-475. [3] Marinova M.M., et al. (2011) *Icaurs*, *221*, 960–985. [4] Stewart S.T., Leinhardt Z.M., (2012) *AJ*, *751*, 32. [5] Minton D.A., Malhotra R., (2010) *Icarus*, *207*, 744-757. [6] Halliday, A.N. (2000) *Earth & Planet. Sci. Lett.*, *176*, 17-30. [7] Kleine T. et al. (2005) *Science*, *310*, 1671–1674.

Compositions of the terrestrial planets in the Grand Tack model. S. A. Jacobson[1,2], E. D. Young[3], D. C. Rubie[2], and A. Morbidelli[1], [1]Observatoire de la Côte d'Azur (seth.jacobson@oca.eu), [2]Universtät Bayreuth, [3]University of California at Los Angeles.

The isotopic compositions of the terrestrial planets are a direct consequence of their accretion histories. The large dissimilarity between Earth, Mars and many of the meteoritic samples suggests that the protoplanetary disk from which the terrestrial planets grew had a diversity of isotopic compositions. Confoudingly, it appears that the giant impact model, which best reproduces the dynamical and chemical constraints, to create the Moon suggests that the last giant impactor, Theia, had nearly the same isotopic composition as the Earth. Other suggested models either require potentially unlikely evection resonance capture or may create too much mantle mixing.

We explore the consequences of matching oxygen, titanium and chromium isotopic compositions of the Earth and Mars using protoplanetary disk models for each of those systems. For every system, we explore a simple gradient model. For oxygen, we also study a more sophisticated model that assumes a specific oxygen isotopic composition for the silicates, iron oxides and water in the disk. The oxygen composition of any given body is determined by the mass ratio of these components.

Given these models, the composition of Theia can be compared directly to the Earth. The compositions of other meteorite samples such as aubrites, angrites, enstatites and HEDs can also be placed within the disk.

The Density and Porosity of Lunar Impact Breccias and Impact Melt Rocks and Implications for Gravity Modeling of Impact Basin Structure

Walter S. Kiefer[1], Robert J. Macke[2], Daniel T. Britt[3], Anthony J. Irving[4], and Guy J. Consolmagno[2], [1]Lunar and Planetary Institute, 3600 Bay Area Blvd., Houston TX 77058, kiefer@lpi.usra.edu , [2]Vatican Observatory, V-00120 Vatican City State, [3]Dept. of Physics, University of Central Florida, Orlando FL, [4]Dept. of Earth and Space Sciences, University of Washington, Seattle WA.

Introduction

NASA's GRAIL mission has provided a highly detailed map of the Moon's gravity field, resulting in fundamental new insights into lunar crustal structure. One important aspect of study involves lunar impact basins. GRAIL data has been used to infer the thickness of the crust in the center of impact basins and the presence of a low bulk density, high porosity collar of ejecta surrounding large basins [1, 2].

Our previous measurements of lunar density and porosity [3] have been an important contribution to studies of lunar gravity data [1, 4, 5] and are essential for interpreting the gravity structure of lunar impact basins. For example, the density of the impact melt sheet in the basin center is a key parameter in estimating the thickness of the crust within the basin, which in turn affects estimates of impactor energy and of post-impact mascon uplift. Our results also have implications for hydrocode models of large impacts. These results for impact breccias include our first measurements of bulk volume by laser scanning.

Methods

We measured both the bulk density, ρ_{bulk}, and the grain density, ρ_{grain}, using non-contaiminating and non-destructive methods. The bulk density is based on the entire volume of the sample, including any pore space. The grain density is based solely on the solid material, excluding the pore space. Bulk density is important for calculation of gravity anomalies, and grain density is used for studying systematic trends in density as a function of rock composition. Porosity is calculated as $P=1-(\rho_{bulk}/\rho_{grain})$. Grain volume was measured by ideal gas pycnometry [6, 7]. Errors are determined by repeated measurements of each sample and are typically 10-20 kg m^{-3} (< 0.6%) for grain density provided that the sample mass exceeds 10 gm. Bulk volume was measured either by laser scanning (15 samples) or by immersion in glass beads (3 samples) [8]. Laser scanning produces results with smaller uncertaintites and less fear of contamination than for bead immersion. Scanning also permits measurements of samples that are too friable or too large to measure by bead immersion.

Samples

We report measurements of the density and porosity of 20 rocks from the Apollo 14, 15, 16, and 17 landing sites that are impact breccias and impact melt rocks formed in large basin-forming impacts. Crystalline matrix breccias and an impact melt rock from Apollo 14 [9, 10] are samples of the Fra Mauro Formation, which is Imbrium basin ejecta. We have measured crystalline matrix breccias collected at a range of distances from the rim of Cone Crater, corresponding to a vertical sample through about 70 meters of the Fra Mauro Formation's stratigraphy. Apollo 15 impact melt rocks with norite clasts represent the melt sheet at the rim of the Imbrium basin [11]. Apollo 16 samples include material from both the Cayley Formation and the Descartes Formation and likely represent ejecta from both the Nectaris and Imbrium basins [12-14]. Excavation of material by both the North Ray and South Ray Craters provides sampling through about 200 meters of the local stratigraphy. Apollo 17 samples include both aphanitic and micropoikilitic impact melt rocks from the North and South Massifs [15, 16]. Chemical and petrological differences among the Apollo 17 sample suite have been interpreted as requiring the presence of material from multiple impact events [17], although the abundances of highly siderophile elements in these samples permit a single impactor [18]. Possible basin sources include Serenitatis, Imbrium [19], and possibly Crisium.

We have also made measurements of many lunar meteorites. Some of these, such as Northwest Africa 482 [20] and Sayh al Uhaymir 300 [21] are impact melt breccias that are likely the product of large impact events. Because of the lack of field context for the origin of these samples, we have not incorporated them into the current study, but those measurements do not alter any of the conclusions described here.

Results: Bulk Densities and Porosities

Figure 1 shows the bulk densities for these samples. Half of the samples occur in a narrow peak at low density (mean 2490 kg m^{-3}, range 2440 to 2520 kg m^{-3}). Many of these samples are clast rich, and the samples with impact melt are highly vesicular. These samples have high porosities (mean 16.5%, range 11.5-21.1%). This is similar to the range of bulk densities and porosities observed around basins such as Orientale and Moscoviense [1].

There is also a more dispersed distribution of higher bulk densities (mean 2720 kg m^{-3}, range 2590-2830 kg m^{-3}). The high bulk density samples have lower porosity (mean 8.8%, range 5.5-15.8%). These samples are dominated by impact melt and the variation in density depends at least in part on the degree of sample vesicularity.

Estimates of the Moon's crustal thickness using GRAIL data depend on the assumed density difference between the crust and mantle. Initial GRAIL results used a crustal density of 2550 kg m^{-3} [1], which is appropriate for most of the feldspathic highlands but may not be correct for basin melt sheets. However, if instead one uses an average bulk density of 2720 kg m^{-3} for the central melt sheet, the inferred crustal thickness increases by 25%. If vesicularity decreases with depth (pressure), then the higher average bulk density would further increase the inferred melt sheet thickness. In turn, this would increase the impact energy required to produce the necessary melt volume.

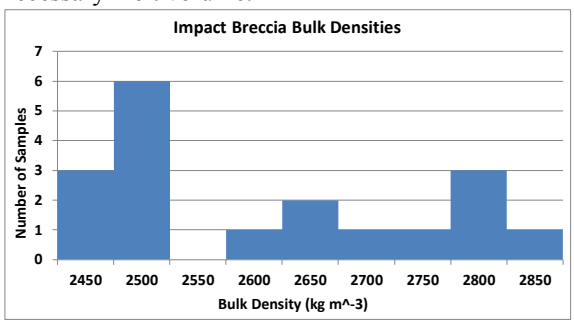

Figure 1: Histogram of impact breccia and melt rock bulk densities. Each bin is 50 kg m^{-3} wide, e.g., the 2500 kg m^{-3} bin includes values from 2475 to 2525 kg m^{-3}.

Results: Melt Sheet Grain Densities

Two competing models for basin melt sheet composition exist. Hydrocode simulations find that most or all of the crust is ejected from the basin (depending on the pre-impact crustal thickness) and that the impact melt pool is composed primarily of mantle material [22, 23]. Alternatively, petrological models of impact melt sheet differentiation assume that about half of the material incorporated into the melt sheet is from the crust [24, 25].

Our results for the grain densities of basin impact breccias and melt rocks show a strong peak between 2990 and 3100 kg m^{-3} (Figure 2). This peak includes material from the Imbrium and Serenitatis rims as well as distal basin ejecta from Apollos 14 and 16. This range of grain densities is consistent with the depth-averaged range of densities predicted by the melt sheet differentiation models [24, 25]. Grain densities between 2800 and 2900 kg m^{-3} in Figure 2 may represent samples from the upper part of a differentiated melt sheet. None of our samples show grain densities of ~3300 kg m^{-3} that would be indicative of a purely mantle origin. This is consistent with the composition of these samples, with Al_2O_3 > 16 weight %, which requires a significant crustal component in the melt. A speculative interpretation is that the observed impact melt grain densities and compositions are due to some form of turbulent mixing between crust and mantle during the initial impact phase that can not be captured in current hydrocode models because of grid resolution and uncertainties in the high stress rheology of shock melts.

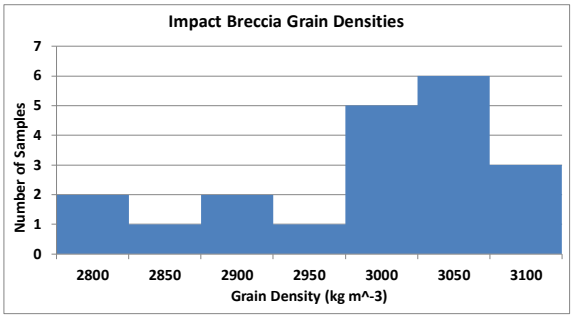

Figure 2: Histogram of impact breccia and melt rock grain densities.

References [1] Wieczorek et al., *Science* 339, 671-675, 2013. [2] Zuber et al., Fall AGU abstract G22-05, 2014. [3] Kiefer et al., *Geophys. Res. Lett.* 39, 2012GL051319, 2012. [4] Kiefer, *J. Geophys. Res.: Planets* 118, 733-745, 2013. [5] Besserer et al., *Geophys. Res. Lett.* 41, 5771-5777, 2014. [6] Consolmagno et al., *Chemie der Erde* 68, 1-29, 2008. [7] Macke et al., *LPSC* 43, abstract 1398, 2013. [8] Macke et al., *Planet. Space Sci.* 58, 421-426, 2010. [9] Simonds et al., *Proc. Lun. Sci. Conf.* 8, 1869-1893, 1977. [10] Lofgren, *Proc. Lun. Sci. Conf.* 8, 2079-2095, 1977. [11] Ryder and Bower, *Proc. Lun. Sci. Conf.* 8, 1895-1923, 1977. [12] Stöffler et al., *Proc. Lun. Planet. Sci.* 12B, 185-207, 1981. [13] James, *Proc. Lun. Planet. Sci.* 12B, 209-233, 1981. [14] Spudis, *Proc. Lun. Planet. Sci.* 15, C95-C107, 1984. [15] Simonds, *Proc. Lun. Sci. Conf.* 6, 641-672, 1975. [16] Dymek et al., *Proc. Lun. Sci. Conf.* 7, 2335-2378, 1976. [17] Spudis and Ryder, *Multi-ring Basins, Proc. Lunar. Planet. Sci.* 12A, 133-148, 1981. [18] Sharp et al., *Geochim. Cosmochim. Acta* 131, 62-80, 2014. [19] Spudis et al., *J. Geophys. Res. 116*, 2011JE003903, 2011. [20] Daubar et al., *Meteoritics Planet. Sci.* 37, 1797-1813, 2002. [21] Hudgins et al., *Meteoritics Planet. Sci.* 42, 1763-1779, 2007. [22] Potter et al., *J. Geophys. Res.: Planets* 118, 963-979, 2013. [23] Melosh et al., *Science* 340, 1552-1555, 2013. [24] Vaughan et al., *Icarus* 223, 749-765, 2013. [25] Hurwitz and Kring, *J. Geophys. Res.: Planets* 119, 1110-1133, 2014.

REMNANTS OF EARLY ARCHEAN IMPACT EVENTS ON EARTH: NEW STUDIES ON SPHERULE LAYERS FROM THE BARBERTON MOUNTAIN LAND, SOUTH AFRICA. Christian Koeberl[1,2], Toni Schulz[2], Seda Özdemir[2], Tanja Mohr-Westheide[3], Wolf Uwe Reimold[3,4], and Axel Hofmann[5]. [1]Natural History Museum, Burgring 7, A-1010 Vienna, Austria (christian.koeberl@univie.ac.at); [2]Department of Lithospheric Research, University of Vienna, Althanstrase 14, A-1090 Vienna, Austria; [3]Museum für Naturkunde Berlin, Invalidenstraße 43, 10115 Berlin, Germany; [4]Humboldt Universität zu Berlin, Unter den Linden 6, 10099 Berlin, Germany; [5]Department of Geology, University of Johannesburg, Johannesburg, South Africa.

Introduction: If a late heavy bombardment during the period from about 3.8 to 4 billion years ago occurred on the Moon, the Earth must have been subjected to an impact flux more intense than that recorded on the Moon. The consequences for the Earth must have been devastating, and may have included partial or total remelting of the crust. So far, no unequivocal record of a late heavy bombardment on the early Earth has been found. The earliest rocks on Earth date back to slightly after the end of the heavy bombardment, although there are relict zircons up to 4.4 Ga old (in which no unambiguous impact-characteristic shock features have yet been found). In terms of evidence for impact on Earth, the first solid evidence exists in the form of various spherule layers found in South Africa and Australia with ages between about 3.2-3.4 and 2.5 Ga; these layers represent several (the exact number is still unknown) large-scale impact events. The oldest documented (and preserved) impact structures on Earth have ages of 2.02 and 1.86 billion years. Thus, the impact record for more than half of the geological history of the Earth is extremely poor, and there is little information about the impact record and its effects during the first 2.5 billion years of Earth history.

Impact structures or ejecta are commonly identified from specific characteristics, including either the presence of evidence for shock metamorphism, and/or geochemical indications of the presence of an extraterrestrial component. Only elements that have high abundances in meteorites, but low abundances in terrestrial crustal and mantle-derived rocks are useful for such studies (such as the PGEs). Elevated abundances of siderophile elements in impact melt rocks or breccias (and impact ejecta), compared to target rock abundances, can be indicative of the presence of either a chondritic or an iron meteoritic component. There are, however, cases in which the PGE interelement abundances might be fractionated.

These problems can, in part, be overcome by the use of isotopic tracers for extraterrestrial components. Most prominent among these are the Os and Cr isotopic methods. The Os isotopic method, which is based on the decay of Re-187 to Os-187, is very sensitive and can detect sub-percent levels of extraterrestrial component in impact breccias and melt rocks, but it is not possible to determine a meteorite type.

In contrast, the Cr isotopic method relies on the fact that all terrestrial rocks have a uniform Cr isotopic composition, whereas different meteorite types have different isotopic anomalies. The Cr isotopic method is, thus, selective not only regarding the Cr source (terrestrial vs. extraterrestrial), but also regarding the meteorite type.

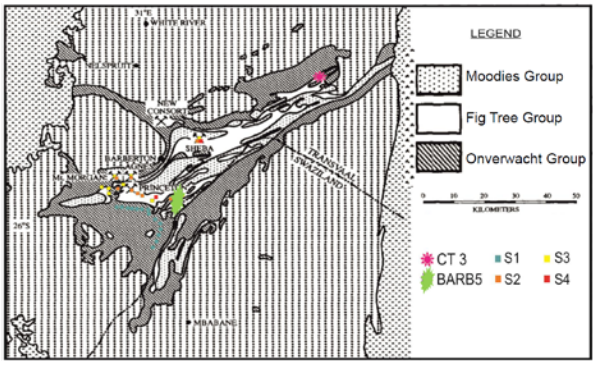

Fig. 1. Location of new spherule layer locations BARB5 (ICDP drill core) and CT3 in the Barberton Mountain Land.

Barberton Greenstone Belt Spherule Layers: Four distinct spherule horizons in the Barberton Greenstone Belt (BGB), South Africa (designated S1 to S4), with ages between about 3.5 and 3.2 Ga, have been proposed as being of impact origin (e.g., [1]). The spherules are mostly spherical to ovoid particles, up to a few mm across, of quenched melt droplets that supposedly formed by condensation from vapor clouds. The spherule layers are coarse-grained and have been interpreted to reflect high-energy depositional events in otherwise low-energy, quiet water environments. The original mineralogical and chemical composition of the spherules has been almost completely changed by alteration. The stratigraphic positions of these layers at different geographic locations are difficult to correlate and the possibility exists that some of the layers represent tectonic duplication. Some samples in these spherule layers show extreme enrichments in the PGEs (in some cases far exceeding the PGE abundances found in chondritic meteorites), unlike modern impact ejecta

deposits. The correlation between the abundances of iridium and arsenic, a very mobile element, in samples from the Barberton spherule layers, all of which have been subject to pervasive transformation into secondary mineral assemblages, indicates remobilization of both elements; this means that the PGE signature in these samples is not primary (e.g., [2]). On the other hand, chromium isotopic anomalies in samples from several of these layers support the presence of an extraterrestrial component [3]. A comprehensive study of sedimentary, petrographic, mineralogical, and geochemical characteristics from a set of new samples of spherule layers between 510 and 512 m depth in the 760-m-long ICDP drill core BARB 5 from the Barite Valley Syncline [4], as well as samples from the CT3 location [5] of the northern Barberton Greenstone Belt has been carried out.

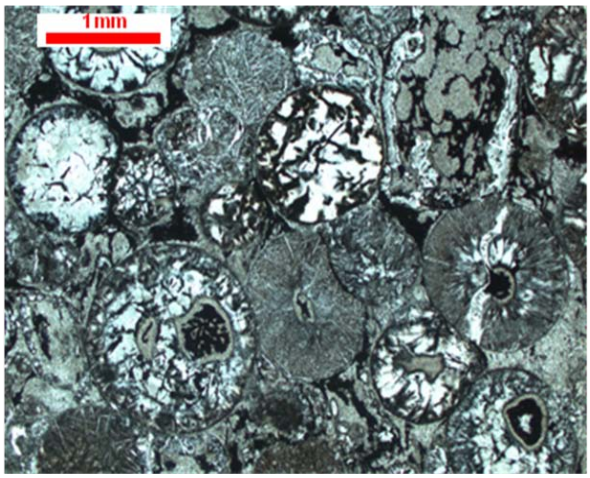

Fig. 2: Examples of spherules in CT3 core, depth 147.5 m.

At BARB5, four new spherule layers, each about 4 cm thick, were identified in the core interval between 511.29 and 511.51 m depth, all separated by shale and chert within the 3.26 to 3.23 Ga old middle Mapepe Formation of the Fig Tree Group [6]. Stratigraphically these spherule layers may belong to the same interval as the previously studied S3 and/or S4 layers. Present day $^{187}Os/^{188}Os$ ratios are in part subchondritic for the spherule horizons (~0.106 to ~0.116) but back-calculated values are indistinguishable from the chondritic $^{187}Os/^{188}Os$ evolution line (~0.105 to ~0.112, compared to ~0.105 for chondrites at ~3.4 Ga). Possible Re loss during hydrothermal or other alteration may obscure the real initial values in these samples, which may also explain the subchondritic $^{187}Re/^{188}Os$ ratios in some samples.

The CT3 drill core contains some 17 spherule layers over a stratigraphic interval of 150 m, occurring along the transition zone between the Onverwacht and Fig Tree groups [6]). Some of these layers might represent tectonic duplication. It is possible, but not yet confirmed, that (some of?) the CT3 layers are correlated to the S2 layer, which occurs in the same stratigraphic unit. Ir and Os contents are comparably low in the country rocks, ranging from ~0.12 to 0.97 ppb for Ir and ~0.25 to 1.3 ppb for Os (which is still higher than average modern continental crust), and are elevated in the spherule horizons (between ~6 and 2068 ppb Ir and ~3 ppb and 4312 ppb Os); similarly, Cr concentrations are low in the spherule-free shale and chert intercalations. The isotopic ratios of $^{187}Os/^{188}Os$ and $^{187}Re/^{188}Os$ vary between the country rocks and spherule horizons (from 0.21 to 1.13 for $^{187}Os/^{188}Os$ and ~4.5 to 99.6 for $^{187}Re/^{188}Os$ ratios in country rocks compared to 0.11 to 0.17 for $^{187}Os/^{188}Os$ and ~0.06 to ~0.33 for $^{187}Re/^{188}Os$ ratios in the spherule horizons).

Conclusions: Our petrographic and geochemical data indicate strong hydrothermal overprint for all lithologies in the studied section of the BARB 5 core. Sulfide mineralization is of secondary origin and may be related to chemical alteration and metamorphism. High Zn concentrations frequently observed along cataclased spinel grains could relate to late secondary overprint. High abundances of the siderophile elements (Ni, Co, Ir, Os, Cr, and Au) are thought to reflect extraterrestrial components. Some high-PGE phases, maybe representing the PGE carriers, have been identified in some samples [7]. Mechanical or chemical concentration of such phases may account for the extreme enrichments in the PGEs that are observed in some samples. Osmium data reveal a trend between the spherule-free horizons (intercalating the spherule layers) and spherule-matrix aggregates. Whereas the former typically exhibit elevated $^{187}Os/^{188}Os$ ratios of up to ~1.2 and low Os and Ir concentrations below several hundred ppt, spherule-matrix aggregates tend to be less radiogenic (down to subchondritic present day $^{187}Os/^{188}Os$ ratios) with Os and Ir concentrations as high as in chondrites. Chromium-Ir correlations for CT3 and BARB5 samples mirror earlier results on S1 to S4 layers and can be interpreted in favor of an impact origin of the investigated spherule horizons. Our ongoing studies provide additional constraints on the early terrestrial impact record.

References: [1] Lowe D.R. et al. (2003) *Astrobiology* 3, 7–48. [2] Koeberl C. and Reimold W.U. (1995) *Precambrian Research* 74, 1–33. [3] Kyte F.T. et al. (2003) *Geology* 31, 283–286. [4] Mohr-Westheide T. et al. (2014) *LPSC 45,* Abstract #1356. [5] Özdemir S. et al. (2014) *77th Meteoritical Society Annual Meeting*, Abstract #5037. [6] Hoehnel D. et al. (2014) *77th Meteoritical Society Annual Meeting*, Abstract #5081. [7] Mohr-Westheide T. (2014) *77th Meteoritical Society Annual Meeting*, Abstract #5235.

WAS AN EPOCH OF LUNAR MAGMATISM TRIGGERED BY THE SOUTH POLE-AITKEN BASIN IMPACT? David A. Kring[1,2] , Patrick J. McGovern[1,2], Ross W. K. Potter[1,2], Gareth S. Collins[3], Marion L. Grange[4], and Alexander A. Nemchin[4], [1]Center for Lunar Science and Exploration, USRA Lunar and Planetary Institute, 3600 Bay Area Blvd., Houston TX 77058, [2]NASA Solar System Exploration Research Virtual Institute, [3]Impacts and Astromaterials Research Centre, Dept. Earth Science and Engineering, Imperial College, London UK, [4]Department of Applied Geology, Western Australian School of Mines, Curtin University, Western Australia (kring@lpi.usra.edu).

Introduction: A compilation (Fig. 1) of zircon analyses [1-6] indicate there was a particularly large magmatic epoch 4.30-4.36 Ga. Zircon is found in a diverse suite of magmatic lithologies (anorthosite, troctolite, gabbro-norite, quartz-monzodiorite, granites, felsites) and in impact breccias that incorporate clasts of those lithologies. The zircon crystals are derived from Apollo landing sites spanning a distance of 1758 km (Apollo 12 to Apollo 17), an area of 878,750 km^2, and involve impact basin deposits that were excavated from depths up to ~60 km (by the Imbrium impact) – providing extensive sampling of magmatic rocks in the nearside crust. The 4.30-4.36 Ga peak in zircon ages is similar to several other ages [7-9], including an urKREEP average model age of 4.368 ± 0.029 Ga [10]. The latter has been interpreted to represent the solidification of the lunar magma ocean, although it is difficult to reconcile that model with ancient lunar zircon ages (up to 4.417 ± 0.007 Ga) without a very complicated petrogenetic model [10].

Lunar Magmatism Hypothesis (LMH): As an alternative, we hypothesize that the magmatic epoch was triggered by the immense, 2500-km-diameter South Pole-Aitken basin impact on the lunar farside, which is the oldest, largest, and deepest impact basin on the Moon. Hydrocode simulations of the South Pole-Aitken impact [11] indicate mantle melting on the farside, leading to an immense differentiated magmatic system [12,13]. Simulations [11,14] also show the impact generated sharp pressure anomalies in the mantle beneath the lunar nearside crust and correspondingly large displacements, strains, and stress changes. Additional modeling shows that those pressure anomalies would have accelerated the ascent of mantle partial melts, producing a concentrated magmatic epoch among nearside lithologies too.

Modeling the SPA Impact and the Magmatic Response. The observed dimensions, gravity structure, and distribution of lithologies of the South Pole-Aitken basin are best fit with a hydrocode impact model using a 170 km diameter asteroid hitting the Moon vertically at 10 km/s [11], or one slightly larger for an oblique impact [14]. In this model, the pre-impact thermal structure of the Moon is such that the lower crust and upper mantle temperatures are at or very close to the solidus between a depth of ~25 and 560 km – the vestige of the Moon's magma ocean.

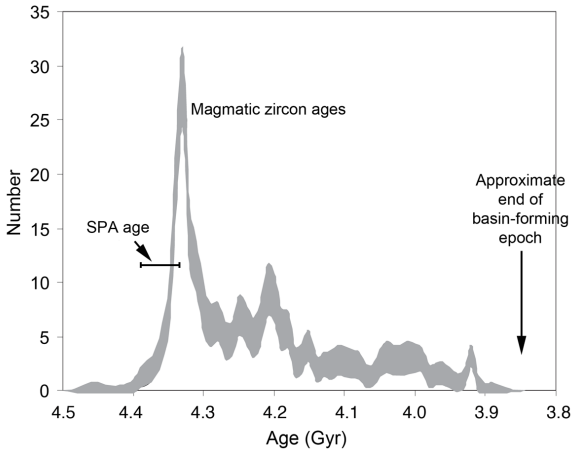

Fig. 1. Distribution of zircon crystallization ages that reflect the production of magma on the Moon [1-6]; the estimated SPA age is from [22].

Here we have extended our analysis of those hydrocode results to evaluate the consequences of the impact on the entire sphere of the Moon, including the upper mantle beneath the nearside crust. Pressure and stress waves generated by the impact event radiated around the Moon, beginning with the shock wave and followed by a train of high-amplitude surface waves. The pressure in the initial shock wave exceeded ~400 MPa (above the lithostatic load) in the upper mantle across the entire Moon; wave focusing would have increased the stress magnitude in a zone around the impact antipode by perhaps as much as an order of magnitude (Fig. 2), depending on the angle of impact [14] and asymmetries in the Moon's figure and internal structure at the time of impact [15]. The consequences of the South Pole-Aitken basin impact were felt around the Moon for hours after the initial shock wave arrived. In particular, the presence of a weak asthenosphere leads to large deformation of the crust during the formation of the basin. Oscillations of the crater floor inside the basin send a series of high-amplitude gravity waves around the Moon, causing displacements of ~1 km and shear stresses sufficient to cause pervasive fracturing of the crust.

The globally distributed dynamic stress changes would have had a profound effect on melt migration by creating new pathways and enhancing forces that drive

melt ascent. In addition to pervasive large-scale fracturing [14], the impact would have catalyzed melt migration at all scales. Estimates of magma ascent velocity and effective buoyancy in dikes [16,17] can be derived from vertical gradients in horizontal stresses via analysis of pressure balances across the dike [18]. For typical locations on the lunar nearside, the averaged stress state during a vertical opening event indicates positive velocities in the lower crust and negative velocities in the upper crust. These findings predict the formation of an intrusive horizon in the lower crust.

Discussion and Final Observations: Thus, we propose the South Pole-Aitken impact mobilized melt around the whole Moon, particularly beneath the antipodal lunar nearside surface that is the provenance of the Apollo sample suite, accounting for the observed spike in magmatic zircon ages. Effectively, the process has the capacity to perturb the normal ascent of partial mantle melts and accelerate them upward, creating a magmatic pulse or cluster of magmatic events over a timescale of several millions of years to produce the observed age spike (Fig. 1).

This process is distinct from the proposed concept of decompression melting beneath the floor of an impact crater [19], a process that fails to generate melt in most impact events [20], with the possible exception of the largest basin-size events. While that process and the processes described here may have enhanced the mobility of melt beneath the South Pole-Aitken impact site, only the process described here has the capacity to generate a period of enhanced magmatism on the lunar nearside.

The 10 km/s impact velocity in our hydrocode model of the South Pole-Aitken basin impact is consistent with an independent assessment of average impact velocities (9 km/s) at that time in lunar history based on the size distribution of craters [21]. A calibration of crater densities on the most ancient portions of the floor of South Pole-Aitken basin also implies an age of 4.33 to 4.39 Ga [22], consistent with the timing needed to generate the subsequent magmatic pulse (Fig. 1). Confirming an age of the South Pole-Aitken basin will be a good test of our hypothesis and is one more reason for a South Pole-Aitken basin sample return mission [23,24].

Interestingly, recent analyses of the production of impact melt within the South Pole-Aitken basin [13] suggest the basin-forming impact event occurred prior to mantle overturn on the Moon. If so, then the same mantle perturbations proposed here to produce an enhanced period of magmatism may have also provided the activation energy needed to initiate that overturn, produce adiabatic melting [25], and further enhanced the amount of magmatism.

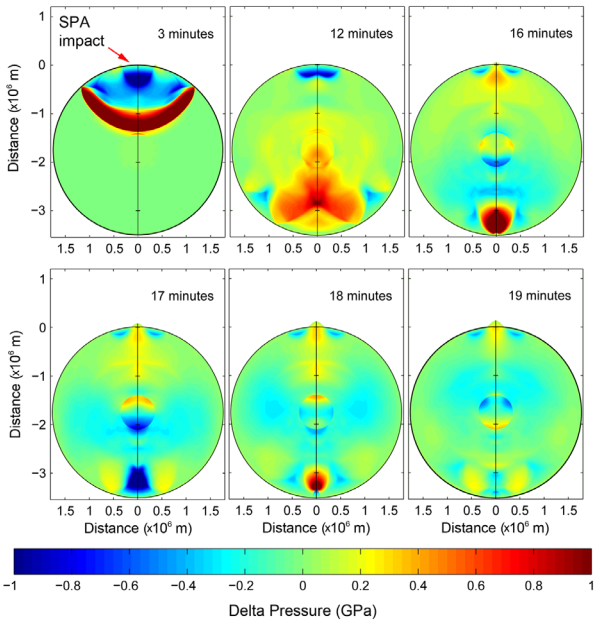

Fig. 2. Pressure variation relative to the initial lithostatic pressure at 3, 12, 16, 17, 18, and 19 minutes after impact. The nearside is at the bottom of each panel.

References: [1] Nemchin A. A. et al. (2008) *Geochim. Cosmochim. Acta, 72*, 668-689. [2] Grange M. L. et al. (2009) *Geochim. Cosmochim. Acta, 73*, 3093-3107. [3] Taylor D. J. et al. (2009) *Earth Planet. Sci. Lett., 279*, 157-164. [4] Nemchin A. A. et al. (2011) *Austral. J. Earth Sci., 59-2*, 277-290. [5] Liu D. et al. (2012) *Earth Planet. Sci. Lett., 319-320*, 277-286. [6] Zhang A. C. et al. (2012) *Geochim. Cosmochim. Acta, 95*, 1-14. [7] Borg L. E. et al. (2011) *Nature, 477*, 70-73. [8] Brandon A. D. et al. (2009) *Geochim. Cosmochim. Acta, 73*, 6421-6445. [9] McLeod C. L. et al. (2014) *Earth Planet. Sci. Lett., 398*, 179-189. [10] Gaffney A. M. and Borg L. E. (2014) *Geochim. Cosmochim. Acta, 140*, 227-240. [11] Potter R. W. K. et al. (2012) *Icarus, 220*, 730-743. [12] Vaughn W. M. and Head J.W. (2013) *Planet. Space. Sci., 91*, 101-106. [13] Hurwitz D. M. and Kring D. A. (2014) *J. Geophys. Res., 119*, 1110-1133. [14] Schultz P. H. and Crawford D. A. (2011) *GSA Spec. Pap., 477*, 141-159. [15] Meschede M. A. et al. (2011) *Geophys. J. Int., 187*, 529-537. [16] McGovern P. J. et al. (2013) *J. Geophys. Res., 118*, doi:10.1002/2013JE004455. [17] McGovern P. J. et al. (2013) *LPS XVIV*, Abstract #3055. [18] Rubin A. M. (1995) *Ann. Rev. Earth Planet. Sci., 23*, 287-336. [19] Jones A. P. et al. (2002) *Earth Planet. Sci. Lett., 202*, 551-561. [20] Ivanov B. A. and Melosh H. J. (2003) *Geology, 31*, 869-872. [21] Marchi S. et al. (2012) *Earth Planet. Sci. Lett., 325-326*, 27-38. [22] Morbidelli A. et al. (2012) *Earth Planet. Sci. Lett., 355-356*, 144-151. [23] National Research Council, *The Scientific Context for Exploration of the Moon*, 107p. [24] National Research Council, *Vision and Voyages for Planetary Sciences in the Decade 2013-2022*, 382p. [25] Elkins-Tanton L. T. et al. (2011) *Earth Planet. Sci. Lett., 204*, 326-336.

THE TERRESTRIAL RECORD OF AN EXTENDED LATE HEAVY BOMBARDMENT. Donald R. Lowe[1] and Gary R. Byerly[2], [1]Dept. of Geological and Environmental Sciences, Stanford University, Stanford, CA 94305 USA, drlowe@stanford.edu. [2]Dept.of Geology and Geophysics, Louisiana State University, Baton Rouge, LA 70803 USA, glbyer@lsu.edu

Introduction: While the primary record of the early bombardment history of the Solar System is preserved on extraterrestrial bodies, it should not be overlooked that there exists a terrestrial record of giant impacts until at least 3.2 billion years ago (Ga). That record includes 8 major impact layers 3.2 to 3.5 Ga discovered and described by the authors from Archean rocks in the Barberton greenstone belt (BGB), South Africa, and Pilbara Block, Western Australia [1,2,3]. These layers have led to the inference that the terrestrial flux of large asteroids during this interval was perhaps several orders of magnitude greater than that of the modern era and that the Late Heavy Bombardment (LHB) had a very long tail that was still depositing large bolides on the terrestrial surface at 3.2 Ga [4,5,6,7]. The known layers represent distal settings, far removed from the impact sites, and contain distinctive spherical particles (spherules) formed by the condensation and solidification of impact-generated rock vapor clouds [2,3]. These impacts also produced globe-encircling tsunamis and widely fractured surface rock layers. Several spherule beds coincide with stratigraphic horizons marking major tectonic events, suggesting that the Earth's crustal development was probably influenced or controlled by impacts to at least 3.2 Ga.

Barberton spherule beds: The BGB spherule beds range from 3.23 to 3.47 Ga in age (Fig. 1). Individual layers reach up to 5 m thick but most have been widely removed by nearly syndepositional erosion. With the possible exception of S7, all include spherules (Figs. 2 and 3) formed by condensation of impact-generated rock vapor clouds. All of the BGB spherule beds represent settings far removed from the impact sites: there is an absence of coarse ballistic ejecta and thick breccia layers, and the spherules more resemble those found in younger distal ejecta blankets [2,3,5]. For the three layers where we have Cr-Mn isotopic analyses (S2, S3, and S4), the results indicate that the bolides were carbonaceous chondrites [8].

The great thicknesses of relatively pure fall-deposited spherule layers, up to 35 cm, their distal depositional settings, and, in a few cases, modeling based on estimated bolide vs target rock contents [9] suggest that all represent bolides larger than 20 km in diameter and some may have exceeded 70 km [6, 7]. All were large compared to virtually all known post-2.5 Ga bolides.

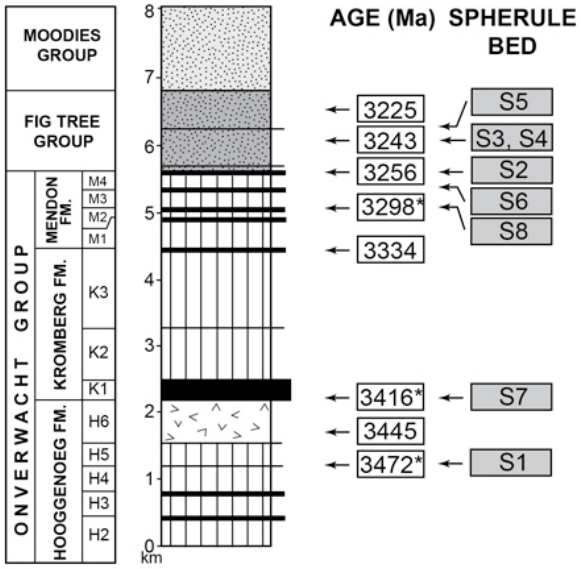

Figure 1. Stratigraphy of the Barberton belt showing distribution and ages of impact layers S1 thru S8. Vertical lines, mafic and ultramfic volcanic rocks; v's, felsic volcanic rocks; black, cherty sediments; stippled, detrital sedimentary rocks. * indicates spherule beds dated by detrital zircon geochronology. Stanford SHRIMP single-zircon analyses with ±3 Ma precision.

These layers document the profound effects that large impacts had on the early terrestrial surface, surface environment, and, probably, life. The detailed records of surface events before, during, and following the individual impacts are quite variable but almost all show evidence of major current- and/or wave-activity that mixed the spherules during and immediately following deposition with debris eroded from the sea floor and surface volcanic rocks. We have interpreted these events as tsunamis generated by the impacts or resulting crustal movements. The inferred distal depositional sites imply that there were few or no large landmasses to impede propagation of the tsunami waves around the globe. Consistent with this observation, the geochemistry and mineral composition of the spherule beds, including the lack of shocked quartz and zircons, and available geochemical modeling of impact layer compositions, indicating that the target rock was mafic crust, collectively suggest that there was a paucity or absence of large continental blocks at that time.

Several of the impacts triggered fracturing of the

crust in the present BGB area. In the case of S2, open fractures extended through at least the upper 100 m of surface rock and were filled by the the downward flowage of surface sediments and loose spherules [10]. At least 2 of the spherule beds, S2 and S8, are associated with major regressive events, and exposure and erosion of the sea floor. Throughout the southern part of the BGB, S2 (3.256 Ga) marks the end of over 250 million years of anorogenic, largely basaltic and ultramafic volcanism and initiation of large-scale, long-term deformation and orogenic activity that culminated 175 myr later in the formation of the Kaapvaal Craton. In the northern part of the belt, this transition occurred somewhat later, about 3.243 Ga, and is marked there by spherule bed S3. Much of the Archean development and evolution of the Earth's crust and geodynamic system may have been triggered by large impacts.

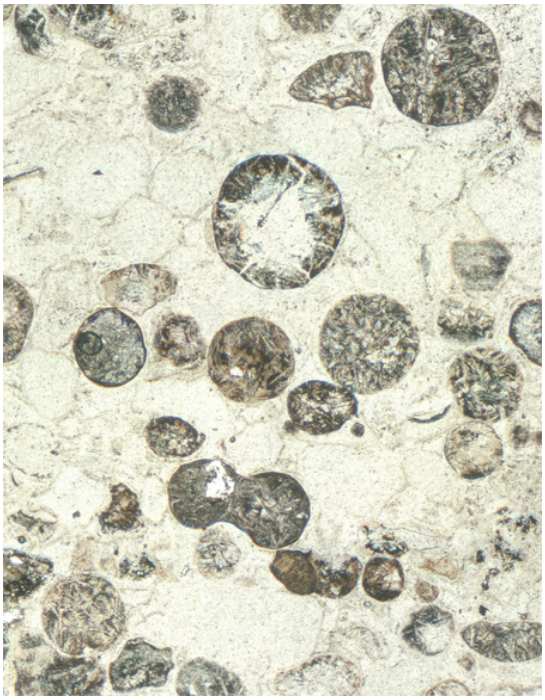

Figure 2. Spherules from the Pilbara Block, Western Australia. This bed correlates with bed S1 in the BGB. The dark spherules show a variety of preserved crystalline textures similar to those seen in chondrules. The light background also consists largely of spherules, now composed of nearly pure microcrystalline quartz.

These early impact layers also hold an accessible record of the latest LHB. While much of the time interval represented by the Barberton greenstone belt is represented by volcanic rocks (Fig. 1), many of the interbedded thin sedimentary layers preserve records of impact events. The frequency of large-body impacts implied by the beds discovered to date exceeds by several orders of magnitude the impact rates for comparably-sized bodies during later geologic time [5]. These results indicate that the Late Heavy Bombardment did not end abruptly at about 3.8 Ga but fell off gradually, with common large impacts persisting until at least 3.2 Ga. These results must be incorporated into models of the bombardment history of the inner Solar System.

Figure 3. Part of a core through spherule bed S3, Sheba-Fairview Mine. The spherules have been slightly flattened by tectonic shortening. Scale in cm. Photo courtesy of Chris Rippon.

Acknowledgments: Funding from Stanford University to Lowe; Louisiana State University to Byerly.

References: [1] Lowe, D.R., and Byerly, G.R. (1986), *Geology*, 32, 83-86. [2] Lowe et al. (1989) *Science*, 245, 959-962. [3] Lowe, D.R., et al. (2003) *Astrobiol.*, 3, 7-48. [4] Lowe, D.R., and Byerly, G.R. (2010) *LPS 41,* Abst. 2563. [5] Lowe, D.R., Byerly, G.R., and Kyte, F.R. (2014*) Geology*, 42, 747-750. [6] Johnson, B.C., and Melosh, H.J. (2012) *Nature,* 485, 75-77. [7] Bottke, W.F., et al. (2012) *Nature*, 485, 78-81. [8] Kyte, F.R., et al. (2003) *Geology*, 31, 283-286. [9] Byerly, G.R., and Lowe, D.R. (1994) *Geochem. Cosmochim. Ac*ta, 58, 3469-3486. [10] Lowe, D.R. (2013) *Geol. Soc. Am. Bull*., v. 125, 894-912.

The Bombardment of the Earth During the Hadean and Early Archean Eras

S. Marchi[1], W.F. Bottke[1], L.T. Elkins-Tanton[2], K. Wuennemann[3], A. Morbidelli[4], D. A. Kring[5]

1. Southwest Research Institute, Boulder, CO, United States; 2. School of Earth and Space Exploration, Arizona State University, Tempe, AZ, United States; 3. Museum fur Naturkunde, Berlin, Germany; 4. Observatoire de la Cote d'Azur, Nice, France; 5. USRA - Lunar and Planetary Institute, Houston, TX, United States.

Our knowledge of the Earth during the Hadean and early Archean eons (ca 4.5-3.5 Ga) is very limited, mainly because few rocks older than 3.8 Ga have been found (e.g. Harrison 2009). Hadean-era zircons have allowed us to glean important insights into this era, but their data has led to considerably different evolution models for the evolution of the early Earth; some predict a hellish world dominated by a molten surface with a sporadic steam atmosphere (e.g. Pollack 1997), while others have predicted a tranquil, cool surface with stable oceans (e.g. Wilde et al 2001; Valley et al 2002). To understand whether either model (or both) could be right, we believe it is useful to quantitatively examine the post Moon-forming impact bombardment of the early Earth.

Over the last several years, through a combination of observations (e.g., Marchi et al 2012), theoretical models (e.g., Bottke et al 2012), and geochemical constraints from lunar rock (e.g. highly siderophile elements -HSE- abundances delivered to the Moon by impactors; the global number of lunar basins; the record of Archean-era impact spherule beds on Earth; Walker 2009; Neumann et al 2012), we have constructed a calibrated model of the early lunar impactor flux (Morbidelli et al 2012). Our results have now been extrapolated to the Earth, where they can make predictions about its post-Moon formation bombardment, the so called *late accretion*.

Using a Monte Carlo code to account for the stochastic nature of major impacts, and constraining our results by the estimated HSE abundances of Earth's mantle (that were presumably delivered by impactors; Walker 2009; Bottke et al. 2010), we find the following trends. In the first ~100-200 Myr after the formation of the Moon, which we assume was created ~4.5 Ga, the Earth was almost entirely resurfaced by impacts. This bombardment, which included numerous D > 1000 km diameter impactors, should have vigorously mixed the crust and upper mantle. Between ~4.1-4.3 Ga, the impactor flux steadily decreased; though an uptick near ~4.1 Ga caused by the so-called Late Heavy Bombardment should have delivered a new round of large impactors striking at a mean velocity ~1.5 times higher than in previous epochs. Overall, only a relatively small fraction of ancient terrain survives unscathed all the way to the early Archean. We speculate that if impacts are involved with Hadean zircon formation, a scenario we find plausible, the apparent preference for ~4.1 Ga ages among Hadean zircons may be a combination of (i) terrain (and zircon) preservation and (ii) the ability of large impactors to create zircons (i.e., ~4.1 Ga would potentially be the "sweet spot" in this competition).

Bottke W.F., et al., Nature 485, 78, 2012.
Harrison T.M., Annu. Rev. Earth. Planet Sci., 37, 2009.
Marchi S., et al., EPSL, 325, 2012.
Morbidelli A., et al., EPSL, 355, 2012.
Pollack H.N. Greenstone belts, Oxford University Press, 1997.
Valley J.W., et al., Geology, 30, 2002.
Walker R.J., Chem. Der Erd., 69, 2009.
Neumann G. et al., AGU 2012.

APPLICATION OF A NEW METHOD FOR EXPLORING THE COPERNICAN CRATERING RECORD.
S. Mazrouei[1], R. R. Ghent[1], W. F. Bottke, [1]Department of Earth Sciences, University of Toronto, Toronto, ON, Canada. [2]Southwest Research Institute and the Institute for the Science of Exploration Targets (ISET), Boulder, CO, USA

Introduction: Here we investigate the Copernican-era lunar impact flux using a new method for determining crater ages.

Customarily, geological maps and crater counting methods have been used to determine the ages of lunar terrains and individual features. Those methods, however, are (i) extremely time consuming, (ii) are limited by image quality, image availability, and the need to identify small craters over datable regions, and (iii) are subject to systematic errors derived from uncertainty in the crater production function and small number statistics. For these reasons, it would be useful to have another way to explore this challenging problem.

It has recently been shown that the rockiness of large craters' ejecta, derived from the Lunar Reconnaissance Orbiter's Diviner thermal radiometer data [2], provides an alternative method for estimating the ages of Copernican craters (younger than roughly one billion years old) [1]. Young surfaces have fresh, sharp rocks, while older terrains have lower rock abundances, with both impacts and thermal cracking producing rock demolition over time [3]. The rate that rocks are eliminated can then be quantified using the rock abundances found on or near lunar craters with known absolute ages. This method is not subject to the constraints of traditional crater counting methods using visible images. The results of [1] show that in essence, only craters younger than ~1 Ga have ejecta blankets with rock abundance values that are higher than the background regolith. This broadly corresponds to the Copernican era [4].

In this work, we counted all craters with visible rocky ejecta, recorded their sizes, and calculated the rock abundance of their ejecta. We first compared the size-frequency distribution of our rocky craters to those craters previously defined as Copernican on the basis of geologic mapping and crater rays [4, 5]. Next, we calculated ages for each of our craters using the regression in [1] in order to determine whether or not the impact rate on the Moon has remained constant over the past billion years. The number and sizes of craters on the lunar surface reflect the number and sizes of impactors that created those craters (i.e., the Earth-crossing object population), which in turn tell us how the main asteroid belt population, particularly the inner main belt population, has changed with time. Therefore, it is possible that Copernican-era impacts can possibly tell us about asteroid disruption events and fragment evolution in the asteroid belt.

Methodology: We investigate the size-frequency distributions and ejecta rock abundances of rocky craters five kilometers and larger, and compare the results to canonical relationships for Copernican craters. The Diviner Rock Abundance (RA) dataset expresses the rock abundance as the areal fraction of a given field of view occupied by rocks large enough to remain warm through the lunar night [2]. Such craters are very distinct in the RA dataset, as shown in Figure 1.

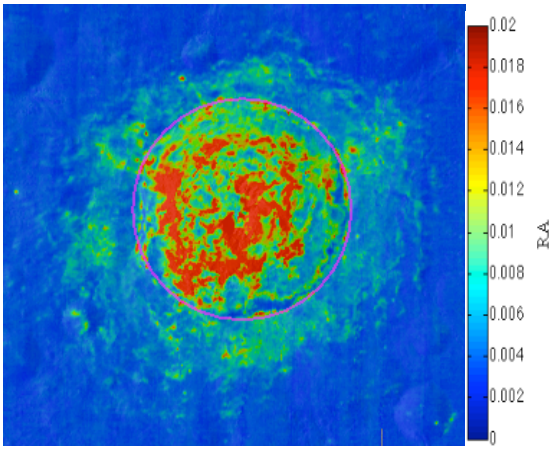

Figure 1: Rock Abundance Map of Jackson Crater (22.4° N, 163.1° W, ~17.4km diameter)

In contrast, older craters have ejecta blankets with RA values similar to the background regolith, as shown in Figure 2.

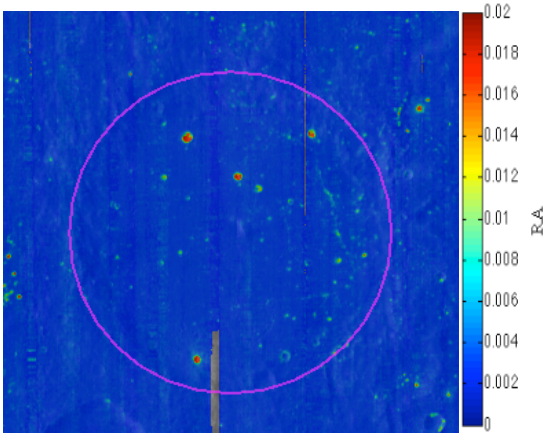

Figure 2: Rock Abundance Map of Alphonsus Crater (13.4° S, 2.8° W, ~120km diameter)

We identify about 620 craters larger than 5 km between 80° N and 80° S with rocky ejecta. Using the regression from [1], shown below, we calculate the crater ages by first finding the 95th percentile RA values.

$$RA_{95/5}=0.27\times(age[m.y.])^{-0.46}$$

Analysis and Results: The preliminary size-frequency distribution of our craters, together with those of Copernican craters identified by [4] and [5], is shown in Figure 3.

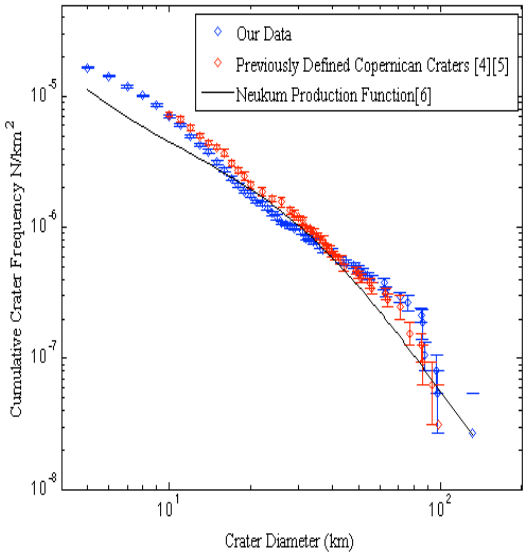

Figure 3: Size-frequency distribution comparison: Copernican Craters shown in red[5], versus identified craters with distinct rock abundance in their ejecta, shown in blue, and the Neukum 2001 Production Function [6].

It is evident from Figure 3 that our Copernican craters are broadly similar in population statistics to those identified by [4] and [5]. We are currently analyzing these size-frequency distributions in order to interpret discrepancies between the two. Furthermore, we are investigating the statistics of sub-populations of this dataset in a range of age bins as calculated using the regression of [1].

Individual craters. When comparing our results with those previously defined as Copernican [4, 5], some are in strong agreement. Giordano Bruno Crater is an example of such craters (Figure 4).

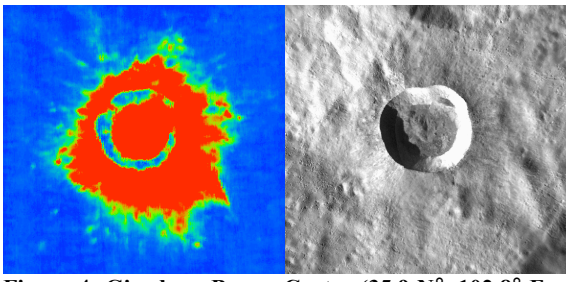

Figure 4: Giordano Bruno Crater (35.9 N°, 102.8° E, ~22 km diameter) shown in the Rock Abundance dataset (left), and LROC WAC Equatorial Mosaic (right)

On the contrary, some specific craters do not show high rock abundance in their ejecta, and we therefore exclude them from our dataset. An example is the Coriolis Y Crater; note the low rock abundance in the ejecta blanket (Figure 5).

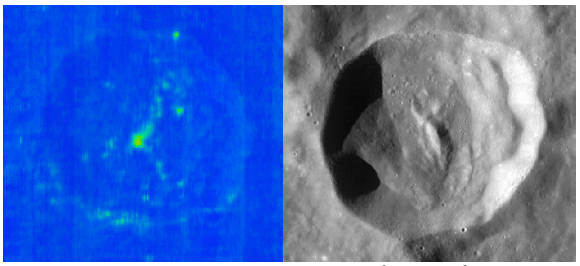

Figure 5: Coriolis Y Crater (3.6 N°, 171.2° E, ~31 km diameter) shown in the Rock Abundance dataset (left), and LROC WAC Equatorial Mosaic (right)

Current Work: As outlined above, we are currently analyzing sub-populations of Copernican craters with ages calculated using the regression of [1]. We will thereby identify any deviations from the Neukum production function [6], and eventually, relate these to events in the asteroid belt.

References: [1] Ghent, R.R., et al. 2014, *Geology, 42,* N10. [2] Bandfield, J.L., et al. 2011, *Journal of Geophysical Research* 116: E12. [3] Delbo, M., et al. 2014, *Nature, 508*. [4] D. E. Wilhelms., et al. 1978, *Planetary Science Conference* 9, 3735-3762. [5] A. S. McEwen., et al. 1997, *Journal of Geophysical Research* 102: E4. [6] B. A. Ivanov., et al. 2002, *Asteroids III*, 89-101.

PULSES OF MAGMA MOVEMENT TRIGGERED BY THE SOUTH POLE-AITKEN BASIN IMPACT. P. J. McGovern[1,2], R. W. K. Potter[1,2], G. S. Collins[3], D. A. Kring[1,2], M. L. Grange[4], and A. A. Nemchin[4], [1]Center for Lunar Science and Exploration, USRA Lunar and Planetary Institute, 3600 Bay Area Blvd., Houston TX 77058, [2]NASA Solar System Exploration Research Virtual Institute, [3]Impacts and Astromaterials Research Centre, Dept. Earth Science and Engineering, Imperial College, London UK, [4]Department of Applied Geology, Western Australian School of Mines, Curtin University, Western Australia (mcgovern@lpi.usra.edu).

Introduction: Basin-scale impacts have profound consequences for the surface and interior evolution of their target bodies. The South Pole-Aitken (SPA) basin, the oldest, widest, and deepest impact basin on the Moon, set off immense global pressure waves, with enormous implications for the structural and magmatic evolution of the Moon. Elsewhere [1], we pose the question of whether a global-scale epoch of magmatism could have been triggered by the SPA impact event, in order to account for a striking peak in magmatic zircon ages at 4.30-4.36 Ga [e.g., 2-3]. Here, we explore in more detail the mechanical effects that such pressure waves would exert on potential magma pathways in the lunar crust and lithosphere, linking hydrocode model results to magma ascent theory.

Method: We examine the stress state in an axisymmetric model Moon struck by a 10 km/s, 170 km diameter impactor [4], as calculated by the iSALE hydrocode [5]. Reported in-plane stresses are rotated into a local horizontal-vertical coordinate system, and when combined with the out-of-plane normal stress (also effectively a horizontal stress) the propensity for opening of potential magma-transporting fractures in both vertical (dikes) and horizontal (sills) orientations can be assessed. For vertical pathways, we assess whether each horizontal stress is less compressive than both the vertical stress at that timestep and the initial vertical stress. For horizontal pathways, we assess whether the vertical stress is less compressive than both of the horizontal stresses at that timestep and the initial horizontal stress. If an assessment is true, the fracture opening criterion is satisfied. Further, variations in stress with depth in the lunar crust are input to a calculation of pressure balance on the walls of potential dikes [6-8], allowing magma ascent velocities to be estimated.

Results:

Intrusion orientations. Variations in stress vs. time for a location at about 20 km depth and about 15 degrees from the impact antipode (Fig. 1a) show quite large excursions from the pre-impact lithostatic (all stress components equal) state. At the earliest stages, the criteria for opening vertical and horizontal fractures are satisfied at apparently alternating times (Fig. 1b). At time $t \sim 90$ minutes, an extended period during which the horizontal stresses are significantly more extensional than the vertical stress commences, lasting for about 38 minutes, predicting opening of vertical fractures (potential magma pathways) during that time. This is immediately followed by a comparably long time interval when the horizontal stresses are strongly more compressional than the vertical, indicating opening of horizontal sill-like pathways for magma movement. Similar excursions in stress magnitudes and intervals of dominance for each potential intrusion orientation are seen at locations farther from the antipode (out to at least 45 degrees from the antipode).

Magma ascent velocities. Stress distributions vs. depth at the angular location (15 degrees from antipode) of the point in Fig. 1 during the 38 minute vertical fracture opening event predict strong, positive magma ascent velocities in the lower crust (Fig. 2a), with a similar result holding for a similar event in a column at 45 degrees from the antipode (Fig. 2b). Ascent velocities are negative in the upper crust for both locations/times, indicating that ascent is inhibited there during the time that vertical fractures are opening.

Discussion: The large, global-scale excursions of stress expected in the crust of the Moon immediately after the SPA impact have enormous implications for transport of magma. Long-duration (10s of minutes) vertical fracture-opening events (Fig. 1) favor magma ascent in dikes, at velocities that allow the entire lower crust to be traversed within the timeframe of the events (Fig. 2). Stress gradients adverse to magma ascent (horizontal stresses becoming more compressional with decreasing depth) result in arrest of the ascending magmas, producing an intrusive horizon in the mid-crust. Further, the lateral spread of magmas at this horizon is favored by subsequent periods of horizontal fracture opening, that are comparable in duration to the vertical fracture opening events. Thus, the mobilized magmas will be widespread and widely available for incorporation into materials that ultimately arrive in the sample record. This pulse of impact-generated magma ascent into the lower crust would produce a complementary pulse of magmatic crystallization ages over a longer, yet still short-duration period of order 10 Myr. In addition, the establishment of widespread intrusive systems introduces mechanical inhomogeneities in the crust that can facilitate magma mobility long after the initial pulse of magma has solidified. While it is not necessary for magmas to erupt to enter the sam-

ple record, local pre-existing perturbations in topography and tectonic structure can provide limited pathways to the surface.

References: [1] Kring D. A. et al. (2014) this volume, Abstract #3009. [2] Nemchin A. A. et al. (2008) *Geochim. Cosmochim. Acta, 72*, 668-689. [3] Grange M. L. et al. (2009) *Geochim. Cosmochim. Acta, 73*, 3093-3107. [4] Potter R. W. K. et al. (2012) *Icarus, 220*, 730-743. [5] Collins, G.S. et al. (2004) *MAPS*, 39, 217-231. [6] Rubin A. M. (1995) *Ann. Rev. Earth Planet. Sci., 23*, 287-336. [7] McGovern P. J. et al. (2013) *J. Geophys. Res., 118*, doi:10.1002/2013JE004455. [8] McGovern P. J. et al. (2013) *LPS XVIV*, Abstract #3055.

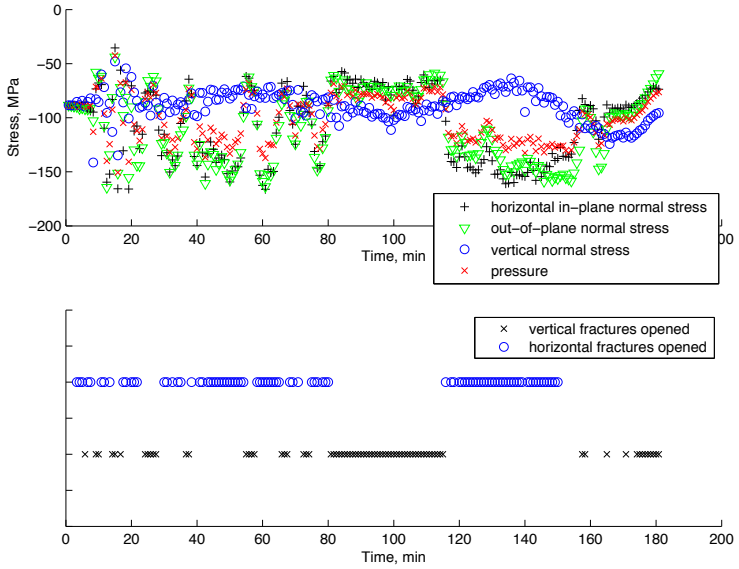

Figure 1. Stresses and fracture opening criteria for a location at ~ 20 km depth and 15 degrees from the SPA impact antipode. a, top) Stresses in MPa as functions of time in minutes. b, bottom) Criteria for opening of horizontal (blue circles) and vertical (black 'x's) as a function of time in minutes. Symbols are plotted at times when criteria are satisfied.

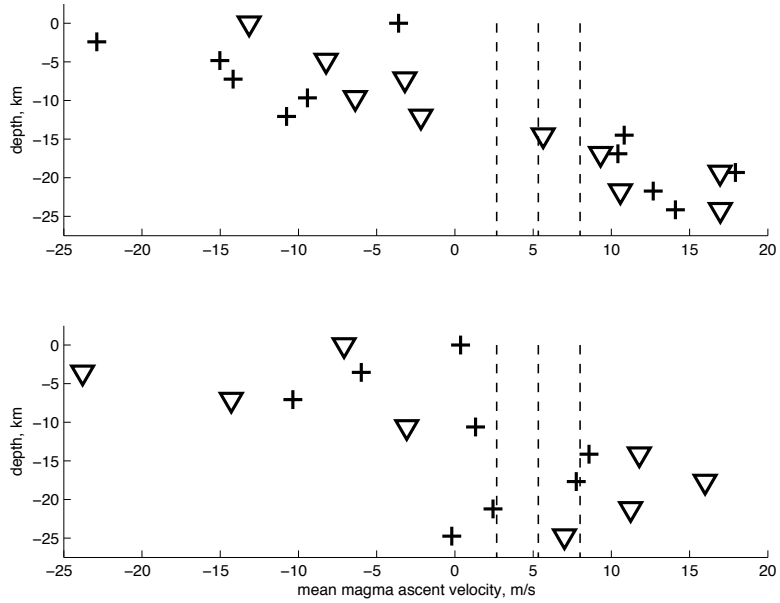

Figure 2. Magma ascent velocity and effective mechanical buoyancy as a function of depth in the lunar crust, for a horizontal opening event of duration 2300 seconds. Plus signs correspond to in-plane horizontal normal stress, triangles to out-of-plane (hoop) stress. Dashed lines delineate effective buoyancies of 200, 400, and 600 kg/m^3 from left to right. a, top) Location 15 degrees from SPA antipode. b, bottom) Location 45 degrees from SPA antipode.

Debris from Borealis Basin Formation as the Primary Impactor Population of Late Heavy Bombardment.
D. A. Minton[1], A. P. Jackson[2], E. Asphaug[2], C. I. Fassett[3], J. E. Richardson[4], [1]Purdue University, Dept. of Earth, Atmospheric & Planetary Sciences, 550 Stadium Mall Dr., West Lafayette, IN 47907, daminton@purdue.edu, [2]School of Earth & Space Exploration, Arizona State University, Tempe, AZ 85287 [3]Department of Astronomy, Mount Holyoke College, South Hadley, MA 010751, [4]Arecibo Observatory, Arecibo, PR 00612

Introduction: Here we investigate a novel Giant Impact Debris (GID) hypothesis to explain a number of observations regarding a period of early solar system history known as the Late Heavy Bombardment (LHB). In the GID hypothesis, the early impact histories of the Moon and Mars are dominated by debris left over from two giant impacts: The Moon-formation impact [1,2], and the formation of the crustal dichotomy on Mars (Borealis Basin) [3,4].

The Moon-formation impact has been constrained to have occurred within the first ~100 My of solar system history [5,6]. Debris left over from the Moon-formation impact would be substantial, but would clear out rapidly and preferentially impact the Earth-Moon system. This debris would therefore produce an Early Heavy Bombardment (EHB), possibly associated with the pre-Nectarian of the lunar cratering record. The timing of the Borealis Basin formation on Mars is not well constrained, other than the obvious fact that it predates all other northern hemisphere basins. Borealis Basin impact debris, though smaller than Moon-formation debris, could preferentially become trapped in a quasi-stable region currently occupied by the so-called Hungaria asteroids, which are not only dynamically distinct, but also compositionally distinct, including a prevailing number of E-type asteroids that are believed to be the source of the unusual, highly reduced enstatite achondrites (aubrites), and possibly the mesosiderites [7].

The dynamical decay lifetime of the Hungaria region is long, having a half life of ~600 My [7,8]. Therefore, it is plausible that Borealis Basin debris trapped in the Hungaria asteroid region could be responsible for the late lunar basins, such as Imbrium and Orientale, which are the most stringent constraints on the timing and existence of the LHB.

Our model makes several testable predictions, and naturally explains several observations that are difficult to reconcile under giant planet instability models, such as the Nice Model, which is the currently most-favored hypotheses for the cause of the LHB [8,9].

Challenges of the Giant Planet Instability Hypothesis for the LHB: Currently, many researchers have adopted a model for the LHB in which late-migrating giant planets destabilized reservoirs of small bodies [9-12] This model has many unresolved challenges [13]. In particular, giant planet instability models, such as the so-called Nice Model, [9,14,15] predict that a large fraction of the LHB-era impactors were comets from a massive icy planetesimal disk beyond Neptune. This is difficult to reconcile with geochemical constraints [16] as well as the size-frequency distribution of the impactors. The currently-favored version of the Nice Model, the so-called Jumping Jupiter model [17], predicts a substantially reduced fraction of destabilized Main Belt and extended inner Main Belt (E-Belt) asteroids to the total lunar impact record [8], compared with the "classical" Nice Model, which predicted roughly equal fractions of asteroidal and cometary impactors [9].

Giant planet instability models for the LHB predict that the impactors sourced from both the Main Belt (and E-Belt) and proto-Kuiper Belt would reach the terrestrial planets in a size-independent way. This was in fact used as evidence for an instability model, due to the close correlation between the derived impactor size-frequency distribution of ancient heavily cratered terrains and the Main Asteroid Belt [11]. However, there is a substantial disconnect between the density of ~100 km craters and the >300 km basins relative to the Main Asteroid Belt [18, 19]. The Main Asteroid Belt is far more abundant in >70 km objects than the putative lunar highlands impactors [19]. Because the abundance of large objects appears to be a primordial feature of both the Main Belt and the Kuiper belt [20, 21], the lack of this feature in the ancient lunar highlands bombardment population suggests that they did not come from either of these reservoirs.

Many authors have also reported evidence of impact "spikes" in the early bombardment record of the Moon and Mars based on counts of craters on top of basins (large craters) [22-24]. However, under a giant planet instability model, in which impactors are delivered to the inner solar system in a size-independent way, such spikes should not be observable. The existence of such spikes indicates either size-dependent preservation [25], or a mass-dependence on the impactor delivery timescale.

Promise of the Giant Impact Debris Hypothesis for the EHB/LHB: The GID hypothesis resolves the issue of cometary impactors by not requiring them. In this model, all impactors are sourced locally from rocky

inner-solar system material. The impactor SFD of both the Moon formation debris (EHB) and the Borealis debris (LHB) would lack the excess of large bodies that are present in the "planetesimal" remnants (the Main Belt and Kuiper Belt). Collisional evolution of these debris remnants would produce a similar SFD for the <10 km objects as observed in the Main Belt [26, 27]. The relative flux of the impactor populations onto the respective planets would be far different than in the giant planet instability models. The EHB impactors would favor the Moon over Mars by as much as a factor of 10, while the LHB impactors would favor the Mars by a factor of ~10-100. This could explain why the pre-Nectarian on the Moon (EHB) includes ~2/3 of all lunar basins, while the equivalent period on Mars, the pre-Noachian, contains proportionally many fewer basins [28].

The timing of the LHB would suggest that the Borealis Basin impact occurred relatively late, coinciding with the start of the Nectarian at 4.1-4.2 Gy [7]. This is well within the plausible timescale of the loss of a "fifth" terrestrial planet under the Planet V hypothesis [29].

References:

[1] W. K. Hartmann and D. R. Davis (1975) *International Astronomical Union*, 24, 504–514. [2] A. P. Jackson and M. C. Wyatt, Mon. Not. of the Royal Astron. Soc., 425, 657–679, 2012. [3] M. M. Marinova, O. Aharonson, and E. Asphaug (2008) *Nature*, 453, 7199, 1216–1219. [4] M. M. Marinova, O. Aharonson, and E. Asphaug, (2011) *Icarus* 211, 2, 960–985. [5] S. B. Jacobsen (2012) *Annu. Rev. Earth. Planet. Sci.,* 33, 1, 531–570. [6] S. A. Jacobson, A. Morbidelli, S. N. Raymond, D. P. O'Brien, K. J. Walsh, and D. C. Rubie (2014) *Nature*, 508, 7, 84–87. [7] M. Ćuk (2012) *Icarus*, 218, 1, 69–79. [8] W. F. Bottke, D. Vokrouhlický, D. Minton, D. Nesvorný, A. Morbidelli, R. Brasser, B. Simonson, and H. F. Levison (2012) *Nature*, 485, 7396, 78–81. [9] R. Gomes, H. F. Levison, K. Tsiganis, and A. Morbidelli (2005) *Nature*, 435, 7, 466–469. [10] H. F. Levison, L. Dones, C. R. Chapman, S. A. Stern, M. J. Duncan, and K. Zahnle (2001) *Icarus*, 151, 286–306. [11] R. G. Strom, R. Malhotra, T. Ito, F. Yoshida, and D. A. Kring (2005) *Science*, 309, 5, 1847–1850,. [12] A. Morbidelli, S. Marchi, W. F. Bottke, and D. A. Kring, Earth and Planetary Science Letters, 355, 144–151, 2012. [13] C. I. Fassett and D. A. Minton (2013) *Nature Geosci,* 6, 7, 520–524. [14] K. Tsiganis, R. Gomes, A. Morbidelli, and H. F. Levison (2005) *Nature*, 435, 7, 459–461. [15] A. Morbidelli, H. F. Levison, K. Tsiganis, and R. Gomes (2005) *Nature*, 435, 7, 462–465. [16] D. A. Kring and B. A. Cohen , (2002) *JGR*, 107, 2, 5009. [17] R. Brasser, A. Morbidelli, R. Gomes, K. Tsiganis, and H. F. Levison (2009) *A&A*, 507, 2, 1053–1065. [18] S. C. Werner (2014) *EPSL*, 400, 0, 54–65. [19] D. A. Minton, J. E. Richardson, and C. I. Fassett (2015) *Icarus*, 247, 0, 172–190. [20] A. Morbidelli, W. F. Bottke, D. Nesvorný, and H. F. Levison (2009) *Icarus*, 204, 2, 558–573. [21] D. Nesvorný, D. Vokrouhlický, W. F. Bottke, K. Noll, and H. F. Levison (2011) *AJ*, 141, 5, 159. [22] M. R. Kirchoff, C. R. Chapman, S. Marchi, K. M. Curtis, B. Enke, and W. F. Bottke (2013) *Icarus*, 225, 1, 325–341. [23] S. J. Robbins and B. M. Hynek (2012) *LPSC XLIII*, 43, 1649. [24] H. Frey (2008) *GRL*, 35, 1320. [25] S. J. Robbins, B. M. Hynek, R. J. Lillis, and W. F. Bottke (2013) *Icarus*, 225, 1, 173–184. [26] D. D. Durda (1993) *PhD Dissertation*. [27] D. P. O'Brien and R. Greenberg (2003) *Icarus*, 164, 334–345. [28] S. C. Werner (2008) *Icarus*, 195, 1, 45–6. [29] J. E. Chambers (2007) *Icarus*, 189, 2, 386–400.

ZIRCONIUM MINERALS FROM MARS, MOON AND EARTH INDICATE CRUSTAL 'REFUGIA' ON EARLY BOMBARDMENT SURFACES. D.E. Moser[1]
[1]University of Western Ontario, London, CAN (desmond.moser@uwo.ca)

Introduction: Zircons are difficult to destroy yet can bear witness to the occurrence and sometimes age of major impact events [e.g. 1]. The zirconium mineral record consequently has implications for the tempo and nature of early bombardment and ultimately the evolution of planetary crusts, hydrospheres and life. Recent models that rescale impactor flux according to a saw-tooth decay in lunar impact frequency [2] deduce 100% to 600% resurfacing of the early Earth by impact-related mafic magmatism [3] and reworking of the outer 20km. It is presumed that other bodies in the inner solar system experienced similar pervasive crustal modification. Ultimately the accuracy of such models hinges on geochronology since a key model input is the interpretation of isotopic data from samples of the Moon and the degree to which those data measure a lunar impact chronology. Until we have achieved direct dating of the major lunar impact basins, other physical evidence must be relied upon to test early bombardment scenarios. Presented here is a synthesis of our recent microstructural investigations of zircon that crystallized at different stages in the early bombardment period (4.4 to 3.8 Ga) from Earth, Moon and Mars as a test of the recent bombardment-driven recycling model [3].

Methods: The advances presented are made possible by integration of electron nanobeam measurements of orientation and chemical microstructure with isotopic analyses, ideally using in situ techniques such as SIMS (UCLA), laser ablation ICPMS (Univ. of Houston), or the relatively new technique of Local Elec-trode Atom Probe (LEAP) Tomography (CAMECA). Electron nanobeam analyses were performed at the Zircon and Accessory Phase Laboratory (UWO ZAPLab) using a Hitachi SU6600 VP-FEG-SEM with cathodoluminescence (CL) , electron diffraction (EBSD), Energy Dispersive Spectroscopy (EDS) [2], and by atomic resolution STEM (CCEM).

Results: EARTH; Pre-3.9 Ga terrestrial zircons are notable for their scarcity, as well as the absence of shock microstructures despite thorough EBSD analysis of grains as old as 4.37 Ga grain [4]. The terrestrial bombardment resurfacing model [3] ascribes the rarity of early zircon to its original paucity in the dominantly mafic crust and/or its destruction by major shock melting events. The early earth crust was most likely mafic in bulk composition and and baddeleyite would have been the dominant Zr phase. Baddelyties are also shock resistant [5] but search for primary pre-3.9 ga in early crust of the Nuvvuagittuq belt has been negative [6]. The absence of shock, and the oxygen isotope compostions indicating surface presence of water, in the surviving grains are reconciled as crystallization characteristics of relatively cool, wet regions at the externides of impact-initiated igneous complexes. Aspects of this argument run counter, however, to empirical evidence that zircon has survived major impact cratering events on Earth at sites such as Vredefort [7] whereas it is noted that inherited zircon is uncommon in impact melt sheets such as at Sudbury.

MOON: The persistence of zircon and baddeleyite through the bombardment period can be seen in both the Apollo sample suite and in lunar meterorites. A study of micrograins of zircon and baddeleyite in meteoritic lunar breccia NWA 2200 [8] exhibit a diversity of microstructures analogous to those in samples from the Vredefort and Ries craters. An example of polystage igneous and impact processes is evident in an anhedral zircon grain, in an apparently undeformed gabbro clast, exhibiting shock microtwin lamellae and crystal-plastic deformation. Spatially correlated SIMS U-Pb dating reveals a 400 million year span of early lunar processes in grains as small as 5 micrometres in diameter. Bombardment has not erased the early lunar Zr mineral record.

MARS: The recent discovery of zircon as old a 4.43 Ga in NWA7533 [9] and related stones such as NWA 7475 [10] presents the first population of pre-bombardment zircons from Mars for investigation of its shock history. The simple fact that hundreds of these grains, and co-existing baddeleyite, have survived in a basaltic-composition suevite as crystal clasts speaks to the persistence of these phases in the planetary mafic crustal record [10]. Results so far suggest a paucity of shocked grains in the population. New results on age age and microstructure will be presented to quantify early martian shock history.

Discussion:

A comparison of Zr mineral phases from Earth, Moon and Mars reveals that a) pre-bombardment minerals survive the bombardment epoch, even through multiple impact reworking, and b) a significant number of the albeit rare pre-bombardment grains show no evidence of shock metamorphism. These observations, together with the already established evidence for relatively cool and hydrous formation conditions for terrestrial Hadean grains, suggest that bombardment-driven melting, reprocessing and burial of early crusts was perhaps

not as pervasive as has been recently modeled, and that islands of primitive crust persisted through the bombardment epoch. On earth these early fragments have been largely destroyed whereas on Mars they remain to be reprocessed by endogenic dynamics.

References: [1] Krogh, T.E., Kamo, S.L., & Bohor, B.F. (1996) Geophys. Monog., 95, 343-353. [2] Morbidelli, A. et al., (2012) EPSL 355-6, 144-151. [3] Marchi, S. et al., (2014) Nature 511, 578-581. [4] Valley, J.W. et al. (2014) Nature Geoscience, 7, 219-223. [5] Moser D.E. et al. (2013). Nature 499, 454-458. [6] Darling, J.R. et al. (2013) Amer. Jnl of Science 313, 844-8, [7] Moser, D. E. et al. (2011) Can. J. Earth Sci. 48, 117–139. [8] Darling, J.R. et al. (abs) (2012) ESBD 2012 CMU, Pittsburgh. [9] Humayun, M. et al., (2013) Nature 503, 513-516. [10] Moser, D.E. et al. (2013) Meteoritical Society, Edmonton, CAN (Abs).

DESTRUCTION AND RE-ACCRETION OF OUTER SOLAR SYSTEM SATELLITES DURING THE LATE HEAVY BOMBARDMENT. N. Movshovitz[1], F. Nimmo[1], D. G. Korycansky[1], E. Asphaug[2], and J. M. Owen[3]
[1]Earth and Planetary Sciences, University of California, Santa Cruz, Santa Cruz CA
[2] School of Earth and Space Exploration, Arizona State University, Tempe, AZ
[3] Lawrence Livermore National Laboratory, Livermore, CA

Introduction: One explanation for the Lunar Late Heavy Bombardment (LHB) can be found in the Nice Model [1], [2]. In this model, an exterior disk of unaccreted planetesimals remains after the main stage of planet formation. Migration due to chance encounters with disk particles brings Jupiter and Saturn to a 1:2 mean motion resonance, causing a period of dynamical instability in the system. With the right choice of initial conditions, the timing of this period can be made to coincide with the timing of the suspected LHB [2].

The above scenario would also lead to a LHB period in the outer solar system and the possible ramifications for the small-to-middle sized satellites of the outer system have already been noted [3]. Here we present the latest results from an extensive Monte-Carlo study of collisional outcomes, focusing on the rate of *catastrophic* impacts. We find that, even with very conservative assumptions, Mimas, Enceladus, Tethys, and Miranda experience at least one catastrophic impact in every simulation. We consider the implications of this for present-day observed properties of these satellites.

Method: We simulate 200 randomized LHB events for many satellites of the outer solar system. We draw random impactor samples (sizes and orbits) from estimated probability distributions [4]–[6] until the total mass delivered to the target exceeds the relative fraction of impactor flux expected to be intercepted by that satellite [7]. We fix the absolute value of delivered mass, $M_{\mathrm{LHB}}^{\mathrm{sat}}$, by scaling to the value suggested in [8] for Callisto.

The result of an individual impact is determined by calculating Q, the effective specific energy of impact (in the target's rest frame), and comparing it with Q_D^*, the energy of an impact that is expected to disperse half the mass or a target of radius R, obtained with the scaling law

$$Q_D^* \approx 0.05\,\mathrm{J/kg} \times \left(\frac{R}{1\,\mathrm{m}}\right)^{1.188}.$$

This scaling law was derived from hydro-code simulations of gravity-regime collisions of ice bodies. In this study, we used the SPH code SPHERAL [9]–[11] to extend the results of [12] to targets in the 100-1000 km range [13].

If $Q > Q_D^*$ we increment a catastrophic impact counter. We also keep track of *super-catastrophic* ($Q > 2Q_D^*$) and *ultra-catastrophic* ($Q > 3Q_D^*$) impacts.

We make the conservative assumption that any ejected mass is quickly re-accreted onto the target. The target's mass and radius thus remain fixed throughout the simulation. This is a conservative approach since if a target were allowed to lose mass between impacts it would become progressively easier to disrupt.

We begin by setting $M_{\mathrm{LHB}}^{\mathrm{sat}}$ for each target to match $M_{\mathrm{LHB}}^{\mathrm{Callisto}}$ as suggested by [8]. We then scale down the delivered mass until all satellites survive 200 simulated LHBs without experiencing a catastrophic impact. The resulting statistics are described below.

Results: Figure 1 shows the fraction of Monte-Carlo runs that included at least one collision with energy greater than one, two, and three times Q_D^*, for 11 outer solar system satellites. Mimas, Enceladus, Tethys, and Miranda experienced a catastrophic impact in every simulation. In most runs, Mimas, Enceladus, and Tethys experienced *multiple* catastrophic impacts, including impacts with energy several times that required to completely disrupt them. These satellites would be heavily modified by a LHB no matter what assumptions we make about the impactor population or re-accretion efficiency. By contrast, the larger satellites (Europa, Ganymede, Callisto, and Titan) are not ex-

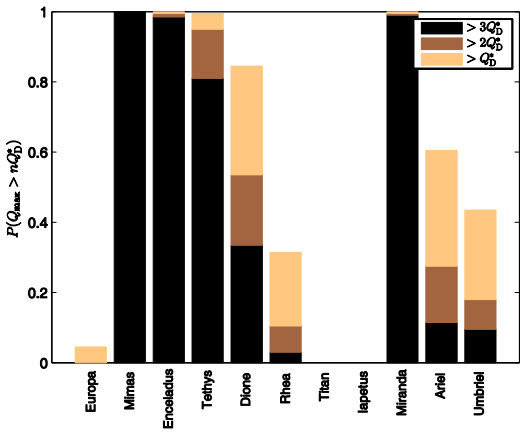

Figure 1. Fraction P of Monte-Carlo runs that included at least one impact with effective specific energy greater than one, two, or three times the catastrophic disruption threshold, Q_D^*. In these runs the mass delivered to each satellite was scaled to deliver $\sim 3 \times 10^{20}$kg to Callisto.

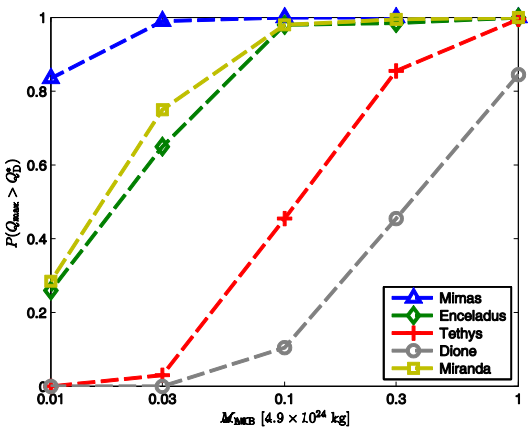

Figure 2. Fraction *P* of simulations that included at least one catastrophic impact, as a function of mass delivered. The upper limit value corresponds to $\mathbf{3 \times 10^{20}}$kg delivered to Callisto.

pected to undergo disruption; nor are very distant objects such as Iapetus.

It may be possible that different initial conditions in the Nice Model would result in less mass delivered to the outer solar system while still being able to explain the lunar LHB [14]. Figure 2 shows how the probability of catastrophic disruption drops when the total mass delivered in the simulation is reduced. A reduction by a factor of 3 is not enough to save Mimas or Enceladus, nor, probably, Tethys or Dione. The mass delivered by a hypothetical LHB must be at least 30 times less than the value predicted by the canonical Nice model to give Enceladus a decent chance of surviving the LHB unmodified, and 100 times less to give Mimas any chance at all.

Implications: The results described above suggest that the inner Saturnian and Uranian satellites were disrupted and re-accreted several times during the putative LHB. Possible implications of this scenario are:

(1) The impact history recorded on the surface of these satellites has been erased. This is consistent with current surface age estimates based on cratering rates [7]. Older surface ages are still conistent for larger satellites (Callisto, Umbriel, Oberon) or for the remotely orbiting Iapetus.

(2) The ice-rock ratio in differentiated bodies may have been affected. This is because, although we assumed perfect re-accretion in order to be conservative, in reality collisions are sure to lead to some mass loss. And probably preferentially that of lighter material. This mechanism can be invoked, for example, to explain the ice-rich nature of Tethys, arguing that Tethys is a byproduct of catastrophic disruption of a larger, differentiated body.

(3) The present day interior of Mimas is expected to be undifferentiated. This is because catastrophic disruption and prompt re-accretion is likely to "scramble" a pre-differentiated satellite. Conversely, if Mimas turns out to have a differentiated interior, then our results suggest either that Mimas is younger than 3.9 Ga, or that a heat source capable of melting Mimas must be invoked (accretional energy without radionuclides would not be sufficient), or that the canonical Nice Model – when applied to the outer solar system – requires significant modification. Interestingly, evidence for a complex interior of Mimas has indeed been suggested recently, based on anomalously large forced librations detected in Cassini Image Science Subsystem images [15].

References: [1] K. Tsiganis, R. Gomes, A. Morbidelli, and H. F. Levison, *Nature*, vol. 435, no. 7041, pp. 459–61, May 2005. [2] R. Gomes, H. F. Levison, K. Tsiganis, and A. Morbidelli, *Nature*, vol. 435, no. 7041, pp. 466–9, May 2005. [3] F. Nimmo and D. G. Korycansky, *Icarus*, vol. 219, no. 1, pp. 508–510, May 2012. [4] S. Charnoz, A. Morbidelli, L. Dones, and J. Salmon, *Icarus*, vol. 199, no. 2, pp. 413–428, Feb. 2009. [5] K. Zahnle, L. Dones, and H. F. Levison, *Icarus*, vol. 136, no. 2, pp. 202–22, Dec. 1998. [6] K. Zahnle, P. M. Schenk, S. Sobieszczyk, L. Dones, and H. F. Levison, *Icarus*, vol. 153, no. 1, pp. 111–129, Sep. 2001. [7] K. Zahnle, P. M. Schenk, H. F. Levison, and L. Dones, *Icarus*, vol. 163, no. 2, pp. 263–289, Jun. 2003. [8] A. C. Barr and R. M. Canup, *Nat. Geosci.*, vol. 3, no. 3, pp. 164–167, Jan. 2010. [9] J. Owen, J. Villumsen, P. Shapiro, and H. Martel, *Astrophys. J. Suppl. Ser.*, vol. 116, pp. 155–209, 1998. [10] J. Owen, in *5th International SPHERIC SPH Workshop*, 2010, pp. 297–304. [11] J. Owen, *Int. J. Numer. Methods Fluids*, vol. 75, pp. 749–775, 2014. [12] W. Benz and E. Asphaug, *Icarus*, vol. 142, pp. 5–20, 1999. [13] N. Movshovitz, D. Korycansky, F. Nimmo, E. Asphaug, and J. Owen, in *Lunar and Planetary Institute Science Conference Abstracts*, 2014, pp. 1–2. [14] L. Dones and H. F. Levison, in *44th Lunar and Planetary Science Conference (2013)*, 2013. [15] R. Tajeddine, N. Rambaux, V. Lainey, S. Charnoz, A. Richard, A. Rivoldini, and B. Noyelles, *Science*, vol. 346, no. 6207, pp. 322–4, Oct. 2014.

THE NATURE OF THE 4.2 GA IMPACT EPISODE ON THE MOON: EVIDENCE FROM NORTH RAY CRATER BRECCIAS, APOLLO 16. M. D. Norman[1], [1]Research School of Earth Sciences, The Australian National University, Canberra ACT 2000, Australia (marc.norman@anu.edu.au).

Introduction: The timing of basin formation on the Moon, and in particular the recurring hints of one or more large events at ~4.1 to 4.3 Ga, remains an outstanding problem. The low-grade, fragmental breccias and associated regolith that were collected at Apollo 16, Stations 11 and 13 around North Ray crater have provided a particularly rich source of material with apparent impact-related ages ≥4.0 Ga [1, 2, 3, 4]. Here we re-examine some of the geochronological data obtained on clasts extracted from these breccias in an attempt to clarify the age relationships and implications for lunar impact history.

Geological setting: The North Ray crater breccias carry a diverse suite of crystalline to glassy lithic clasts in a lightly welded and variably shocked matrix of finely communited mineral fragments. Crystalline lithic clasts are primarily anorthositic with a range of igneous to metamorphic textures (Fig 1a). Dark clasts with abundant mineral fragments in a rapidly quenched melt matrix are also abundant (Fig. 1b).

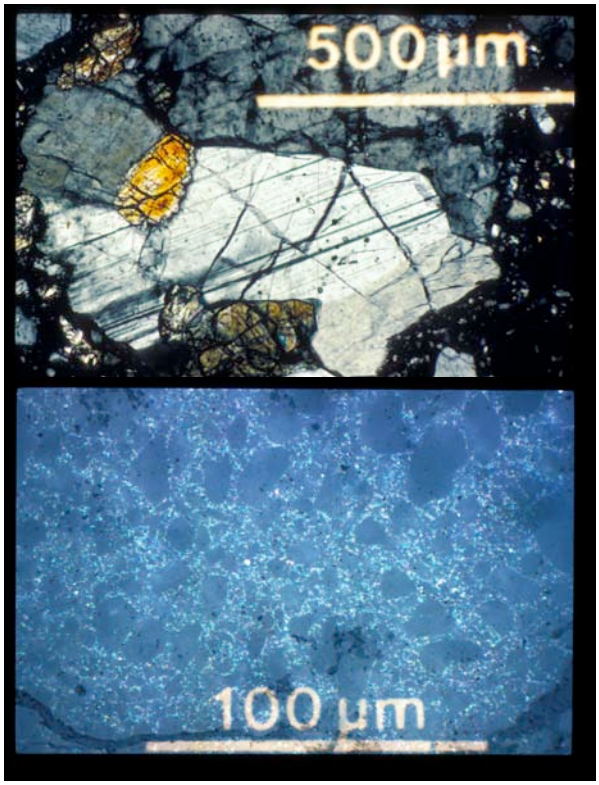

Fig. 1. *Photomicrographs of lithic clasts from North Ray crater breccia 67016. (1a - upper) ferroan noritic anorthosite, transmitted light. (1b - lower) fragment-laden, melt matrix clast, reflected light.*

The provenance of these breccias and their genetic relationship to major basins such as Imbrium and Nectaris has been a matter of debate since they were collected by the Apollo 16 mission. Post-mission geological interpretations concluded that they were most likely emplaced as ejecta from either Imbrium or Nectaris, and relatively little progress toward resolving this uncertainty has been made. Since the early 1980's the consensus has favored an origin as Nectaris ejecta for the North Ray crater breccias [5]. However, many of the anorthositic clasts have ^{40}Ar-^{39}Ar ages that are identical with the commonly accepted age of Imbrium and KREEP-rich clasts have been recognized in these breccias [3, 5]. These observations tend to support an origin for these breccias as Imbrium ejecta.

Ages: ^{40}Ar-^{39}Ar plateau ages ≥4.0 Ga are commonly, but not exclusively, obtained from the fragment-laden, melt matrix clasts such as those shown in Fig. 1b. For example, melt-matrix clasts extracted from North Ray breccia 67016 have apparent plateau ages of 4.02 to 4.25 Ga, compared to 3.84-3.87 Ga for anorthositic clasts from the same breccia (Fig. 2).

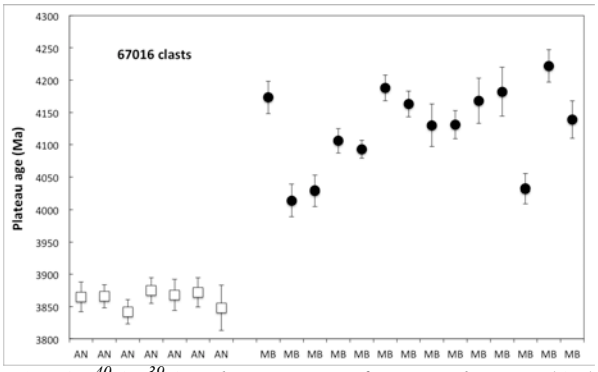

Fig. 2. *^{40}Ar-^{39}Ar plateau ages for anorthositic (AN) and melt-matrix (MB) clasts from North Ray breccia 67016. Data from [3].*

The range of apparent plateau ages obtained from these breccias and the associated regolith may imply an extended record of impacts on the Moon prior to the canonical Terminal Cataclysm. This possibility may be supported by ^{40}Ar-^{39}Ar ages obtained from other lunar anorthosites and granulitic breccias [4, 6], U-Pb ages of some lunar zircons and other U-bearing phases [7, 8], and the Re-Os isotopic composition of impact melt rock 67935 [9]. Fernandes [4] has proposed that the ^{40}Ar-^{39}Ar characteristics of some igneous lunar crustal rocks reflects exhumation by basin-scale impacts, but

petrographic characteristics of the melt matrix clasts that yielded the older Ar ages suggest that they represent relatively small volumes of melt compared to the clast-poor crystalline melt rocks that have been linked to the lunar cataclysm.

An additional consideration is the extent to which the isotopic record of impact ages in these samples may have been obscured by subsequent events. Both Shuster et al [2] and Norman et al. [3] illustrate possible effects of younger thermal events on ^{40}Ar-^{39}Ar step release patterns of clasts extracted from the North Ray breccias and associated regolith. In addition, the fragment-rich nature of many of the melt matrix clasts (Fig. 1b) raises concerns about inheritance of older, incompletely degassed components.

Based on available data, it seems clear that the melt-matrix clasts typically carry a higher proportion of inherited Ar than do the crystalline anorthosite lithic clasts from these same breccias. For example, a number of the melt matrix clasts studied by [3] have high-T steps with apparent ages ≥4.4 Ga, while these are rare in the data from the crystalline anorthosite clasts examined by that study. In addition, the slopes of the step-release plateaus obtained from 67016 melt breccia clasts are often steeper than those of the anorthosite clasts from this breccia (Fig. 3, 4). Intercept ages calculated from the plateau steps are systematically younger than the plateau ages themselves, also reflecting the slopes on those plateaus (Fig. 3, 4). In contrast, the anorthositic clasts have intercept ages that agree well with the plateau ages, as expected for well-behaved step-release plateaus (Fig. 3, 4).

Implications for impact history: The petrology and well-defined crystallization age of the melt rock protolith of lunar sample 67955 show that the North Ray crater breccias do preserve evidence for a 4.2 Ga basin-scale impact on the Moon [8]. However, the apparent range of ^{40}Ar-^{39}Ar ages obtained from clasts extracted from the North Ray breccias may reflect variable resetting of ejecta that was originally associated with that 4.2 Ga basin rather than a number of distinct impact events. This possibility is suggested by the step release patterns of melt matrix clasts which often show a quasi-continuous increase in apparent ^{40}Ar/^{39}Ar age that approaches an upper limit of ~4.2 Ga prior to the high-T steps (Fig. 3). Frequency distributions of melt rock ages aimed at representing lunar impact flux may wish to consider this potential bias in the data. Geochemical characteristics of 67955 suggest that the provenance of the 4.2 Ga basin was likely within the PKT rather than representing Nectaris [8]. Possible links between other records of a 4.2 Ga impact on the Moon and this PKT basin remain to be explored.

References: [1] Maurer P. et al. (1978) *GCA, 42*, 1687-1720. [2] Shuster D. L. et al. (2010) *EPSL, 290*, 155-165. [3] Norman M. D.et al. (2010) *GCA, 74*, 763-783. [4] Fernandes V. A. et al., (2013) *MAPS, 48*, 241-269. [5] Stoffler D et al. (2006) *Rev. Mineral. Geochem., 60*, 519-596. [6] Hudgins J. A. et al. (2008) *GCA, 72*, 5781-5798. [7] Grange M. L. et al. (2009) *GCA, 73,* 3093-3107. [8] Norman M. D. and Nemchin A. A. (2014) *EPSL, 388*, 387-398. [9] Fischer-Gödde M. and Becker H. (2012) *GCA, 77*, 135-156.

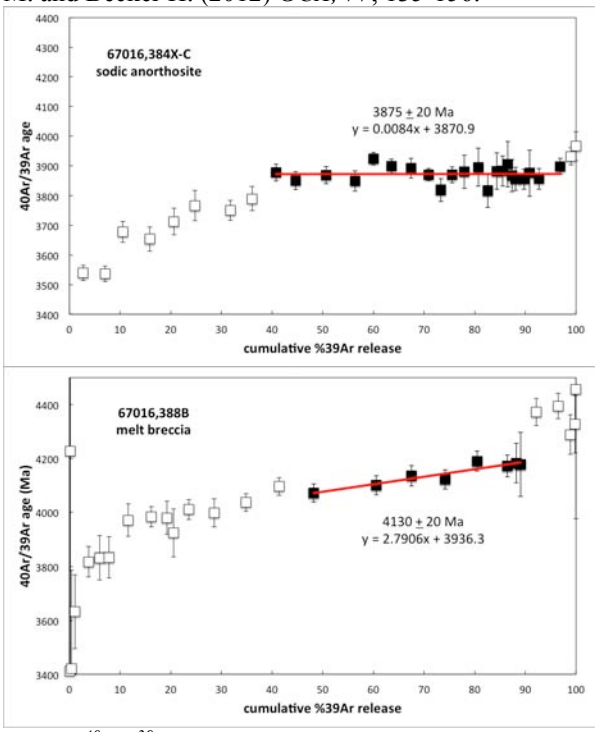

Fig. 3. *^{40}Ar-^{39}Ar step release patterns for (a) a crystalline anorthosite clast and (b) a fragment-laden melt matrix clast from 67016 illustrating calculation of slopes and intercept ages from the plateau steps (filled squares). Data from [3].*

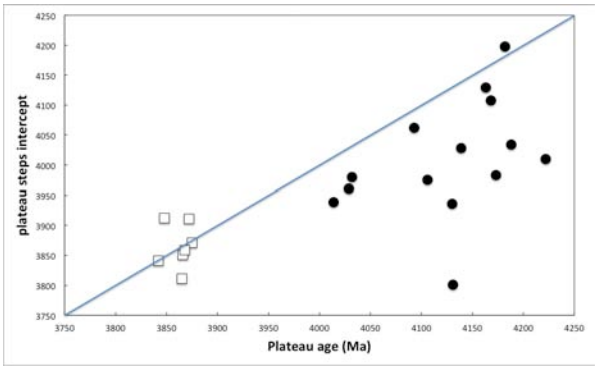

Fig. 4. *Fragment-laden melt matrix clasts from breccia 67016 have systematically older plateau vs. intercept ages, illustrating the consistently greater slope on the melt clast release patterns. Data from [3].*

THE LUNAR INCLINATION AS A MONITOR OF LATE STAGE TERRESTRIAL ACCRETION. K. Pahlevan and A. Morbidelli, Lagrange Laboratory, Observatoire de la Côte d'Azur, Nice, France (pahlevan@oca.eu)

Introduction: The Moon is generally thought to have formed from the debris ejected by the impact of a planet-sized object with the proto-Earth towards the end of planetary accretion. While the "lateness" of this event during the Earth's accretion has been assumed and/or favored for over a decade [1], it has never been quantitatively demonstrated nor precisely quantified. Here, we identify a new mechanism – differential momentum transfer during three-body encounters – for tilting the primordial lunar orbit. We show that the inclination of the lunar orbit is a sensitive recorder of dynamical events in the Earth-Moon system and that the smallness of its value (~5 degrees at present) is a reflection of the occurrence of the Moon-forming event towards the very end of Earth's accretion. With this mechanism, we can quantify how dynamically pristine the Earth-Moon system is, constrain the largest post-lunar-formation impacts with the Earth, and limit the angular momentum change of the system via collisional and collisionless interactions with remnant bodies following the Moon-forming event.

The Moon-forming impact is thought to have generated a compact debris disk (within < 10 Earth radii) from which the Moon rapidly accreted. Like Saturn's rings, the proto-lunar disk is expected to have become an equatorial disk on a timescale rapid relative to its evolutionary timescale. Hence, so long as the proto-lunar material disaggregated into a disk following the giant impact, the Moon is expected to have accreted within ~1 degree of the Earth's equator plane [2]. Tidal evolution calculations suggest that for every degree of inclination to the Earth's equator plane at an Earth-Moon separation of 10 R_E, the lunar orbit will exhibit half a degree of inclination to Earth's orbital plane at its present separation of 60 R_E [3, 4]. Hence, the present ~5 degree lunar inclination – without external influences – translates to a ~10 degree primordial inclination relative to Earth's equator shortly after lunar formation. This ~10x difference between the modern system and theoretical expectations has become known as the lunar inclination problem.

Previous work: Prior work on this problem has sought to identify mechanisms such as a gravitational resonance between the newly formed Moon and the Sun [5] or the remnant proto-lunar disk [6] that can excite the lunar inclination to its present high value. However, neither one of the proposed mechanisms has been established as the former requires particular values of the tidal dissipation parameters while the latter has only been shown to be viable in an idealized system where a single Moon interacts with a single pair of resonances in the proto-lunar disk. Here, we identify three-body encounters as an excitation mechanism that can – in fact – generate inclinations much larger than that which is observed. We then ask a different question: why isn't the inclination of the lunar orbit greater than it is? We then use the *smallness* of the observed value of the inclination to set constraints on the amount and character of accretion experienced by the Earth-Moon system following its origin.

Context: After the giant impact and lunar accretion, lasting at most ~10^3 years [7, 8], the Moon begins a steady outward tidal evolution. On a timescale rapid relative to the timescale between large impacts in the final stage of planet formation (~10^6-10^7 years) [9], the lunar orbit expands through the action of tides to an Earth-Moon separation of ~20-30 R_E, transitions from precession around the spin-axis of the Earth to precession around the vector normal to its heliocentric orbital plane [3], and its inclination becomes insensitive to the shifting of the Earth's equator plane via impacts [10]. However, the lunar inclination remains sensitive – indeed becomes more sensitive – to excitation via differential momentum transfer as orbital expansion proceeds. While the lunar eccentricity may be damped via tidal dissipation in the Moon, the lunar inclination is largely preserved via tidal evolution over geologic time and carries information about dynamical events in the history of the Earth-Moon system. The present lunar orbit is therefore a reflection of the dynamical environment prevailing in the inner Solar System at the time of the lunar-forming event.

Model/Results: We have developed a model tracking the early orbital evolution of the Earth-Moon system subject to tides and gravitational encounters from interloping bodies. We use the model to follow interactions with the nascent Earth-Moon system in the tens of millions of years followings its formation. We find that both collisional and collision-less interactions with the Earth-Moon system can significantly excite the system dynamically (Fig. 1). While the effects of in-plane perturbations excite the eccentricity and can be erased via tidal dissipation over geologic time, out-of-plane perturbations will excite the lunar inclination and will be largely preserved over the subsequent history. Importantly, encounters of remnant bodies with the nascent terrestrial planets are expected to be in the "dispersion" regime, that is, isotropic [10]. Statistical constraints can therefore be placed on the remnant bodies, including constraints on the size distribution

[11] of remnant populations and on the most massive member (after the Moon-forming impactor).

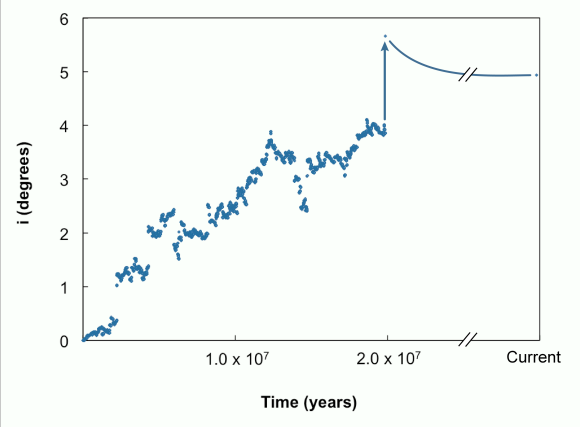

Fig. 1 – A simulation of lunar inclination excitation via collisionless and collisional interactions with a single massive body of ~0.01 M_E. Both cumulative collisionless and impulsive collisional excitation (at ~20 Myrs) contribute significantly to the final excitation. In this simulation, subsequent tidal evolution via planetary tides alone reproduces the observed inclination of the modern Moon.

Due to the stochasticity inherent in this problem, we have performed a large number of simulations to quantify the statistical constraints on likely outcomes. We will present results showing the sensitivity of the excitation to the amount and nature of post-impact accretion as well as sensitivity to early tidal evolution rates.

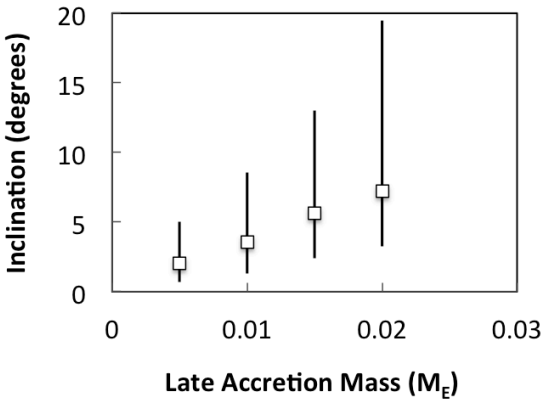

Fig. 2 – A summary of several hundred simulations used to characterize likely outcomes of three-body interactions in the Earth-Moon system. Displayed are the median values and 1σ intervals of inclination excitation versus the mass of late accretion delivered in a single massive body with k2/Qp = 0.03.

Dynamical environments: There is currently an active, vigorous debate regarding the nature of the Moon-forming impact, with ideas ranging from the classic Mars-mass impactor onto a nearly-formed proto-Earth [1, 12, 13], to a nearly symmetric collision between two ~half-Earth-mass bodies [14], to a high-velocity, nearly head-on collision with a rapidly-rotating Earth [15] to a Moon-forming impact that is described as a hit-and-run event [16]. While we do not attempt to determine which – if any – of these impacts corresponds to *the* Moon-forming event, we note that these distinct impacts correspond to distinct dynamical environments in the inner Solar System that can be identified.

Conclusions: The Moon-forming giant impact has generally been assumed to take place towards the very end of terrestrial accretion. The isotopic similarity observed between silicate Earth and Moon has been used to set constraints on post-Moon-formation terrestrial accretion, but such a constraint requires assumptions about the composition and differentiation state of accreting bodies and their behavior upon impact. Here, we have identified a mechanism – three-body interactions – that can naturally reproduce the lunar orbital excitation and sets direct constraints on the number and mass of remnant bodies in the terrestrial planet region at the time of the Moon-forming giant impact. The implications of this constraint for the dynamical environment in the inner solar system at the time of lunar formation will be discussed.

References: [1] Canup R. M. and Asphaug E. (2001) *Nature*, 412, 708-712. [2] Ida, S., Canup, R. M., and Stewart, G. R. (1997) *Nature*, 389, 353-357. [3] Goldreich, P. (1966) *Rev. Geophys.* 4, 411-439 [4] Touma, J. and Wisdom, J. (1994) *Astron. J.,* 108, 1943-1961. [5] Touma, J. and Wisdom, J. (1998) *Astron. J.,* 115, 1653-1663. [6] Ward, W. R. and Canup, R. M. (2000) *Nature*, 403, 741-743. [7] Salmon, J. and Canup R. M. (2012) *Ap.J.*, 760, 83. [8] Thompson, C. and Stevenson, D.J. (1988) *Ap. J.*, 333, 452-481. [9] Agnor, C. B., Canup, R. M. and Levison, H. F. (1999) *Icarus,* 142, 219-237. [10] Canup, R. M. (2004) *Annu. Rev. Astron. Astrophys.* 42, 441-475. [11] Bottke, W. F. (2010) *Science*, 330, 1527-1530. [12] Canup, R. M. (2004) *Icarus*, 168, 433-456. [13] Canup, R. M. (2008) *Icarus*, 196, 518-538. [14] Canup (2012) *Science*, 338, 1052-1055. [15] Cuk and Stewart (2012) *Science*, 338, 1047-1052. [16] Reufer et al. (2012) *Icarus* 221, 296–299.

TESTING THE COLLISIONAL EROSION HYPOTHESIS FOR THE HADEAN EARTH

Ross W. K. Potter[1,2,3] and David A. Kring[2,3], [1]Dept. Earth, Environmental and Planetary Sciences, Brown University, Providence, RI, 02912, USA, [2]Center for Lunar Science and Exploration, Lunar and Planetary Institute, 3600 Bay Area Boulevard, Houston, TX, 77058, USA, [3]NASA Solar System Exploration Research Virtual Institute; ross_potter@brown.edu.

Introduction: Impact cratering is a fundamental geologic process involved in the original accretion and subsequent evolution of planetary bodies throughout the Solar System. Impacts have the ability to add or remove material from their target body and, therefore, affect their target's geochemical make-up.

Geochemical studies have shown that Earth, relative to chondritic and/or solar abundances, is depleted in heavy halogens (Cl, Br, I) [1]; has a superchondritic Fe/Mg ratio (possibly by erosion of silicates relative to metals) [2], and; a superchondritic Sm/Nd ratio [3-5]. O'Neill and Palme [2] proposed the concept of collisional erosion, whereby impact events lead to the preferential removal of Earth's enriched crustal material, to explain these geochemical signatures.

To be consistent with the abundances modeled, collisional erosion of Earth, if it occurred, must have taken place early in its history during the Hadean period (~4.5 to 3.8 Ga). O'Neill and Palme [2] suggest collisional erosion could have either (i) stripped refractory lithophile element (RLE)-rich crust from planetesimals that then accreted to form the Earth or (ii) stripped RLE-rich crust from an initially chondritic Earth during the final stages of accretion. Current data allow a fairly well constrained test of scenario (ii) relative to scenario (i). Here, therefore, analytical methods are used to assess removal of Earth's crustal material from the time of the proposed Moon-forming impact through the end of the Late Heavy Bombardment (LHB) when impacts were sufficiently large to potentially erode significant amounts of crust.

Methods: We test the collisional erosion model with four plausible impactor size-frequency distributions (SFDs) derived from examining crater size distributions on the Moon [6]. The lunar crater size distributions imply impactor SFDs similar to that among main belt asteroids [6,7], whose flux can then be scaled from the Moon to the Hadean Earth [8,9]. These size distributions include impactors up to, nominally, 1000 km in diameter.

To determine the fraction of impact-excavated crust that escapes Earth's gravity (V_{esc} > 11.2 km/s) during the Hadean, the mass of material (M) ejected was calculated using an equation from [10]:

$$\frac{M(V_{esc})}{m} = 0.1398\left[\frac{V_{esc}}{U}\left(\frac{\rho}{\delta}\right)^{\frac{4}{33}}\right]^{-1.65} \quad (1)$$

where m is the impactor mass, U is the impactor velocity, ρ is the target density, and δ is the impactor density. Impact velocities between Earth's escape velocity (11.2 km/s) and 35 km/s were analyzed, with impactor and target densities assumed to be the same (3000 kg/m^3). The constants in Equation 1 incorporate a number of parameters, with values appropriately chosen for impacts into rock [10-13]. Equation 1 defines the mass ejected above a given velocity in terms of impactor properties; crater properties are, therefore, not significant.

The presence, volume, extent, and persistence of crustal material during the Hadean period is unknown and remains a contentious issue [14 and references therein]. Here, the mass of crust was defined as a fraction of the silicate Earth mass (4x10^{24} kg). To be consistent with previous studies [2,15] crustal mass fractions of 0.002 (similar to Earth's oceanic crust today) to 0.08 (a suitable value for the lunar crust) were considered. As with [2], a basaltic crust was assumed.

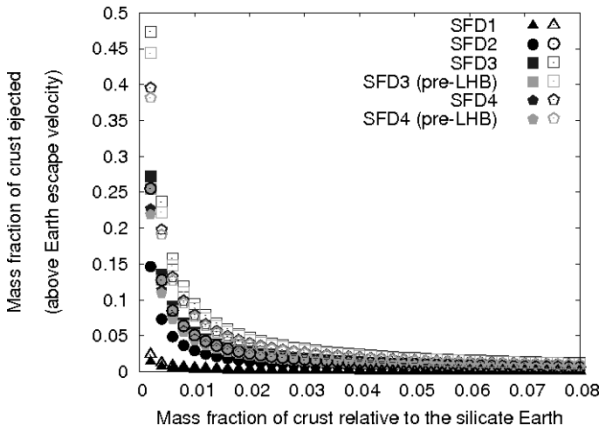

Figure 1: Mass fraction of crust ejected above Earth escape velocity as a function of crustal mass fraction relative to the silicate Earth for 25 km/s (solid symbols) and 35 km/s (open symbols) impact velocities.

Results: Figure 1 plots the mass fraction of crustal material ejected above V_{esc} as a function of mass fraction of crust relative to the silicate Earth for two sets of impact velocities (solid symbols: 25 km/s; open symbols: 35 km/s) for the four impactor SFDs. The results demonstrate that the higher the impact velocity, the

greater the crustal fraction ejected above escape velocity. Size-frequency distributions 3 and 4 are divided into total and pre-LHB populations. These illustrate that the vast majority of crustal material for these respective distributions (>95%) is removed from Earth prior to, rather than during, the LHB.

Discussion: Removal of a greater percentage of crustal material prior to, rather than during, the LHB is a consequence of the greater number and size of impactors in the early Hadean. No SFD, however, removed more than 50% of the crust. The total percentage of crust ejected could be increased by considering very large (albeit low probability) impactors that were present during this time (up to 4000 km in diameter [9]). Figure 2 illustrates the outcome with one of the SFDs supplemented by a 2000, 3000, or 4000 km diameter impactor. This demonstrates that the addition of one very large impactor can help this SFD remove enough crustal mass to be consistent with the chemical constraints of collisional erosion scenarios [2,15]. The successful scenarios, though, require impact velocities of >25 km/s, which are possibly greater than the average impact velocities prior to the LHB (11 km/s [7]).

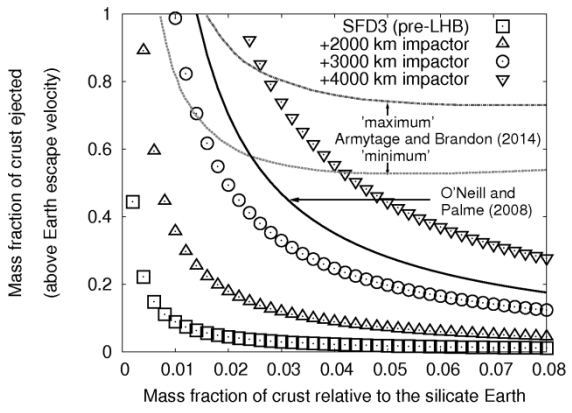

Figure 2: Mass fraction of crust ejected above Earth escape velocity as a function of crustal mass fraction relative to the silicate Earth for SFD3 supplemented by one 2000, 3000, or 4000 km diameter impactor (all impacts at 35 km/s). Data points that plot along or above the data from O'Neill and Palme [2] and Armytage and Brandon [15] represent successful collisional erosion scenarios, where enough crustal mass has been removed to satisfy geochemical constraints.

The work of [2] requires the removal of crustal material with a mass equivalent to 1.4% of Earth's mass and, therefore, a volume of ~10^{10} km^3. If this crustal volume covered Earth's entire surface it would be equivalent to a global crustal layer 70 km thick. Estimates of crustal thicknesses in the Hadean, however, range from ~20-40 km [e.g., 16]. Thus, the model only works if that volume was removed serially via multiple impacts.

Geographical distribution of crust will also heavily influence its removal. If all crustal material was concentrated in a single area, it could potentially be removed by a single impact, such as scenarios recently suggested for the proposed Moon-forming impact [17]. Additionally, if any continental crust was present on the Hadean surface, removal of a given volume of this would alter Earth's geochemical to a greater extent than the same volume of basaltic crust due to its enrichment in a number of RLE [18].

Conclusions: Collisional erosion during the Hadean is a viable mechanism to explain Earth's observed geochemical signatures only if certain dynamical considerations are met. It requires an impactor size-frequency distribution containing at least one very large (>2000 km diameter) impactor and average impact velocities >25 km/s. The vast majority of crustal material would likely have been removed prior to the Late Heavy Bombardment if those dynamical constraints existed.

References: [1] Sharp, Z. D. and Draper, D. S. (2013) *EPSL*, 369-370, 71-77. [2] O'Neill, H. St. C. and Palme, H. (2008) *Phil. Trans. R. Soc.*, 366, 4205-4238. [3] Boyet, M. and Carlson, R. W. (2005) *Science*, 309, 576-581. [4] Armytage, R. M. G. and Brandon, A. (2013) *LPSC XLIV*, #1708. [5] Campbell, I. H. and O'Neill, H. St. C. (2012) *Nature*, 483, 553-558. [6] Strom, R. G. et al. (2005) *Science*, 309, 1847-1850. [7] Marchi, S. et al. (2012) *EPSL*, 325-326, 27-38. [8] Abramov, O. et al. (2013) *Chemie der Erde*, 73, 227-248. [9] Marchi, S. et al. (2014) *Nature*, 511, 578-582. [10] Housen, K. R. and Holsapple, K. A. (2011) *Icarus*, 211, 856-875. [11] Housen, K. R. et al. (1983) *JGR*, 88, 2485-2499. [12] Schmidt, R. M. and Housen, K. R. (*1987) Int. J. Impact Eng.*, 5, 543-560. [13] Holsapple, K. A. (1993) *Ann. Rev. Earth Planet. Sci.*, 21, 333-373. [14] Harrison, T. M. (2009) *Ann. Rev. Earth Planet. Sci.*, 37, 479-505. [15] Armytage, R.M.G. and Brandon, A. (2014) *LPSC XLV*, #1883. [16] van Thiesen, P. et al. (2004) *Phys. Earth Planet. Int.*, 142, 61-74. [17] Ćuk, M. and Stewart, S. T. (2012) *Science*, 338, 1047-1052. [18] Taylor, S. R. and McLennan, S. M. (1985) *The continental crust: its composition and evolution*, Blackwell, Oxford.

Theian Orbital Evolution Amidst the Planetary Leftovers B. Quarles[1] and J. J. Lissauer[1], [1]NASA Ames Research Center, Space Science and Astrobiology Division, MS 245-3, Moffett Field, CA 94035-1000 (billy.l.quarles@nasa.gov)

Introduction:

The formation of the Earth's Moon commonly involves a theory where Theia, a Mars-sized object [1,2], encounters the proto-Earth via a Giant Impact. Updated measurements based on lunar samples indicate an age of the Moon to be roughly 70-110 Myr [3,4] younger than the Calcium Aluminum Inclusions in the chondritic meteorites. This implies that Theia likely existed for 20-80 Myr as one of five surviving terrestrial embryos [5] embedded in a planetesimal disk leftover from the late stage of planetary accretion [6,7].

Simulations of a Moon-forming giant impact using smooth particle hydrodynamics have been successful in providing insight into what initial conditions are required with respect to the collision parameters and compositions [8]. But the mass of the impactor is largely unconstrained and can vary depending on the chosen model [9,10]. Using a dynamical 5 terrestrial planet model we present our current work to understand how the penultimate orbit of Theia influences the early bombardment history of the terrestrial planets.

Method:

We use a custom dynamical model (an improved version of [11]) in which the collision parameters are determined just before a collision [5]. Using this model, we investigate a broad parameter space for starting values of the semimajor axis and eccentricity of Theia, which we present only a sample case. The corresponding starting conditions of the proto-Earth are determined through conservation of angular momentum with the current Earth-Moon system. All other orbital parameters for the other terrestrial and giant planets are taken from a recent common ephemeris. Mass ratios of between the proto-Earth and Theia (8:1 and 4:1), are considered within a range of semimajor axis (0.76 – 1.55 AU) and eccentricity (0.0 – 0.1).

This model assumes a Solar System architecture of giant planets, however this may not have been the case for the era in question. Thus we investigate an alternate giant planet architecture consistent with the Nice model [12] configuration for the 4:1 mass ratio to determine the possible consequences of the Nice model on the early bombardment. We prescribe a disk of planetesimals for this epoch consisting of ~600 bodies with a total mass ranging from 0.02 to 0.2 Earth masses. The starting orbital parameters of these bodies are chosen from statistical distributions. We begin with 1000 test particles and select those that survive the first ~2 Myr of evolution. The next step in our simulations will use the results of these distributions as a representative sample of the likely sample of early bombardment impactors.

Preliminary Results:

We show the results of a test particle simulation considering the Solar System to include five terrestrial planets and the present giant planet configuration. The starting semimajor axis of Theia is 1.10 AU for the simulations shown and the starting semimajor axis of the proto-Earth is adjusted based on angular momentum conservation [5]. The starting semimajor axis distribution was chosen to be uniform from 0.6 to 1.6 AU containing 10 planetesimals in increments of 0.01 AU.

Figure 1 shows the starting distribution (solid line) in semimajor axis along with the distribution of surviving test particles after ~2 Myr of evolution. The surviving population (dashed lines) of test particles show random variations from the starting uniform distribution. Additionally, there does not appear to be a dependence on the mass ratio assumed.

The eccentricity the planetesimals considered was selected from a Rayleigh distribution (solid line) with a scale parameter of 0.1. Figure 2 demonstrates the resulting eccentricity distributions (dashed lines) that follow a similar shape to the starting distribution. The planetesimals are excited over this 2 Myr simulation, which is likely due to secular perturbations from the giant planets.

Discussion:

Distributions of planetesimals are evolved for ~2 Myr under a five terrestrial planet Solar System model. On the this timescale, the test particles are randomized in semimajor axis and excited in eccentricity. The results presented will be part of a larger study evaluating the contribution of Theia's gravitational influence within this early epoch. Our future work will consider simulations for an additional 200 Myr, track the bombardment of this population onto the terrestrial planets, and determine what influence a disk of debris has on a late Giant Impact of Theia with the proto-Earth.

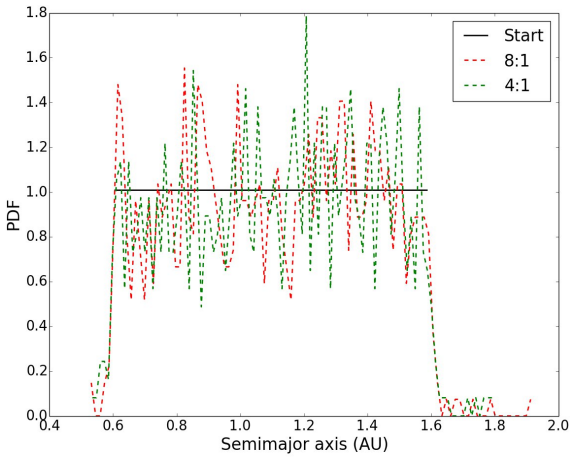

Figure 1: The semimajor axis distribution after ~2 Myr of evolution considering the 8:1 and 4:1 mass ratios. The starting values for the planetesimals were chosen from a uniform distribution ranging from 0.6 to 1.6 AU.

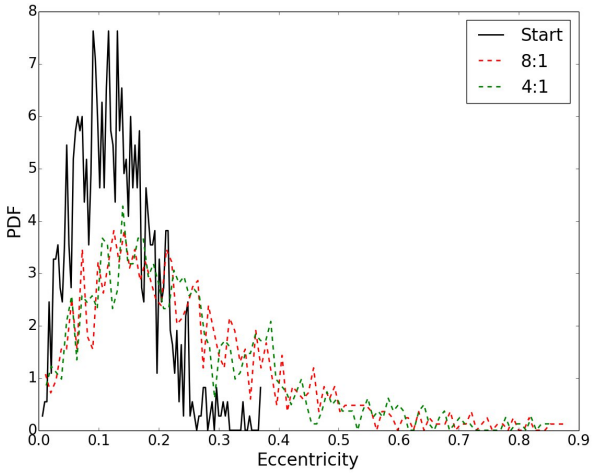

Figure 2: The eccentricity distribution after ~2 Myr of evolution. The starting values of eccentricity for planetesimals were drawn from a Rayleigh distribution with a scale parameter of 0.1.

References:

[1] Hartmann, W. K. and Davis, D. R.,. Icarus 24, 504–514 Apr. 1975.
[2] Cameron, A. G. W. and Ward, W. R., LPSC VII, 120-121 Mar. 1976.
[3] Brandon, A., Nature 450, 1169-1170 Dec. 2007.
[4] Borg, L. E., Connelly, J. N., Boyet, M., and Carlson, R. W., Nature 477, 70-72 Sep. 2011.
[5] Quarles, B., and Lissauer, J.J. Icarus (in Press) Nov. 2014
[6] Jacobson, S., and Morbidelli, A., Phil. Trans. A. 372 20130174 (2014)
[7] Jacobson, S.A, Morbidelli, A., Raymond, S.N., et al., Nature 508, 84-87 April 2014
[8] Cameron, A. G. W., LPSC XXXI, 133-144, Mar. 2000.
[9] Canup, R. M., Science 338, 1052, Nov. 2012
[10] Cuk, M. and Stewart, S. T., Science 338, 1047, Nov. 2012
[11] Rivera, E. J., Ph.D. thesis, State University of New York at Stony Brook, 2002
[12] Morbidelli, A., Tsiganis, K., Crida, A., Levison, and H. F., Gomes, R., AJ 134, 1790–1798, Nov. 2007

RE-EVALUATION OF HSE DATA IN LIGHT OF HIGH P-T PARTITIONING DATA: LATE CHONDRITIC ADDITION TO INNER SOLAR SYSTEM BODIES NOT ALWAYS REQUIRED FOR HSE.

K. Righter[1], [1]Mailcode XI2, NASA Johnson Space Center, 2101 NASA Parkway, Houston, TX 77058 (kevin.righter-1@nasa.gov).

Introduction: Studies of terrestrial peridotite and martian and achondritic meteorites have led to the conclusion that addition of chondritic material to growing planets or planetesimals, after core formation, occurred on Earth, Moon, Mars, asteroid 4 Vesta, and the parent body of the angritic meteorites [1-4]. One study even proposed that this was a common process in the final stages of growth [5]. These conclusions are based almost entirely on the 8 highly siderophile elements (HSE; Re, Au, Pt, Pd, Rh, Ru, Ir, Os), which have been used to argue for late accretion of chondritic material to the Earth after core formation was complete (e.g., [6]). This idea was originally proposed because the D(metal/silicate) values for the HSE are very high (>10,000), yet their concentration in the terrestrial mantle is too high to be consistent with such high Ds. The HSE in the terrestrial mantle also are present in chondritic relative abundances and hence require similar Ds if this was the result of core-mantle equilibration. The conclusion that late chondritic additions are required for all five of these bodies is based on the chondritic relative abundances of the HSE, as well as their elevated concentrations in the samples. An easy solution is to call upon addition of chondritic material to the mantle of each body, just after core formation; however, in practice this means similar additions of chondritic materials to each body just after core formation which ranges from ~ 4-5 Ma after T_0 for 4 Vesta and the angrites, to 10-25 Ma for Mars, to 35 to 60 Ma for Moon and perhaps the Earth [7].

Since the work of [6] there has been a realization that high PT conditions can lower the partition coefficients of many siderophile elements, indicating that high PT conditions (magma ocean stage) can potentially explain elevated siderophile element abundances [8,9]. However, detailed high PT partitioning data have been lacking for many of the HSE to evaluate whether such ideas are viable for all four bodies. Recent partitioning studies have covered P, T, fO_2, and compositional ranges that allow values to be predicted at conditions relevant to these five inner solar system bodies. Because the D(HSE) metal/silicate are lowered substantially at higher PT conditions and natural compositions (FeNi metallic liquids and peridotites) it is natural to re-examine the role of core formation on the HSE patterns in a variety of inner solar system bodies. Here I will discuss other processes (including high PT core formation for Mars, Moon and Earth) that can produce the observed HSE patterns, and demonstrate that there are viable hypotheses other than the "one size fits all" hypothesis of late chondritic additions.

Mars – Compilation of HSE partitioning data for metal/silicate Ds, as well as martian samples led Righter et al. (2014) [10] to conclude that the HSE concentrations in the martian mantle could have been established by an early magma ocean stage for Mars. Such conditions would have been established near the end of growth of Mars during accretion, where metal and silicate equilibrated at 14 GPa, 2400 K, ΔIW = -1.5 and peridotite mantle and S- and C-bearing metallic core. These conditions also satisfy the concentrations of moderately siderophile elements (MSE; Ni, Co, Mo, W), and a number of other siderophile elements (Mn, V, Cr, Ga, Ge, etc.; [11-12]). These results indicate that a late chondritic addition is not required to explain the HSE concentrations in the martian mantle as proposed by a number of investigators, some of whom (e.g., [3]) deferred on evaluating the possibility of high PT core-mantle equilibrium due to lack of appropriate data.

4 Vesta – Studies of diogenites have revealed high and somewhat chondritic relative HSE abundances that have been interprteted as due to late chondritic additions to the mantle of 4 Vesta [5]. In addition, recent Si isotopic data for 4 Vesta [13] that are distinct from chondrites were interpreted as due to core formation at reduced conditions (IW-4) followed by addition late chondritic materials to satisfy the HSE. There are several aspects to these interpretations that are problematic, and an alternative explanation is necessary. First, core formation at IW-4 would leave the Vestan mantle nearly FeO-free. Addition of a small mass late chondritic material would not raise the FeO content to values that are consistent with current geochemical or geophysical estimates [14]. Second, most of the diogenites are pieces of the crust that have experienced chondritic contamination and brecciation. It would require only a small amount of chondritic metal in << 1 modal %, to explain the HSE patterns measured in diogenites. Other non-brecciated diogenites are also from the crust and have experienced post-shock annealing of brecciated diogenitic material [15]. Finally, the HSE patterns for diogenites are variable and fractionated [5], especially compared to the terrestrial primitive upper mantle. A more plausible explanation is that

Vesta experienced a magma ocean at IW-2.5, and diogenites experienced either addition of core metal by impact deformation [16] or simple addition of chondritic materials to the diogenitic breccias, this producing the widely variable but sometime chondritic relative HSE patterns. The latter are post core formation additions, but to the crust not the mantle.

Angrites – Angrites exhibit a wide range of rock types (including breccias, and cumulate or igneous textured rocks), and their HSE patterns also demonstrate high and somewhat chondritic relative abundances. This led [4] to conclude that the angrite parent body also experienced late chondritic additions. Although the angrites are certainly depleted in siderophile elements, and may have experienced core formation [17], their detailed geochemistry (elevated Ge and Ir) and their petrography suggests that they more plausibly formed as impact melts [18]. In this case, there may have been chondritic impactor that provided HSE. This was not the same as late chondritic additions to post-core formation mantle, but instead due to impacts that are quite common in the meteoritic record.

Earth and Moon - HSE studies of lunar materials have demonstrated some elevated concentrations and some chondritic relative patterns that have been attributed to late chondritic additions, or to stochastic late chondritic additions. However, a recent study [19] showed that in both the post core formation mantle and subsequent liquids in equilibrium with anorthosite, the HSE Ru, Pd and Au are fractionated by several orders of magnitude and not chondritic. If there had been post core formation but pre-anorthosite crust genesis addition of chondritic material to the lunar mantle, the HSE patterns would be elevated and chondritic relative, but they are not. Therefore late chondritic additions to the lunar mantle, if they occurred at all, must have been after anorthosite genesis, which means later than 100-200 Ma after T_0; this is a young event and more syncontemporaneous with heavy bombardment history.

Earth remains the only body to have compelling evidence for a late chondritic addition, but the uniqueness of this interpretation is also being challenged. The elevated and chondritic relative HSE patterns in the terrestrial PUM have been explained numerous times by addition of the "late veneer" or late chondritic additions after the core formed. This interpretation is due entirely to the inability of available (low PT) metal/silicate partition coefficients to explain the higher concentrations in the mantle. As new studies have ben completed at higher PT conditions and on more Earth-like compositions (peridotite and Fe-bearing metallic liquids that also contain a light element), it is clear that partition coefficients decrease substantially at the conditions that are more relevant to nature. Recent studies [20] at high PT conditions conclude decrease of D(HSE) metal/silicate, but nonetheless argue the need for late veneer because the Ds are not lowered enough. This however, was for metallic liquid that contained no light element. When calculated for the high PT conditions of core formation for Earth (~ 40 GPa), metal/silicate partition coefficients for Au, Pd, and Pt are all low enough to allow an equilibrium explanation for the concentrations in the primitive upper mantle (~600±200). The other five HSE elements – Re, Rh, Ru, Ir, and Os – are less well understood at these extreme conditions, but extension to high pressure conditions and to peridotites and FeNi metallic liquids with C, Si, O, and S may reveal possible solutions to the HSE abundances that do not require a late veneer or late chondritic additions. Sulfur alone has a substantial lowering effect that can almost explain several additional HSE [21]. For the Earth, lack of a late veneer would be consistent with recent other geochemical evidence such as water and D/H ratios also not requiring late additions of volatiles, as once had been argued [22].

Each of these five bodies possesses unique and specific aspects of their early history. Only Earth has compelling evidence for late chondritic additions, and this may also require revision in light of high PT metal-silicate partitioning data.

References: [1] Morgan, J.W. et al. (2001) MaPS 36, 1257–1275; [2] Bottke, W. et al. (2010) Science 330, 1527–1530; [3] Brandon, A. et al. (2012) GCA **76**, 206-235; [4] Riches, A. et al. (2012) EPSL 353/4, 208-218; [5] Day, J.M.D. et al. (2012) Nat. Geos. 5, 614-617; [6] Chou, C. (1978) PLPSC 9, 219-230. [7] Kleine, T. and Rudge, J. F. (2011) Elements *7*, 41-46; [8] Righter, K. (2003) AREPS 31, 135-174; [9] Righter, K. et al. (2014) In Treatise on Geochemistry (2nd Edition), edited by H.D. Holland and K.K. Turekian, Elsevier, Oxford, 449-477; [10] Righter, K. et al. (2014) MaPS; DOI: 10.1111/maps.12393; [11] Yang, S. et al. (2014) MaPS; DOI: 10.1111/maps.12384; [12] Righter, K. and Chabot, N.L. (2012) MaPS 46, 157–176; [13] Pringle, E.A. et al. (2013) EPSL 373, 75-82; [14] Mandler, B. E. and Elkins- Tanton, L. T. (2013) MaPS 48, 2333-2349; [15] Papike, J.J. (2000) MaPS 35, 875-879; [16] Rushmer, T. et al. (2006) 37th LPSC, #1936; [17] Righter, K. (2008) 39th LPSC, #1936; [18] Shirai, N., et al. (2009) 40th LPSC, #2122; [19] Sharp, M. G. et al. (2014) MaPS; DOI: 10.1111/maps.12396; [20] Mann, U. et al. (2012) GCA 84, 593-613; [21] Laurenz, V. et al. (2013) GCA 108, 172-183; [22] Sarafian, A. et al. (2014) Science 346, 623-626.

^{40}Ar/^{39}Ar AGE OF HORNBLENDE-BEARING R CHONDRITE LAP 04840. K. Righter[1] and M. Cosca[2] [1]Mailcode XI2, NASA Johnson Space Center, 2101 NASA Pkwy., Houston, TX 77058; [2]US Geological Survey, Denver Federal Center, MS 963, Denver, CO 80225.

Introduction: Chondrites have a complex chronology due to several variables affecting and operating on chondritic parent bodies such as radiogenic heating, pressure and temperature variation with depth, aqueous alteration, and shock or impact heating [1]. Unbrecciated chondrites can record ages from 4.56 to 4.4 Ga that represent cooling in small parent bodies. Some brecciated chondrites exhibit younger ages (<<4 to 4.4 Ga) that may reflect the age of brecciation, disturbance, or shock and impact events (<< 4 Ga).

A unique R chondrite was recently found in the LaPaz Icefield of Antarctica – LAP 04840 [2]. This chondrite contains ~15% hornblende and trace amounts of biotite, making it the first of its kind. Studies have revealed an equigranular texture, mineral equilibria yielding equilibration near 650-700 ºC and 250-500 bars, hornblende that is dominantly OH-bearing (very little Cl or F), and high D/H ratios [3,4,5]. To help gain a better understanding of the origin of this unique sample, we have measured the ^{40}Ar/^{39}Ar age (LAP 04840 split 39).

Results: The ^{40}Ar/^{39}Ar experiments were conducted at the U.S. Geological Survey in Denver, CO. Individual grains of amphibole were separated by crushing and hand-picking and loaded into platinum tubes and irradiated in the central thimble position of the USGS TRIGA reactor for 80 mega watt hours. The biotite GA1550 was used as the standard. Samples were evacuated within a custom built stainless steel extraction line, incrementally heated using a 25 W CO_2 laser, exposed to a cryogenic trap maintained at -130 ºC and a hot SAES GP50 getter and then expanded into a Thermo Fisher ARGUS-VI mass spectrometer. Argon isotopes (40, 39, 38, 37, 36) were analyzed in two separate experimental configurations. One grain was analyzed in multi-collection mode, with all argon isotopes measured simultaneously during 300 seconds of data collection, and another grain was analyzed using only the ion counter in peak hopping mode during 10 cycles of data collection. Both experiments yielded identical ^{40}Ar/^{39}Ar plateau ages of 4290 +/- 30 Ma (2 sigma); only the age spectrum obtained from the multi collection experiment is presented here. Ages were calculated after correction for blanks, detector intercalibration (<0.1%), radioactive decay subsequent to irradiation, and interfering nucleogenic reactions.

Discussion: The plateau age of 4290 +/- 30 Ma is younger than one would expect for a sample that has cooled within a small body [6], and one might instead attribute the age to a younger shock event. On the other hand, there is no evidence for extensive shock in this meteorite (shock stage S2; [3]), so this sample may have been re-annealed after a shock event. Indeed, detailed textural and petrographic studie of LAP 04840 have revealed evidence for post-shock annealing [7], which is consistent with the chronologic data obtained here. This age is similar to Ar-Ar ages determined for some other R chondrites [8,9]. R chondrites in general have yielded older impact ages (or annealing ages) than most other ordinary chondrites which show a wide range of ages from 4.4 to <1.0 Ga [10].

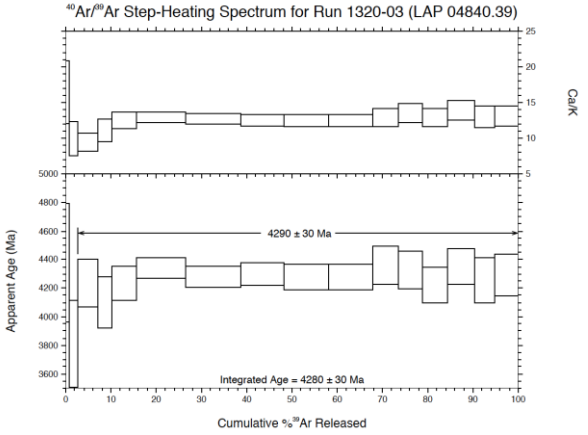

References: [1] Bogard, D. (2011) Chemie der Erde-Geoch. 71, 207-226. [2] Satterwhite, C.E. and Righter, K. (2006) Ant. Met. Newsl. 29, no. 1. [3] McCanta, M. et al (2008) GCA 72, 5757-5780. [4] Righter, K. and Neff, K. (2007) Polar Sci. 1, 25-44; [5] Ota, K., et al. (2009) J. Mineral. Petrol. Sci. 104, 215-225; [6] Bennett and McSween, H.Y., Jr. (1996) MaPS 31, 783–792. [7] Rubin, A.E. (2014) MaPS 45, 1057-1075; [8] Dixon, E. et al (2003) MaPS 38, 341-355. [9] Nagao,

K. et al (1999) Ant. Met. Res. 12, 81-93; [10] Swindle, T. et al. (2014) *Geol. Soc. Lon. Sp. Pub. 378*, 333-347.

THE AGE OF THE RHEASILVIA BASIN – HOW THE TWO GEOLOGICAL INTERPRETATIONS AND CHRONOLOGY SYSTEMS DIFFER. N. Schmedemann[1], T. Kneissl[1], A. Neesemann[1], G. Michael[1], H. Hiesinger[2], R. Jaumann[1,3], C. A. Raymond[4], C. T. Russell[5], [1]Institute of Geological Sciences, Freie Universität Berlin, Berlin, Germany, [2]Institut für Planetologie, Westfälische Wilhelms-Universität, Münster, Germany, [3]German Aerospace Center, Institute of Planetary Research, Berlin, [4]JPL, Caltech, Pasadena, CA, USA, [5]University of California, Los Angeles, CA, USA. (nico.schmedemann@fu-berlin.de)

Introduction: The highly successful Dawn mission [1] finished data collection at Vesta in 2012 and is now on its way to the dwarf planet Ceres, where it will arrive in spring 2015. A high number of papers presenting data and results from the Dawn at Vesta mission have already been published and are discussed in the scientific community. The complex interaction of many different processes in the low gravity environment represent a formidable challenge for correct interpretation and data analysis. With respect to the published results [2,3,4,5,6] on the formation age of the Rheasilvia basin and related chronology systems these difficulties became evident. While the protagonists of this discussion exchange very detailed arguments the broad community is confused about the results of crater retention ages on Vesta. In our presentation we will clarify the discussion by presenting three major reasons for the differing results in the asteroid-flux and lunar-like systems [7] by focusing on the results related to the Rheasilvia basin, because its formation influenced Vesta on a global scale.

Geologic Setting: Rheasilvia is both the largest and the youngest known basin on Vesta [8], not being superimposed by any other basin. The signature of its ejecta is visible over large parts of the Vestan surface [9] and they also are not superimposed by any younger basin. Rheasilvia cut one half of the underlying and smaller basin Veneneia. The outline of the remaining basin is preserved as a relatively shallow mountain range that intersects with the Rheasilvia basin rim.

Disagreement I – Which geologic unit should be used for dating Rheasilvia?: Studies by [2,3,4,5] (asteroid-flux system) use the floor of the Rheasilvia basin in order to use its crater retention age as basin formation age. Thus, these studies assume that the floor of the Rheasilvia basin was not significantly resurfaced after the basin formed. [6] (lunar-like system) use several areas on the Rheasilvia ejecta blanket, the top of the central peak of Rheasilvia as well as areas in the northern hemisphere of Vesta, that clearly show contemporary resurfacing events affecting crater diameters smaller than 40 to 60 km. The floor of the Rheasilvia basin is not used, because its sloping surface allows for regolith creeping, which "resurfaces" the basin floor. Impacts into the sloped basin floor could trigger repeated resurfacing events. The underlying assumption in this view is that the floor of the Rheasilvia basin is resurfaced subsequently and, thus only provides a minimum age but not necessarily the formation age of the basin. Topographically high standing areas with shallow slopes on top of the central peak and on the ejecta blankets of the Rheasilvia basin give more reliable basin formation ages. Furthermore, tectonic relationships [8] and hydrocode modelling by [10,11] suggest that the Rheasilvia impact is responsible for the formation of Divalia Fossae and for strong mechanical disturbance with temporal lifting of the top regolith layer in large parts of the Vestan northern hemisphere.

Data and results presented by [3] imply that Rheasilvia ejecta on the floor of the neighboring Veneneia basin is dated with about 2.1 Ga in the asteroid-flux system. In addition, according to Fig. 14c in [12] the formation of Divalia Fossae took place about 2 Ga ago in the asteroid-flux system, too. Thus, presented data in both publications indicate a Rheasilvia formation that predates the floor of Rheasilvia by about 1 Ga in the asteroid-flux system. Hence, the assumption in the asteroid-flux system of an unchanged floor of Rheasilvia since short after its formation is flawed. Therefore, the floor of the Rheasilvia basin cannot be used in order to date the basin formation.

Disagreement II – Crater Production Function (PF): The asteroid-flux system relies on a crater PF that is based on the observed average population in the asteroid Main Belt. Frequencies in the size range of unobservable (< ~1 km) projectiles are derived from models of collisional cascades [13]. Projectile sizes are scaled to impact crater sizes under the given impact properties on Vesta (in which both groups roughly agree). The underlying assumption in this view is, that each part of the asteroid Main Belt contributes roughly equally to the total impacting population on Vesta. Furthermore, it is assumed that the small crater distribution on Vesta reflects the average projectile distribution derived from collisional debris, regardless of the higher radiation force mobility of smaller pieces [14]. The lunar-like system is based on a crater PF that scales the very well-known lunar crater PF to the impact conditions at Vesta. The lunar cratering record is well known down to a few tens of meters crater diameter. Such craters are formed by very small projectiles, far smaller than the observational completeness in the

Main Belt. Thus, no extrapolation to small crater sizes is necessary in the lunar-like system. The underlying assumption in this view is, that the projectile size distribution on the Moon is exactly the same as for Vesta and only the flux differs. This implies that whatever forces and processes cause bodies to drift into the Main Belt resonance zones, from where they are excited into planet-crossing orbits, leading them eventually to impact the Moon, are the same forces and processes as bring the projectiles into the track of Vesta. That includes all kinds of forces acting on Main Belt asteroids such as size dependent radiation forces as well as size independent gravitational forces.

Data and results presented by [6,15,16,17] show that the small crater size distribution on 4 different Main Belt asteroids is clearly steeper than predicted by collisional cascade models and is as steep as the small crater size distribution observed on the Moon. Thus, extrapolated small crater size distributions based on models of collisional cascades do not seem to fit the data well. Such models are used in the asteroid-flux system and the related shallow PF is the reason why the Rheasilvia formation age derived from the floor of Veneneia [3] and the Divalia Fossae formation [12] is only ~2 Ga and not at least 3.5 Ga. ~3.5 Ga is the age of Rheasilvia in the lunar-like system, which chronology gives even younger ages than the asteroid-flux system chronology for ages higher than ~3 Ga.

Disagreement III – Chronology Function: The chronology function in the asteroid-flux system is built upon dynamical models of the Solar System evolution [18,19]. Because the location of Vesta is radially outside the proposed E-belt region but the Moon is inside and much more affected by E-belt projectiles than Vesta, the chronology functions between the Moon and Vesta are significantly different for the time of the LHB (late heavy bombardment) although they are based on the same set of dynamical models. The underlying dynamical models have been derived in order to explain a number of observations in the outer Solar System. In its early form the Nice model [20] was used to explain the idea of a "Terminal Lunar Cataclysm" [21] that is one way of interpretation of radiometric ages of lunar rock samples that show a pronounced peak of Ar-Ar ages around 3.9 Ga in many samples of different locations (Apollo landing sites). In the lunar-like chronology for Vesta the chronology curve has exactly the same smoothly decaying shape and thus the same time dependence in projectile flux like on the Moon [15], if the peak in Ar-Ar ages around 3.9 Ga is interpreted under consideration of sampling bias. The Vestan chronology curve is vertically offset w.r.t. the lunar chronology according to the much higher projectile flux at Vesta. This chronology assumes a relatively stable Solar System over at least the last ~4 Ga in which only the number of available projectiles inside the Main Belt decreased in a way that is resembled by the shape of the lunar impact rate that shows a smooth decline for about the first billion years of Solar System history. The lunar-like and asteroid-flux chronologies are nearly identical for the last ~3 Ga. For ages older than that differences of up to ~1 Ga occur for the same measured crater frequency.

Applying the lunar-like PF in combination with the asteroid-flux chronology the areas located on Rheasilvia ejecta and the central peak result in ages of ~4.4 Ga [6]. That is before the large impact events took place that are recorded in the Ar-Ar age distribution of brecciated, Vesta derived, HED meteorites [22,23]. Since Rheasilvia is the youngest basin on Vesta either the large events recorded in the Ar-Ar chronometer are not reflected by morphologically visible large impact structures or the asteroid-flux chronology results in too high absolute ages. Applying the lunar-like PF in combination with the lunar-like chronology to the same crater counts, and areas results in a reasonably good agreement with the youngest and most prominent peak in the Ar-Ar age distribution of brecciated eucrites between 3.3 and ~4 Ga [6]. That is well in agreement with the stratigraphic position of the Rheasilvia basin.

Implications for the LHB: Since [18] the smoothly decaying lunar chronology [15] is indistinguishable from the one based on the Nice model for the last 4.1 Ga. The chronology model test at Vesta shows that the lunar-like chronology gives more reasonable results than the asteroid-flux chronology. Thus, from this point of view a sudden discharge of projectiles during the heavy bombardment time period is not necessary. It looks more like the smooth tail of planetary accretion.

References: [1] Russell C.T. et al. (2012) Science, 336, 684-686; [2] Marchi S. et al. (2012) Science, 336, 690-694; [3] Schenk P. et al. (2012) Science, 336, 694-697; [4] O'Brien D.P. et al. (2014) PSS, 103, 131-142; [5] Marchi S. et al. (2014) PSS, 103, 96-103; [6] Schmedemann N. et al. (2014) PSS, 103, 104-130; [7] Williams D. A. et al. (2014) Icarus, 244, 158-165; [8] Jaumann R. et al. (2012) Science, 336, 687-690; [9] Reddy V. et al. (2012) Science, 336, 700-704; [10] Ivanov, B. A. and Melosh, H. J. (2013) JGR, 118, 1545-1557; [11] Bowling T.J. et al. (2013) JGR, 118, 1821-1834; [12] Williams D. A. et al. (2014) Icarus, 244, 74-88; [13] Bottke W. F. et al. (2005) Icarus, 179, 63-94; [14] Bottke W. F. et al. (2006) Annu. Rev. Earth Planet. Sci., 34, 157-191; [15] Neukum G. and Ivanov B. A. (1994) Crater size distributions and impact probabilities on Earth from Lunar, terrestrial planet, and asteroid cratering data. In: Gehrels T. (ed) Hazards due to comets and asteroids. University of Arizona Press, Tucson, 359–416; [16] Chapman C. R. et al. (1996) Icarus, 120, 77-86; [17] Chapman C. R. et al. (1996) Icarus, 120, 231-245; [18] Morbidelli A. et al. (2012) EPSL, 355,144-151; [19] Bottke W. F. et al. (2012), Nature, 485, 78-81; [20] Gomes R. et al. (2005) Nature, 435, 466-469; [21] Tera F. et al. (1974) EPSL, 22, 1-21; [22] Bogard D. D. and Garrison D. H. (2003) MaPS, 38, 669-710; [23] Bogard D. D. (2011) Chem. d. Erde; 71, 207-226.

THE CRATER PRODUCTION FUNCTIONS FOR MIMAS. N. Schmedemann[1], R. J. Wagner[2], G. Michael[1], T. Denk[1], T. Kneissl[1], [1]Institute of Geological Sciences, Freie Universität Berlin, Berlin, Germany, [2]German Aerospace Center, Institute of Planetary Research, Berlin. (nico.schmedemann@fu-berlin.de)

Introduction: The highly successful Voyager [1,2] and Cassini [3] imaging experiments revealed high quality imaging data that allows for a reasonably good analysis of the crater distributions on the Saturnian satellites [4,5,6]. The observed crater distributions appear to conflict with theoretical crater distributions that are derived from observed projectile populations [6,7]. In order to compare relative crater frequencies across different diameter ranges of measured craters a model of the crater production function is required. This function is fitted to the measured crater distribution and crater frequencies at a specific reference diameter can be determined from the function. Crater frequencies from measurements on high- and low-resolution imaging data or large and small areas can be compared relative to each other at the reference diameter. This technique is also used for the determination of absolute surface ages were the absolute age is derived from a chronology function, which is valid only at one specific crater diameter. If the used crater production function does not reflect the observed crater size-frequency distribution over large diameter ranges reasonably well, relative stratigraphy as well as absolute dating of the investigated surfaces becomes nearly impossible. In this presentation we compare crater production functions for Mimas that are derived from the observed size-distribution of comets [7] and from the lunar crater size-distribution [8] with the observed crater distribution on Mimas.

Scaling the lunar crater production function to Mimas: For the scaling of the production function we rely on the Ivanov scaling laws [9], which require knowledge about several parameters. They are mostly well known or can be deduced from known parameters or observations. In the case of the Saturnian satellites the projectile densities and impact velocities are not well known, because the source of the impacting projectiles is still in discussion. Because of missing apex-/antapex asymmetries and the missing focusing effect of Saturn [6], we assume a planetocentric projectile source with impact velocities on the order of 600 m/s. Furthermore, scaling the lunar crater production function [8] to Mimas requires the transition from a basaltic to an icy target. The affected scaling parameters are the simple to complex transition and the strength to gravity transition. On Mimas the ~135 km Herschel crater is clearly of complex character. If the classic 1/g approach [10] is applied using the lunar value of 15 km [8], the smallest simple crater on Mimas is expected to be ~380 km in diameter. This is clearly in disagreement with the complex character of Herschel. Because of its larger size and higher gravity, the simple to complex transition can be deduced much better from Iapetus (transition at 15 km) [6]. Utilizing values from Iapetus the 1/g approach gives a value of ~53 km for the simple to complex transition on Mimas. This value is in agreement with the transitional character of crater Arthur (~64 km) on Mimas. The strength to gravity transition is not known for both bodies. It is approximated for Iapetus and Mimas from a ratio equation utilizing strength to gravity transition and simple to complex transition on Vesta [11] with similarly low surface gravity. The result for Mimas is ~1.64 km. The lunar-like crater production function for Mimas (Fig. 1) is derived using the discussed parameters and a target density of 0.9 g/cm³ [6] as well as a projectile density 0.6 g/cm³.

[7] proposed two cases of crater production functions derived from the size-frequency distribution of observed comets and the assumed size-distribution of secondary projectiles within the Saturnian system (Fig. 1).

Measured crater size-frequency distribution: The crater size-frequency distribution on Mimas is measured within 7 areas that cover crater sizes from ~400 m up to ~135 km. The measurements within the Herschel crater and its proximal ejecta blanket give similar diameter coverage and crater frequencies. Thus, they are combined for better statistics (A235). The areas and measurements not affected by Herschel ejecta broadly overlap in common crater size bins (A6, A8, A9). Since Herschel and its ejecta superimpose the heavily cratered plains, it is stratigraphically younger. Relative crater frequencies that represent the formation of Herschel are about a factor of 6 lower than crater frequencies of the heavily cratered plains. Measurement A7 shows a resurfacing effect at its small crater sizes, which is likely caused by Herschel ejecta, because A7 is located at the outer margin of the continuous ejecta blanket of Herschel. Large craters in A7 show the same frequencies like measurements from the heavily cratered plains.

Comparison of the measured crater distribution with crater production functions: In order to utilize the small crater size-frequency distribution of the Herschel areas (A235) the related measurement is vertically shifted (factor: ~6) until it aligned with measurements of the heavily cratered plains in equal diameter

bins. This technique is described by [12]. The shifted measurement is termed "A235 normalized". Measurements of the heavily cratered plains are presented as they were measured. Fig.1 shows all mentioned measurements.

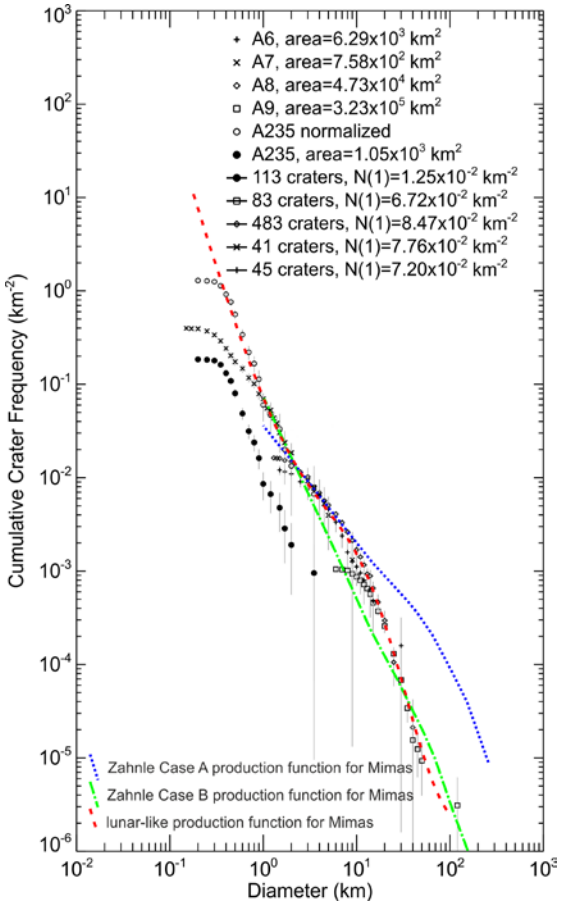

Fig. 1: Crater measurements on Mimas and proposed crater production functions. Zahnle Case A (blue,dotted) and Case B (green, dash-dot) are published by [7]. The lunar-like function is derived from the lunar cratering record and scaled to partly assumed impact conditions on Mimas (see text).

Results: The highly similar crater frequencies in areas A6-A9 that probe the heavily cratered plains indicate a globally homogeneous age of Mimas' surface. Thus, no regional geologic activity obliterated the observable cratering record except for the Herschel impact that clearly shows lower crater frequencies. If vertically shifted about a factor of 6 upwards, the crater distribution of the younger Herschel areas align well between 1 and 3.5 km with the distribution of the older heavily cratered plains. This section of the crater size-frequency distribution contains a change in its slope. The Zahnle crater production functions fit either the shallower slope at larger diameters (Case A) or the steeper part towards smaller diameters (Case B). At diameters > 3.5 km both production functions by [7] divert significantly from the measured crater distribution. The lunar-like crater production function for Mimas shows much higher similarity with the observed crater distribution. Although this function is based on partly assumed projectile parameters that need to be verified yet, the lunar-like solution gives much more reasonable results than both Zahnle functions. The good agreement of the lunar crater size-frequency distribution with Mimas' cratering record implies a collisionally evolved projectile distribution. Whether this distribution is only compatible with the projectile distribution that impacts the Moon or is the result of Kuiper Belt projectiles or even a product of a collisional cascade within the Saturnian system remains uncertain.

References: [1] Smith B. A. et al (1981) Science, 212, 163-191; [2] Smith B. A. et al (1981) Science, 212, 504-537; [3] Porco C. C. et al. (2004) Space Science Reviews, 115, 363-497; [4] Neukum G. (1985) Advances in Space Research, 5, 107-116; [5] Kirchoff M. R. and Schenk P. (2010) Icarus, 206, 485-497; [6] Dones L. et al. (2009) Icy Satellites of Saturn: Impact Cratering and Age Determination. In: Dougherty M. K., Esposito L. W., Krimigis, S. M. (eds) Saturn from Cassini-Huygens. Springer Netherlands, 613-635; [7] Zahnle et al. (2003) Icarus, 163, 263-289; [8] Neukum G. and Ivanov B. A. (1994) Crater size distributions and impact probabilities on Earth from Lunar, terrestrialplanet, and asteroid cratering data. In: Gehrels T. (ed) Hazards due to comets and asteroids. University of Arizona Press, Tucson, 359–416; [9] Ivanov B. A. (2001) Space Science Reviews, 96, 87-104; [10] Pike R. J. (1980) Icarus, 43, 1-19; [11] Schmedemann N. et al. (2014) Planetary and Space Science, 103, 104-130; [12] Neukum G. and Wise D. U. (1976) Science, 194, 1381-1387.

SIZES OF ASTEROIDS RESPONSIBLE FOR LARGE IMPACT BASINS ON THE MOON DURING THE LATE HEAVY BOMBARDMENT . P. H. Schultz, Department of Earth, Environmental, and Planetary Science, Box 1846, Brown University, Providence, RI 02912, peter_schultz@brown.edu

Introduction: Scaling relations derived from laboratory experiments and dimensional analysis [1] provide first-order estimates for the diameters of objects responsible for craters on the planets. At basin scales, however, the final crater rim may not be preserved due to rim collapse. Assumptions about impactor speed, angle, and density further preclude a unique determinations. As a result, the sizes of asteroids (or comets) colliding with the Moon during the Late Heavy Bombardment (LHB) are very poorly constrained. Independent estimates for impactor sizes, however, can be determined from the pattern of ejecta generated by oblique impacts [2]. This contribution reviews this strategy and considers the implications for asteroid sizes during the Late Heavy Bombardment.

Strategy: Laboratory impact experiments reveal the evolving crater shapes as a function of impact angle [3]. At planetary scales (craters and basins 30km to 300km in diameter), however, such asymmetries may be lost due to the much higher impact speeds or crater collapse, which circularizes crater shape. Nevertheless, the distribution of ejecta around large craters clearly indicates an evolving cratering flow-field as expressed by the uprange zone of avoidance [3] or curved ray patterns [4,5]. The initial conditions leading to this asymmetry has been identified in the ejecta velocity distribution generated by impacts into particulate targets at late [6] and early times [7]. At much large scales, the Deep Impact collision captured the identical evolution of the ballistic ejecta [5]. Experiments using particulate targets, however, result in a final crater diameter 20 to 50 times the projectile size. Consequently, early asymmetries expressed by the growing crater shape (in plan) are masked as the source region becomes very small relative to the final crater.

Impacts into strength-controlled targets, however, retain the footprint of the early coupling stage. As a result, the final crater diameter may be only 5-7 (vertical) down to 3-5 (oblique) times the projectile diameter. Moreover, the early-time scour pattern in the target closely resembles in-flight ejecta trajectories from impacts into particulates [6,7]. For strength-controlled targets, however, early time scours remain on the surface (**Fig. 1**). Some of these patterns emanate from the first point of contact and relate to processes associated with the failed projectile re-impacting the surface downrange. Conversely, scours that converge uprange relate directly to the dimensions of the projectile. The identical pattern can be documented in hydrocode models at planetary scales [8, 9].

Such observations, then, provide a possible strategy for constraining the diameter of impactor: map the pattern of radial and non-radial ejecta scours associated with large impact basins (**Fig. 2**). This strategy best works at the largest scales where the ratio of the transient crater diameter to the projectile diameter reduces to a value comparable to a strength-controlled crater due to decreased cratering efficiencies with increasing size for gravity-controlled growth. Note that this is an independent determination for projectile size: there is no assumption about impactor speed, angle, or density or the size of the transient crater or target materials.

Observational Results: Several large lunar impact basins were selected for mapping: *Schrödinger* (~310 km), *Moscoviense* (630 km), *Orientale* (930 km), and *Imbrium* (1100 km), all of which have well-documented signatures for an oblique trajectory. Only signatures of the initial momentum were of interest; hence, orientations were mapped only for grooves, flow lineations, scours, and secondaries (breached downrange).

Schrödinger Basin: Two pronounced rimmed grooves converge uprange rather than the center of the basin. Such long grooves require low-angle impacts and are consistent with the decapitated projectile fragments decoupling from the event but striking downrange. There are also numerous finer scale features reflecting the same pattern. These features typically are covered near the crater rim, consistent with formation prior to arrival of late-stage ejecta. Extrapolations of the major grooves converge uprange of the final crater rim. Consequently, the impacting object could not have been located there. Nor could it have been within the crater rim or slumped walls because there would have been an expression of this contact zone. If the first contact on the pre-impact surface had occurred just inside the wall zone, then it would be occur on the uprange side of the elongate inner ring, resulting in an impactor diameter of 45 km.

Moscoviense Basin: Twice as large as *Schrödinger* and much older. Nevertheless, both LOLA topography and low-sun angle illumination views clearly reveal grooves that converge near the southwest rim. Convergence of these grooves yields an impactor diameter of 100 km (placed inside the outer raised rim) to 130 km (placed inside the second outermost ring). Computer simulations (incorporating strength and shear) result in a basin that closely matches the former result [10].

Orientale Basin: The last of the major basins to form during the Late Heavy Bombardment. The overall pattern of ejecta [11], basin outline (and offset mascon) [12] indicate that this impact was the result of an oblique impact. Convergence of extrapolated great circles from grooves and secondaries yields a diameter of 140 km for the contact point just uprange (northeast) of the *Outer Rooke* mountains.

Imbrium Basin: An oblique trajectory based on the distribution of ejecta [13] and NW-SE oblong shape of the innermost ring plus NW-offset mascon [12]. In this case, the convergence pattern of ejecta grooves to the northwest and northeast (uprange) clearly set the uprange limit for the impact point. The pattern of convergence downrange (southeast) of the *Imbrium* basin yielded a well-determined impactor diameter of 250 km ± 25 km (**Fig. 3**).

Scaling Considerations: The derived impactor sizes are consistent with extrapolations of scaling relations. For example, gravity scaling for wet sand [1] yields a transient apparent diameter of 205km for the peak-ring basin *Schrödinger* (v = 20km/s, θ = 30°). After a 25% correction for slumping and conversion to the apparent diameter), the final diameter (rim-to-rim) becomes 320km, consistent with the observed rim-to-rim diameter (~330km). For *Moscoviense*, the impactor diameter of 100 km best matches the basin

diameter for a slower impactor (10 km/s). For *Orientale*, however, a higher impact speed is required in order to match the its larger basin diameter yet similar impactor diameter. Specifically, the transient cavity is calculated to be about 510 km (20km/s at 30°), coincident with the Inner Rooke Mountains. If this were the case, then the Outer Rooke Mountains would approximate the collapsed transient rim and the Cordillera scarp, an outer slump block. For *Imbrium*, the calculated (pre-collapse) the impactor diameter is about 780 km (also 20km/s at 30°). Increasing the apparent transient diameter by 25% (for the transient rim-rim diameter), the calculated final basin diameter becomes 970 km, a diameter consistent with a transient basin extending from inside the northwest rim of Sinus Iridum (first contact) to just inside the Apennines. In all of these calculations, the impactor speed, impact angle, and density (3g/cc) all had to been assumed, which allows for minor leeway in the estimates.

Implications: The derived impactor diameters indicate that the large impact basins represent collisions by large objects, perhaps asteroids from the proposed E-belt [14]. In contrast with other estimates, however, these objects are comparable to the largest asteroids now remaining in the main asteroid belt and much larger than the objects remaining in the E-belt today. For example, the Imbrium impactor would be about 4.5×10^{22}g, which is smaller than asteroid Hygeia. The similarity in size between the *Moscoviense* and *Orientale* basins yet very different outer ring diameter suggests that *Orientale* impactor must have struck at a speed much higher than the object responsible for *Moscoviense*. Such a conclusion is consistent with dynamical models that indicate that impactors from the E-Belt at the beginning of the LHB would have speeds from 9 – 24 km/s but would have become much higher toward the end [14]. If the South-Pole-Aitken Basin also was formed during the earliest stages of migration from the E-Belt, then the asteroid responsible for this basin would be consisteppnt with a lower speed collision (10 km/s) and a diameter of 800 km [15].

The total mass of the asteroids that could have produced just these four impact basins amounts to $>6 \times 10^{23}$ g (~ 10 lunar masses), which contrasts with estimates of the total mass hitting the Moon during the LHB 3-8 x 10^{21} g based on just stirring the main asteroid belt [16]. This result further justifies the need for an E-belt of asteroids. But it also suggests that there must have been large proto-planetary objects in this belt before they were dynamically stirred into collisions or oblivion.

Surface curvature results in impactor decapitation reaching farther downrange and decreasing overall cratering efficiency [17]. In addition, significant portions of the impactor may survive and escape at nearly the same initial impact speeds for very large basins (Imbrium and SPA) or highly oblique impacts (Crisium). Such debris would have been in earth-crossing orbits, further contributing to the LHB.

[1] Holsapple, K.A. (1993), *Annual Revs. Earth and Planet. Sci.*, 21, 333-373; [2] Schultz, P. H. and Papamarcos, S. (2010), *LPSC* 41, # 2480; [3] Gault, D., and Wedekind, J., (1978), *Proc. of the 9th Lunar Science*, 3843-3875; [4] Schultz, P. H. et al. (2009), *LPSC* 40, # 2496; [5] Schultz, P. H. et al. (2007), *Icarus* 190, 295-333; [6] Anderson, J. L. B. et al. (2003), *J. Geophys.Res.Vol. 108*, No. E8, 5094, 10.1029/2003JE0020 75; [7] Hermalyn, B. et al. (2013), *LPSC 44*, #1102; [8] Schultz, P. H. and Wrobel, K. (2012), *Jour. Geophys.* 117, E04001, doi:10.1029/2011JE003843; [9] Schultz, P. H. et al. (2013), *Large Meteorite Impacts and Planetary Evolution V*, #3109; [10] Crawford, D. A. and Schultz, P. H. (2013), *Large Meteorite Impacts and Planet. Evol. V,* #3047; [11] McCauley, J. F (1977), *Phys. Earth Planet. Int*. 15, 220-250; [12] Schultz, P. H. (2005), *LPSC 26*, 1251-1252; [13] Baldwin, R. (1963), *The Measure of the Moon,* U. Chicago Press; [14] Bottke et al., *Nature* doi:10.1038/nature10967; [15] Schultz, P. H. and Crawford, D. A. (2014), *LPSC 45*, #1961; [17] Gomes, R. et al. (2005), *Nature* 435, 466-469; [17] Schultz, P. H. and Crawford, D. A. (2011), *Geol. Soc. Sp. Paper* 477, 141-159.

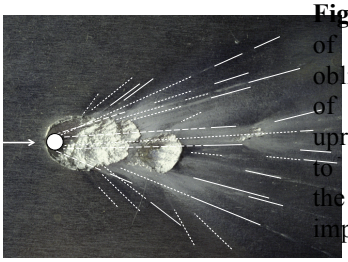

Figure 1: Convergence of scours created by an oblique impact. One set of scours converge uprange and corresponds to different portions of the the failed projectile impacting downrange.

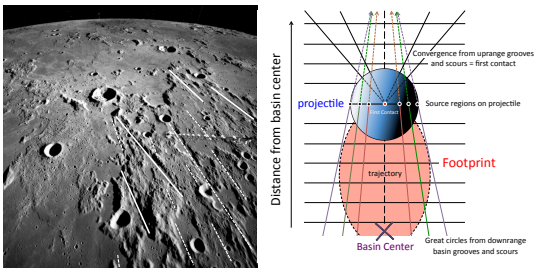

Figure 2: Different sets of grooves/scours appear to converge uprange within the Imbrium Basin (left, **Fig. 2A**). Extrapolations of sets uprange of the impact limit the position of the contact point, whereas as the convergence of grooves and scours downrange of the impact constrain the dimensions of the projectile (right, **Fig. 2B**).

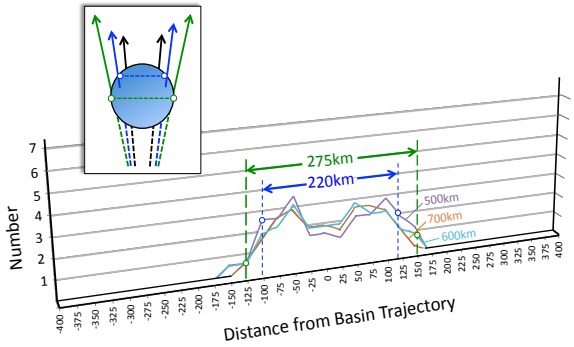

Figure 3: Estimates for the diameter of the Imbrium impactor based on where extrapolations of mapped grooves cross great circles orthogonal to the trajectory at different distances from the basin center (**Fig. 2B**).

DAMAGE DUE TO GIANT IMPACTS INTO DIFFERENTIATED BODIES: A MECHANISM FOR LARGE-SCALE TROUGH FORMATION ON VESTA. A. M. Stickle[1], D.L. Buczkowski[1], and K.A. Iyer[1]. [1]Johns Hopkins University Applied Physics Laboratory, Laurel MD, angela.stickle@jhuapl.edu

Introduction: The Dawn mission observed two sets of linear faults on the surface of the asteroid 4 Vesta [1-3]. Though they appear to be slightly offset from the basin centers, observations indicate that these features are likely related to the two large impact basins on the south pole of Vesta: Rheasilvia and Veneneia [2]. Our experimental and numerical results show that this is a natural consequence of oblique impacts into a spherical, differentiated target. Experiments and models show that large impacts generate different patterns of tensile stress and pressure for differentiated v. undifferentiated targets. Further, sets of discrete shear planes develop within the subsurface of the body following impact [4-5]. These subsurface features can propagate to the surface under combined tensile-shear loading to create sets of approximately linear faults on the surface. We focus on the asteroid Vesta here, but similar deep-seated damage is expected at any solar-system body experiencing giant impacts [e.g., 6].

Experimental Details and Model Setup: Impact experiments into spherical PMMA targets, performed at the NASA Ames Vertical Gun Range (AVGR), track the time-resolved evolution of subsurface damage in spherical targets [e.g., 5]. Here, the spherical targets were impacted by a 6.35-mm Pyrex projectile at angles ranging from 40°-65° and 5 km/s. High-speed imaging tracked the damage within the spheres at a high time resolution, which was then compared with three-dimensional CTH calculations [7].

For the direct comparison, the CTH calculations were done with identical impact conditions to the experiments to identify observed failure conditions observed inside the targets. Adaptive Mesh Refinement was used to track high-pressure regions in detail [7-8]. Pyrex was assumed to behave as a geologic material with a pressure-dependent yield surface; the PMMA spheres assume a von Mises plasticity model coupled to the Johnson-Cook Fracture damage model (JCF), which is used here to track shear deformation [9]. Tensile failure is considered separately.

Laboratory simulations provide important information about the processes occurring following oblique impacts as well as provide confidence for interpreting large-scale models. For this study, we considered impacts into the asteroid 4 Vesta. To provide constraints on trough system formation, we studied the effects of impact angle (15°, 30°, 45°, and 90°), projectile size, internal structure of Vesta (e.g., un-, partially-, and fully- differentiated, as well as varying the core size), and material properties of the asteroid itself. Fully differentiated models included an iron core, dunite mantle and either basaltic or basalt-analog crusts. The basalt-analog materials have fully described equation of state (EOS) and strength models known to undergo brittle fracture and have densities similar to the modeled basalt crusts. All impacts were at 5 km/s, the expected impact velocity in the asteroid belt. Oblique impacts examined the effects of a 100-km dunite projectile into a fully differentiated Vesta, with structure after [10]; the calculation included self-gravity for the asteroid and the impactor. Normal impacts were simulated into three structures representing ancient Vesta: undifferentiated Vesta, and a two- or three-layer Vesta [after 11]. All models are of a ~530 km sphere, with core sizes ranging from 164-220 km.

Results and Discussion: The combination of laboratory experiments and numerical models allow us to track the state of the material, the modes of deformation, and the damage and fracture growth following impact (at both small and large scales).

Laboratory Experiments and Small-Scale CTH. Direct comparisons between observations of damage growth in the AVGR experiments and corresponding CTH models explain failure modes within the target. A typical failure pattern from the AVGR experiment is shown in Figure 1B. Observation of damage evolution coupled with CTH models indicate that the near-surface failure haze results from incipient spallation at the far-side of the target, the central damage stalk is a result of tensile strain, while the sub-parallel failure planes form due to high magnitudes of shear stress (Figure 1A). The orientation of these damage structures depends on impact angle and velocity, but all evolve similarly.

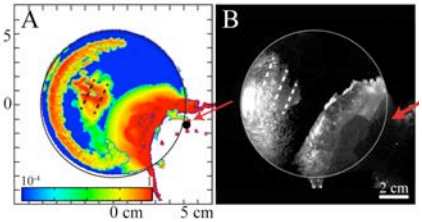

Figure 1. Comparison of lab-scale CTH simulations with AVGR experiment showing shear failure planes. (left) CTH simulation showing damage from both shear and spallation overlain onto each other, (right) Final damage from the AVGR experiment, with failure planes shown by white dotted lines. After [5].

Large-scale CTH models of Vesta. Large-scale CTH simulations, in conjunction with insights gained from laboratory experiments, provide new clues into the resultant damage expected from giant impacts. Ex-

ploring a large parameter space with these models allows examination of the effects of impact parameters on subsurface damage and possible formation scenarios for the large-scale fracture systems on 4 Vesta.

Models examining the effect of differentiation on internal damage and fracture indicate that Vesta was likely differentiated at the time when Rheasilvia and Veneneia formed. The results of these models show that different patterns of fracture (Fig. 2) and pressure (Fig. 3) develop in a differentiated sphere (Fig. 2 center and right; Fig. 3, right) compared to an undifferentiated sphere of the same material and diameter (Figs. 2, 3, left). Though these first-order models do not yet fully mimic the observations of troughs on Vesta, they do demonstrate that the density contrast in Vesta's differentiated interior affects the stresses resulting from the Rheasilvia and Veneneia impacts. It is this impedance mismatch that is suggested to be responsible for the development of Vesta's planet-like troughs [2]. Similar differences between differentiated and undifferentiated targets are seen for models of oblique impacts.

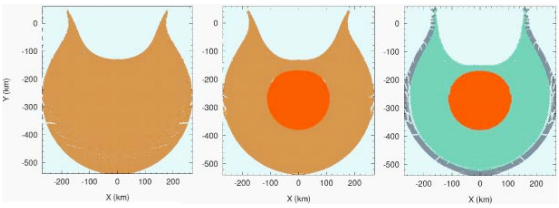

Figure 2. CTH hydrocode models of giant impact into Vesta showing materials following impact. Red is iron, green is dunite, brown is higher-density basalt analog and grey is lower-density basalt analog. Fracture due to tensile stresses changes depending on the amount of differentiation [4].

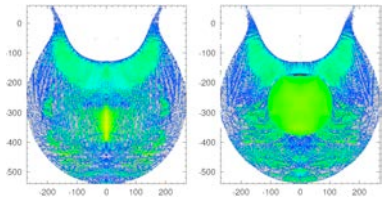

Figure 3. CTH models of a giant impact into an undifferentiated (left) and differentiated (right) Vesta yield very different pressure profiles depending on the presence or absence of a core. Though pressure values are not given in this image, changes in patterns of pressure can be observed [4].

In both normal and oblique impact cases, large regions of Vesta are subjected to tensile stresses great enough to generate fracturing. Because they include a damage model tracking shear deformation, the oblique impact models also show that these regions overlap with, or form directly prior to, regions of high shear stress. Temporally, the combination of these two stress states suggests that the subsurface of Vesta may be damaged or fractured due to tensile stresses after the passage of the shock wave but then fail and slide due to high shear-stresses set up behind the shock wave. This pattern is seen even to late times, as the shock, rarefaction, and shear waves reflect and coalesce throughout the body. The combination of high shear-stress magnitudes overprinting weakened or pre-damaged material lasts for hundreds of seconds, and during this time damaged material is continually subjected to high shear stress (Figure 4). This combination creates localized shear planes that then propagate to the surface. Thus, the linear features observed on Vesta may be the surface expression of large-scale subsurface shear failure and faulting from deep in the interior, similar to what is seen in laboratory experiments.

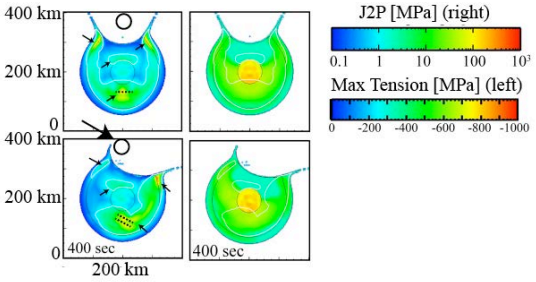

Figure 4. Large-scale time sequence of CTH simulation results showing maximum tensile stress (left) and the magnitude of shear stress (right) within Vesta. (top) center plane of Vesta on a plane perpendicular to the impact trajectory; (bottom) center plane parallel to the impact trajectory. The initial impactor size (100 km) and trajectory (30°) are shown for scale. Note here that the south pole of Vesta would be at the top of these images. After [5].

These general results are true for varying impact angle (30-45°) as well as different impactor and core sizes (50-100 km and 164-220 km, respectively). For 15° impacts, a large portion of the projectile decapitates and decouples from the impact, significantly reducing subsurface stress and damage formation. The results from differing impact angles may also allow constraints to be placed on impact trajectory. If the subsurface shear planes observed in the laboratory experiments are small-scale analogs to the trough features on Vesta, then the orientation of the damage region might also be used to constrain the impact trajectory and location by comparing the angle of the damage offset from the impact crater antipode.

References: [1] Jaumann, R. *et al.* (2012) *Science*, 336, 687-690; [2] Buczkowski, D. *et al.* (2012) *Geophys. Res. Let.,* 29, L18205; [3] Sierks, H. et al. (2011), *Space Sci. Rev*., *163*, 263-327; [4] Buczkowski, D.L., et al. (2012) Paper presented at the GSA Annual Meeting; [5] Stickle, A.M. et al. (2015) *Icarus* 247, 18-34; [6] Schultz, P.H. and D.A. Crawford (2011), *GSA Spec. Paper 477;* [7] McGlaun, J.M. et al. (1990) *Int. J. Imp. Eng*. 10, 351-360; [8] Crawford, D.A. (1999) Paper presented at 15th US Army Symposium on Solid Mechanics, April 12-14; [9] Johnson, G.R. and W.H. Cook (1995) *Engr. Frac. Mech*, 21, 31-48; [10] Ruzicka, A.J *et al*. (1997) *Met. and Planet. Sci*. 32(6), 825-840; [11] Raymond, C.A., et al (2012) *43rd LPSC* Abs. 1007.

WAS THERE A CONCENTRATION OF LUNAR AND ASTEROIDAL IMPACTS AT ~4000 Ma? T. D. Swindle[1,2] and D. A. Kring[2,3], [1]Lunar and Planetary Laboratory, University of Arizona, Tucson AZ 85721-0092, tswindle@lpl.arizona.edu, [2]NASA Solar System Exploration Research Virtual Institute, [3]Center for Lunar Science and Exploration, Lunar and Planetary Institute, 3600 Bay Area Blvd, Houston TX 77058.

Introduction: Ever since the first suggestion that there was a clustering in the ages of the Apollo lunar samples at ~3900 Ma [1, 2], the question of whether that clustering represented an increase in the impact flux, as suggested by [1, 2], or something else [3, 4], has been debated. Since the rate of impacts with time is a critical input parameter for dynamical models [5], as well as having a large effect of the evolution of the surfaces of planets, moons and asteroids, this is a critical question. And it is a question that is still unresolved. This abstract will not completely answer the question, but will lay out a framework for addressing the question.

Two basic approaches to the question:

Identify samples from specific events. A natural way to address the problem of the impact flux of the Moon is to identify samples from specific basins, using their chemistry or the geology of the landing site, and find the ages of the basins by finding the ages of those samples. In practice, that has generally proven difficult. The benchmark paper for this approach is the review by [6], which discusses attempts at determining the ages of the Imbrium, Serenitatis, Nectaris, and Crisium basins in this fashion (the age of the young basin Orientale can be constrained, though not precisely dated, through the ages of samples, as well). But the age of Crisium is constrained by ages of only a few Luna samples, and there is increasing doubt about the age of Nectaris (addressed later). This highlights the difficulty of interpreting the provenance of rocks within the heavily-mixed lunar regolith.

Try to interpret overall patterns of ages. Although less satisfying, this approach makes it possible to use samples that lack geological context, such as lunar meteorites, random clasts within Apollo samples that may have come from remote locations, and asteroidal meteorites (where the relationship of the impacts to the well-studied lunar basin-forming events is completely unknown). The simplest version of this approach, akin to the initial observations of [1, 2], simply looks at the distribution of ages of samples. More sophisticated approaches incorporate texture and chemical composition of lunar samples, and chemical classification (presumably identifying specific, if generally unknown, parent bodies) for asteroid meteorites. A particularly fertile set of samples for this approach has been the Apollo 16 breccias, since they may – or may not – record the crucial age of the Nectaris basin [7-9].

Two things the community seems to agree on:

There were impacts before 4000 Ma. G. Ryder argued for a cataclysmic bombardment of the Moon, based in part on his contention that no impact events older than 4000 Ma on the Moon had been definitively identified [10, 11]. However, the idea that there were no impacts before 4000 Ma has been conclusively disproven on both the Moon and among meteorites. The lunar case has recently been reviewed by [12]. In meteorites, the most prominent feature in the impact record of LL chondrites is one or more impact events at ~4200-4300 Ma [13], although there are no recorded impact events in the H or L chondrites in that time period [14]. There are also a number of impact events at >4400 Ma recorded in meteorites [14]. These could be the result of an accretional leftover population (an underlying assumption of [15]), although [16] suggested that many of them may be the result of the spread of ejecta from the Moon-forming impact on Earth.

A significant number of impacts shortly after Orientale is recorded in both lunar and asteroidal meteorites. Early papers on the Ar-Ar ages of lunar samples showed scant evidence for impact events on the Moon shortly after ~3800 Ma (e.g., [1]), but such events clearly exist. Studying the ages of recrystallized impact melt clasts from lunar meteorites, [17] argued for a cataclysmic bombardment based on the lack of ages >4000 Ma, but also showed that many of the ages were 3000-4000 Ma, not in a spike at ~3900 Ma. A similar situation obtains for meteorites. [18, 19] showed that HED meteorites experienced a bombardment (on Vesta?) that lasted until ~3400 Ma. H and L chondrites have similarly extended bombardment histories [14]. The distributions of impact ages for these groups of meteorites, while yielding more ages of ~3900 Ma than older (~4300 Ma) or younger (~3000 Ma), but also has a much broader peak that begins at ~4100 Ma, and hence seems to require an increase in impact flux earlier than the ~3900 Ma envisioned by [11].

The community doesn't seem to agree on:

The age of the Nectaris impact. Although it was originally assumed that the Apollo 16 breccias were produced by the Nectaris impact, and hence would yield the age of that event, there has been increasing doubt about whether they actually result from that basin [20, 21]. The age of Nectaris is crucial to the understanding of the Apollo 16 site. In addition, it has broader implications, since it has been suggested that

the impactors from the time of Nectaris on represent a different population than pre-Nectarian impacts [22]. The difficulty in determining the age of Nectaris should also serve as a cautionary tale for attempts to determine the ages of other basins by sampling a few carefully selected sites in future exploration missions. In particularly, it is clear that it will be very difficult to attribute the age of a specific Near Side sample with a specific basin other than Imbrium, given the Imbrium overprint that is so prevalent [4]. Imbrium will not have as much of an effect on Far Side samples, but selection of the appropriate samples will still be difficult. It is likely that agreement on the ages of specific basins will only come after a sufficient number of samples have been analyzed from a variety of locations.

Whether there was a concentration of lunar and asteroidal impacts at ~4000 Ma. Given the apparent agreement that there were multiple impacts recorded on the Moon and in asteroids both before and after the original apparent spike noted by [1, 2], is there any reason to think that there was anything different about the impact cratering environment at ~4000 Ma, other than the Imbrium impact shortly thereafter? We believe there are two reasons to think there was an increase, although not the cataclysmic spike discussed by [11].

One line of evidence comes from the Moon, specifically from Apollo 16 breccias. Three studies in the past decade have looked at clasts from Apollo 16 breccias and concluded that there were multiple events between 3800 Ma and 4000 Ma that were recorded. First, [7] analyzed 25 samples, and concluded that the data fall into four clusters, depending on composition. Next, [8] analyzed multiple splits of each of six clasts, and found that while the age for any single clast was reproducible, the clasts, which had different chemical compositions, clearly had ages distinct from one another. Finally, [9] analyzed another group of >20 clasts from Apollo 16 breccias, and again found that the samples naturally cluster into different groups based on age and chemistry. All of these are inconsistent with a single resetting event (Imbrium), unless many of the samples experienced partial resetting, with the amount of resetting being virtually identical across a single clast and among clasts of similar chemical composition. While this scenario is not impossible, it is worth noting that there are cases where samples from a group of Apollo 16 breccias appear to give a range of ages, but the older-than-Imbrium ages often disagree from split to split within a clast, and there do not appear to be clusterings other than at an Imbrium age [20]. The latter case is explained well by Imbrium being the only event influencing the ages, but the others all suggest that there were multiple events recorded between 3800 Ma and 4000 Ma. It is not clear how many of them represent basin-sized events, but there is not similar evidence for that many distinct impact events in such a short time period at any other time in lunar history.

The other line of evidence comes from meteorites. As mentioned, H chondrites, L chondrites and HED meteorites all appear to have broad peaks in impact ages between ~4100 Ma and ~3400 Ma [14, 19]. It is clear that these are not a result of the Imbrium event, either directly (which is obvious) or indirectly (since they extend to times both before and after Imbrium).

Hence it appears that there is an increased impact flux at ~4000 Ma. Two recent models [15, 23], both of which are based on dynamical models but include isotopic and other constraints from the Moon and Earth, respectively, suggest that the data is best described by a "sawtooth" pattern, with an increase at 4100-4200 Ma. This provides a good explanation for the asteroidal meteorite patterns of impact ages, and also explains the extended bombardment history of the Moon seen in lunar meteorites and the multiple events in the 3800-4000 Ma timeframe seen in the Apollo 16 breccias. The lack of strong evidence for multiple events between 4000 and 4100 Ma remains puzzling, but perhaps it would be found at sites other than Apollo 16.

The "sawtooth" model [15, 23] is almost certainly a closer approximation to the history of the inner Solar System impact flux than is the "cataclysm" model of [11], just as that model was more accurate than earlier models with a continuously declining flux. However, the actual history may yet be even more complicated, as [2] suggested 40 years ago.

References: [1] Turner G. et al. (1973) *Proc. LSC 4th*, 1889-1914. [2] Tera F. et al. (1974) *EPSL, 22*, 1-21. [3] Hartmann W. (1975) *Icarus, 24*, 181-187. [4] Haskin L. et al. (1998) *MAPS, 33*, 959-975. [5] Gomes R. et al. (2005) *Nature, 435*, 466-469. [6] Stöffler D. and Ryder G. (2001) *Space Sci. Rev, 96*, 9-54. [7] Norman M. et al. (2006) *GCA, 70*, 6032-6049. [8] Niihara T. et al. (2013) *LPS 44*, Abs. #2083. [9] Haber T. et al. (2014) *LPS 45*, Abs. #1693. [10] Dalrymple G. and Ryder G. (1993) *JGR, 98*, 13,085-13,095. [11] Ryder G. (1990) *EOS, 71*, 313, 322-323. [12] Fernandes V. et al. (2013) *MAPS, 48*, 1-29. [13] Dixon E. et al. (2004) *GCA, 68*, 3779-3790. [14] Swindle T. et al. (2014) *Geol. Soc. (London), SP-378*, 333-347. [15] Morbidelli A. et al. (2012) *EPSL, 355*, 144-151. [16] Bottke W. et al. (2014) *LPS 45*, Abs. #1611. [17] Cohen B. et al. (2000) *Science, 290*, 1754-1756. [18] Bogard D. (1995) *Meteoritics, 30*, 244-268. [19] Bogard D. and Garrison D. (2003) *MAPS, 38*, 669-710. [20] Norman M. et al. (2010) *GCA, 74*, 763-783. [21] Norman M. and Nemchin A. (2012) *LPS 43*, Abs. #1368. [22] Marchi S. et al. (2012) *EPSL, 325*, 27-38. [23] Marchi S. et al. (2014) *Nature, 511*, 578-582.

THE TUNGSTEN ISOTOPE COMPOSITION OF THE MOON: NEW CONSTRAINTS ON THE GIANT IMPACT. M. T. Touboul[1], I. S. Puchtel[1] and R. J. Walker[1], [1]Department of Geology, University of Maryland, MD 20742, USA (rjwalker@umd.edu).

Introduction: Discovery of small enrichments in $^{182}W/^{184}W$ in some Archean rocks, relative to the modern terrestrial mantle [1,2], suggests both exogeneous and endogenous modifications to highly siderophile element (HSE) and moderately siderophile element (MSE) abundances in the mantle. Collectively these isotopic enrichments indicate the formation of chemically fractionated reservoirs in the terrestrial mantle that survived the putative Moon-forming giant impact, and may also provide support for the late accretion hypothesis. The lunar mantle sources of volcanic glasses and basalts were depleted in HSE relative to the terrestrial mantle by at least a factor of 20 [3]. The most likely explanations for the disparity between the Earth and Moon are either that the Moon received a disproportionately lower share of late accreted materials than Earth, such as may have resulted from stochas-tic late accretion, or the major phase of late accretion occurred prior to the Moon-forming event, and the putative giant impact led to little drawdown of HSE already present in the mantle at that time.

Day et al. [3] proposed that late accretion of materials with chondritic bulk compositions added ~0.4 to 0.8 wt. % of mass to the Earth, and ~0.05 wt. % mass to the Moon. Consequently, if late accretion to the mantles of the Earth and Moon largely postdated the formation of the Moon, and the Moon formed with the same W isotopic composition as Earth, then mass balance calculations predict that the $^{182}W/^{184}W$ of the lunar mantle should now be higher than for the Earth by 10 to 30 ppm, as the greater proportion of late accreted materials added to Earth would have lowered the $^{182}W/^{184}W$ of the terrestrial mantle towards the isotopic composition of chondrites (~ -200 ppm relative to present Earth) more than for the lunar mantle.

Accurate and precise measurement of the $^{182}W/^{184}W$ of the lunar mantle is, therefore, critical to test this prediction. Because of the effects of cosmic rays on ^{182}W, particularly production resulting from cosmic ray interactions with ^{181}Ta [4], most prior studies of the W isotopic composition of the lunar mantle have focused on Ta-free metal, separated from impact melt rocks and basalts [e.g., 5]. Touboul et al. [6] measured the W isotopic compositions of lunar basalts and impact melt rocks. Because of the terrestrial composition of W found in the lunar metals, separated from lunar basalts and impact melt rocks, that study interpreted the data to mean that the Moon formed ≥52 Myr after formation of the solar system, and also that the lunar magma ocean crystallized after ^{182}Hf was no longer extant, ≥60 Myr after solar system formation. However, the measurements for that study were made with with ±25-30 ppm precision, so the effects of disproportional late accretion could not be tested by it. In order to examine this issue further, we have applied our new measurement techniques, which provide W isotopic data with ~±5 precision (2σ SD) [7].

Methods: Apollo 16 KREEP-rich impact melt rocks 68115 and 68815 were chosen for study because they formed from target rocks with high W, and experienced only short-term exposure to cosmic rays. Given W concentrations typical of KREEP, together with typical contributions of siderophile elements to lunar impact melt rocks, we estimate the W present in the metal separates is >99% endogenous lunar W.

The samples were crushed in an agate mortar and separated into several size fractions using nylon sieves. Magnetic fractions were separated using a hand-magnet, and further purified by repeated grinding, magnetic separation and ultrasonication in distilled ethanol. The purity of the metal separates were checked to be free of visible silicate or oxide grains under the binocular microscope. The subsequent analytical procedures used for W purification and isotopic analysis were reported in [7]. In brief, samples were processed through anion and cation exchange columns, and the highly-purified final W fractions were analyzed by negative thermal ionization mass spectrometry using the UMd *ThermoFisher Triton* mass spectrometer.

Metal separates from the impact melt rocks 68115,114, 68815,394 and 68815,396 have $\mu^{182}W$ values (where $\mu^{182}W$ is the deviation in ppm of the $^{182}W/^{184}W$ ratio of the sample from that of the modern terrestrial mantle) of +23.3 ± 3.8 (n=3, 2σ SD), +18.1 ± 2.5 and +20.4 ± 2.9, respectively, which are identical within analytical uncertainty (**Fig. 1**). The average $\mu^{182}W$ value of +20.6 ± 5.1 (2σ SD) for the three metal separates provides the current best estimate of the W isotopic composition of their parental KREEP reservoir, and most likely, the lunar mantle. These data are in good agreement with the previously published data for the same samples [6], but are considerably more precise. Of greatest note, the W isotopic compositions of the metals are now well resolved from the isotopic composition of the silicate portion of the modern Earth.

Discussion: The positive W isotopic offset between the Moon and silicate Earth can be attributed to one of

several possible causes, including: 1) cosmogenic exposure effects, 2) contribution of W from the basin-forming impactor that created the melt rocks, 3) radiogenic ingrowth of ^{182}W in a high Hf/W domain within the lunar mantle while ^{182}Hf was extant, or 4) disproportional late accretion to Earth and Moon.

Possibilities 1 and 2 can be easily dismissed based on the measured, very low Ta/W of the metal separates, and based on mass balance estimates for W in KREEP-rich rocks, relative to possible impactors. Enrichment in ^{182}W as a result of radioactive decay can't be discounted at this time, although the magnitude of the offset is inconsistent with current estimates for the Hf/W of the bulk silicate Moon, and the mantle source of KREEP. We conclude that the most likely cause for the offset is disproportional late accretion to the Moon and Earth, especially given that it is an excellent match to the predicted offset [8].

If the W isotopic difference between the Moon and Earth really is the result of disproportional late accretion, then the results provide some important additional constraits on the nature of the putative giant impact that generated the Moon. First, an interpretation of disproportional late accretion requires the assumption that at the time of Moon formation, the Earth and Moon had the same W isotopic composition. This requirement follows other evidence for isotopic similarity between the Moon and Earth in elements such as O, Ti and Cr. One possible cause for this isotopic match is that the giant impactor happened to have been built from very similar building blocks as the Earth coincidentally winding up with essentially the same isotopic compositions for elements that show genetic variability in their isotopic compositions. The W isotopic composition of the silicate portion of the impactor, however, was an outcome of radiogenic decay of ^{182}Hf, coupled with the Hf/W history of its mantle. Consequently, it is exceptionally unlikely that the impactor would have evolved to the same W isotopic composition as Earth at the time of the impact. Thus, an interpretation of disproportional late accretion greatly favors giant impact scenarios that seek to explain the isotopic similarities between the Moon and Earth as a result of high temperature equilibration processes, rather than accretionary happenstance [e.g., 9].

An additional requirement for an interpretation of disproportional late accretion is that the late accretionary accumulation clocks for the Moon and Earth began at the time as the giant impact. Thus, the giant impact would have to have been a clearinghouse event for HSE that were present in the terrestrial mantle prior to the impact. This means that at least some of the metal from the core of the impactor efficiently extracted the HSE from the silicate Earth while transiting to merge with the core.

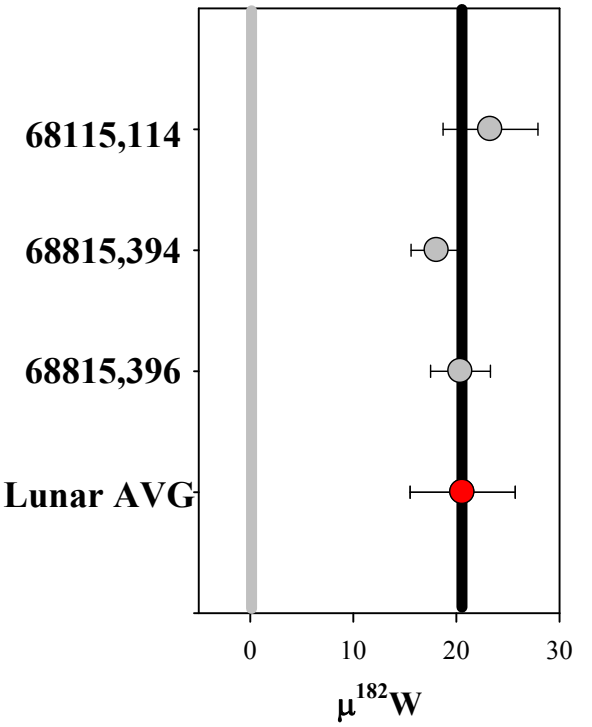

Figure 1: μ^{182}W of lunar metals separated from Apollo 16 KREEP-rich impact melt rocks 68115,114, 68815,394 and 68815,396. The gray vertical bar represents the composition of the bulk silicate Earth. The red circle corresponds to the average value of the 3 individual analyses of the metals (+20.6 ± 5.1 2σ SD), which is our current best estimate for the W isotopic composition of the Moon.

References: [1] Willbold M. et al. (2011) *Nature* **477**, 195-198. [2] Touboul M. et al. (2012) *Science* **335**, 1065-1069. [3] Day et al., *Science* **315**, 217-219. [4] Leya et al. (2000) *EPSL* **175**, 1-12. [5] Kleine et al. (2005) *Science* **310**, 1671-1674 [6] Touboul et al. (2007) *Nature* **450**, 1206-1210. [7] Touboul M. and Walker R.J. (2012*) IJMS* **309**, 109-117. [8] Walker R.J. (2014) *Phil. Trans. Roy. Soc. A* **372**, 20130258. [9] Pahlevan K. & Stevenson D.J. (2007) *EPSL* **262**, 438-449.

Acknowledgement: This study was supported by NASA Cosmochemistry grant NNX13AF83G. This source of support is gratefully acknowledged.

HIGHLY SIDEROPHILE ELEMENT CHARACTERISTICS OF LUNAR IMPACT MELT BRECCIAS: A PICTURE BEGINS TO EMERGE. R. J. Walker[1], O.B. James[2], D.A. Kring[3], J. Liu[4], M.G. Sharp[1], and I. S. Puchtel[1] - [1]Dept. of Geology, Univ. Maryland, College Park, MD 20742. rjwalker@umd.edu, [2]Emeritus US Geological Survey, Reston, VA 20192, [3]Lunar & Planetary Institute, Houston, TX 77058, [4]Dept. Earth & Atmos. Sci., Univ. Alberta, Edmonton, AB T6G 2E3

Introduction: It has long been hypothesized that the Earth-Moon system, and likely the entire inner solar system, underwent a phase of late accretion, termed *late heavy bombardment* (LHB), within the interval of time from ~4.1 to ~3.8 Ga [1-3]. Although the putative LHB had a major effect on shaping the surface of the Moon, it likely involved much less mass than is envisioned for late accretion as a whole. Even generous estimates for the mass of the LHB place the mass of materials involved as no more than about 10% of estimates for the overall mass of late accretionary additions. Nevertheless, the LHB may have delivered substantial water, and other volatile species, including organic molecules, to the Earth and Moon, so it is important to characterize the chemical nature of the materials involved.

The primary means to examine the chemical characteristics of materials from the LHB has been to analyze lunar impact melt rocks that were created as a result of the basin-forming impacts. The bulk of the highly siderophile elements (HSE: including Re, Os, Ir, Ru, Pt, and Pd) present in lunar impact-melt rocks were derived from meteoritic materials incorporated in the melt fraction. The relative abundances of the HSE in these rocks can provide diagnostic chemical fingerprints of the impactors because pristine lunar crustal rocks have extremely low concentrations of these elements [4], and possible impactors, such as chondrites and iron meorites have comparatively high abundances of these elements [5]. Several recent studies have utilized isotope dilution techniques to measure HSE concentrations and have also reported $^{187}Os/^{188}Os$ ratios, in order to characterize multiple pieces of a given melt rock. When the data for a given sample are collectively plotted, the slopes of the linear trends generated from plots of Ir versus other HSE, and $^{187}Os/^{188}Os$, define the relative abundances of HSE in the impactors associated with lunar basin formation [6-9].

There is now a sizable database for HSE present in impact melt rocks from Apollo 14, 15, 16 and 17 landing sites, as well as for several lunar meteorites. Comparison of data from the diverse locations provides a new way of considering the nature of late heavy bombardment to the Moon and Earth.

Discussion: In approximately half of the rocks examined, the results of plots of Ir versus each of the other HSE within each rock measured yield linear trends with intercepts indistinguishable from 0, within regression uncertainties. In such cases, the trends can be assumed to represent mixing trends between a single exogenous impactor and the HSE devoid lunar target rocks.

Puchtel et al. [6] and Sharp et al. [8] reported and interpreted data mainly for Apollo 17 impact melt rocks. Both studies reported a "dominant" component for the site, most notably characterized by suprachondritic Re/Os (as measured by $^{187}Os/^{188}Os$), Ru/Ir, Pt/Ir and Pd/Ir, comparable to the results from Norman et al. [10]. They interpreted the results to suggest that the dominant source of HSE to the site, most likely the Serenitatis basin impactor, shared broad similarities to some chondritic meteorites (enstatite chondrites), but sampling a composition not presently found in our meteorite collections. A distinct, feldspar-rich component in some of these rocks as well as in other lunar impact melt rocks, termed *granulite*, was found to be characterized by relative abundances of HSE more similar to ordinary chondrites.

Fischer-Gödde and Becker [7] focused most of their attention on impact melt rocks from the Apollo 16 site. Here they found HSE ratios extending much higher than known chondrites, and even well beyond the range of the Apollo 17 rocks. They also analyzed some granulitic rocks and reported, like prior studies, that this component (or components) is most like ordinary chondrites. Of note, the study recognized that virtually all of the HSE data for Apollo samples (i.e., among multiple rocks) form linear trends when plotting Ir versus other HSE or $^{187}Os/^{188}Os$. They interpreted this to mean that all of the Apollo impact melt rocks incorporated two major 2 HSE-rich components at the time of their formation. One was very similar to ordinary chondrites, and is the major component in granulitic rocks. The other component most resembles a chemically evolved group IVA iron meteorite. Consequently, they proposed that both components became variably mixing during basin forming impacts, but were not substantially modified by HSE derived from the basin-forming impactors that created the rocks.

Most recently Liu et al. [9] reported considerable additional data for Apollo 15 and 16 impact melt rocks, continuing to note, as with [7], that all lunar data plot along what appears to be continuous linear trends ranging from a composition that is similar to ordinary chondrites, to an endmember with $^{187}Os/^{188}Os$, Ru/Ir and Pd/Ir ratios far above those of

known chondrites. All of the existing data plotted in **Figure 1a-c**.

Possible scenarios to explain the observed trends include: 1) Variable mixing between an earlier granulitic contaminant(s) with chondritic HSE and a series of impactors that happen to have co-linear, suprachondritic Re/Os, Ru/Ir, Pt/Ir and Pd/Ir. 2) Variable mixing between earlier granulitic contaminant(s) and a series of metallic impactors related by crystal-liquid fractionation, resulting in variably suprachondritic Re/Os, Ru/Ir, Pt/Ir and Pd/Ir. 3) Variable mixing between an earlier impactor contaminant in the crust characterized by fractionated HSE abundances (e.g., fractionated metal), and a series of impactors with chondritic HSE that led to creation of the basins. 4) Variable mixing between two components present in the lunar crust prior to the last basin forming impacts. One component (or suite of components) was chondritic in composition, the other component had fractionated HSE, and could have been an isolated core fragment (this is the model of [7]). At this time, these models cannot be discriminated and await genetic testing using nucleosynthetic anomalies characteristic of some siderophile elements.

References: [1] Turner G. et al. (1973) *Proc. 4th Lunar Sci. Conf.*, 1889-1914. [2] Tera F. et al. (1974) *EPSL, 22*, 1-21. [3] Spudis P. D. and Ryder G. (1981) *Proc. Lunar Planet. Sci. Conf. 12A*, 133-148. [4] Day J. M. et al. (2010) *EPSL 289,* 595-605. [5] Horan M. F. et al. (2003) *Chem. Geol.* 196, 5-20. [6] Puchtel I. S. et al. (2008) *GCA, 72***,** 3022-3042. [7] Fischer-Gödde M. & Becker H. (2012) *GCA 77*, 135-156. [8] Sharp M. et al. (2014) GCA 131, 62-80 [9] Liu J. et al. (in review) *GCA*. [10] Norman M. D. et al. (2002) *EPSL 202*, 217-228. [11] Walker R.J. et al. (2002) GCA 66, 4187- 4201. [12] Horan M.F. et al. (2003) *Chem. Geol. 196*, 5-20. [13] Fischer-Gödde et al. (2010) *GCA 74*, 356-379 [14] McCoy T.J. et al. (2011) *GCA 75*, 6821-6843.

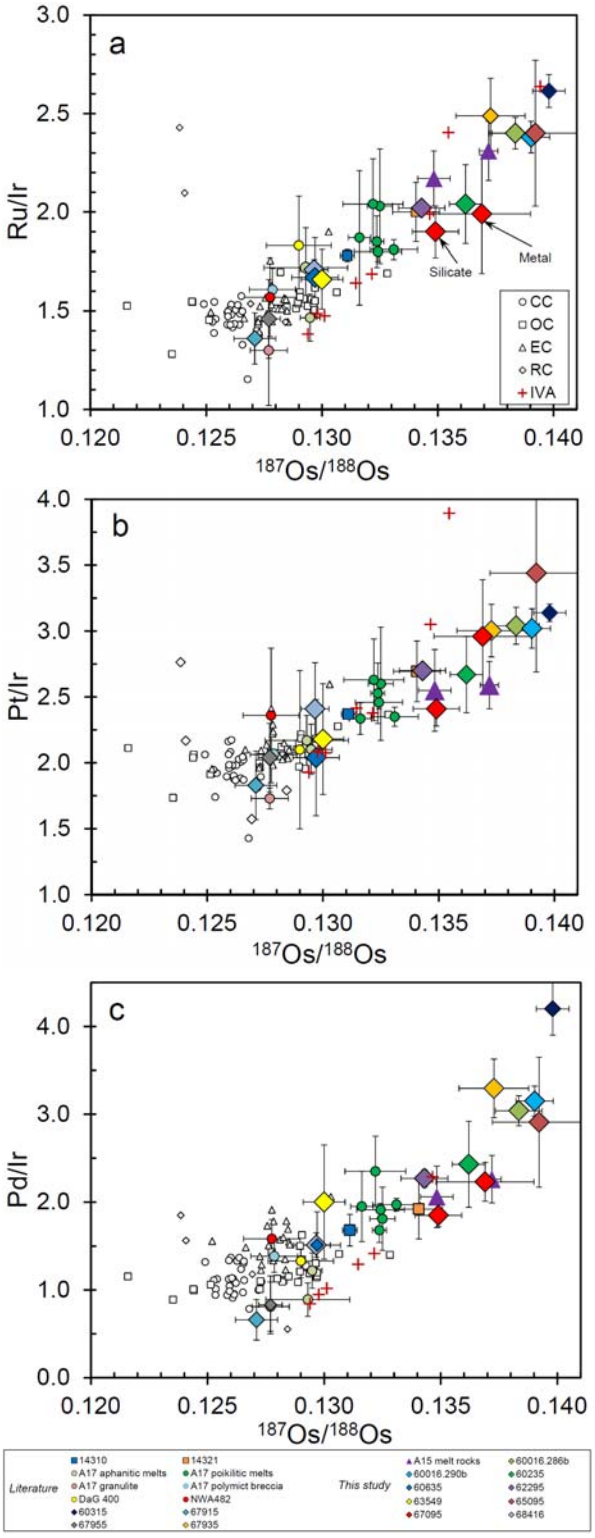

Figure 1a-c. Average $^{187}Os/^{188}Os$ *vs*. Ru/Ir (a), Pt/Ir (b), and Pd/Ir (c) for the impactor components incorporated in the lunar impact melt rocks examined here and in the literature, in comparison with ratios of chondrites (gray symbols), and IVA iron meteorites (red crosses). Lunar data are from references [6-9]. Data sources for chondrites are from references [11-13] and for IVA iron meteorites are from [14]. Figures are from [9].

ZIRCON FORMATION IN IMPACT MELTS: COMPLICATIONS FOR DECIPHERING PLANETARY IMPACT HISTORIES. M. M. Wielicki[1] and T. M. Harrison[1], [1]Earth, Planetary, and Space Sciences, UCLA, 595 Charles Young Drive East, Los Angeles, CA 90095.

Introduction: The impact history of the solar system remains controversial. Early investigation of lunar samples, returned by Apollo astronauts, led to the 'Late Heavy Bombardment' (LHB) concept [1,2] which hypothesized a sharp increase in bolide flux centered around ~3.9 Ga. Evidence for this cataclysm was first derived from whole-rock U-Pb and Rb-Sr ages [2] but subsequently more on ^{40}Ar-^{39}Ar data [3,4]. However, interpretations of lunar ^{40}Ar-^{39}Ar geochronology can be problematic [5]. Recent studies [6,7] have focused on using U-Pb dating of zircon as a new tool with which to identify ancient large-scale impact events, such as the LHB, on the Earth-Moon system.

Background: Poikilitic zircon, which appears as branching, interstitial networks of zircon enclosing other phases, within the melt matrix from lunar meteorite SaU 169 and Apollo 12 samples, have been interpreted [6–8] as growing during equilibrium crystallization of impact melts. U-Pb geochronology of such grains have been used to constrain the age of the Imbrium basin and as such would introduce an important new means with which to probe planetary impact histories [7,8]. Although poikilitic textures are observed in zircon and other phases [10], they are rare in terrestrial environments.

Recently, Hadean zircons from Western Australia have been proposed to form from large scale melting of the Hadean crust by impacts [7]. If so, the age distribution of this population may provide insights into the bolide flux on early Earth. However, identifying zircons that formed in impact melts can be challenging.

Here we evaluate the formation conditions and inheritance probability of zircon in impact melts and the implications of using zircon geochronology to investigate planetary impact histories. Specifically we examine the likelihood of zircon crystallization within simulated lunar impact events, such as the formation of poikilitic zircon within lunar meteorite SaU169, and report SIMS U-Pb geochronology of similar textured zircons found within the melt matrix of the largest terrestrial impact (Vredefort, South Africa) to test the hypothesis that such grains crystallized within an impact melt. We also model the occurrence and crystallization temperature spectrum for zircon in simulated impact melts on an ancient terrestrial surface to assess the role of impacts in the formation of the Hadean zircons from Western Australia and their use in identifying the impact flux on early Earth.

Results: Modeled crystallization temperature spectra for zircon growth in lunar impact melts indicate that zircon crystallizes in only ~2% of the simulations, reflecting the high [Zr] necessary to nucleate zircon in predominantly mafic lunar compositions [11]. Interestingly, model temperatures, which range from ~850-1050^0 C, are typically ~100-200°C higher than those reported by [12] for terrestrial impacts, presumably reflecting the anhydrous nature of lunar melts. Modeled temperatures are significantly lower than Ti-in-zircon crystallization temperatures reported for lunar grains [12,13]. A modeled result for an ancient terrestrial surface predicts a crystallization temperature spectrum significantly above that seen in the Hadean zircon population [15].

Zircons isolated from the granophyre unit of the Vredefort impact show an intimate relationship with Mg-rich pyroxene (i.e. poikilitic texture) similar to that discovered in lunar meteorite SaU 169 [16]. Twelve of twenty isolated grains were analyzed, as the others were so inter-grown that no continuous surface was available to place the ion beam without excessive common Pb contamination. One grain was rejected due to high common Pb presumably contributed from contaminated areas or from the inter-grown pyroxene. Results indicate that all the grains were inherited from the Archean target, with a crystallization age of 3077±74 Ma, and a lower intercept of 1984±150 Ma (MSWD = 2.6), consistent with the impact age. No grains appear to have grown or been 'reset' within the impact melt.

Discussion: Modeled crystallization temperatures appear to argue against most lunar zircons forming in response to impact melting. Dissolution and growth of zircon in an impact melt is a function of: 1) the solubility of Zr, which itself is a function of composition (i.e. cation ratio 'M' = (Na+K+2Ca) / (Al·Si); 2) the diffusivity of Zr; and 3) the temperature and rate of cooling [15–17]. For lunar zircons incorporated within predominantly mafic melts (SaU 169 M = 3.32), a high degree of resorption is likely given the propensity of high 'M' magmas (e.g., M ≈ 3.0), to dissolve zircon. For the composition of SaU 169, growth of zircon would require twenty times higher [Zr] (50,000 ppm) than that reported by [6], essentially ruling out the possibility of this grain growing in equilibrium with the impact melt. Our observation of Vredefort zircon with inherited U-Pb systematics and apparent poikilitic textures further supports our conclusion that poikilitic

grains from Apollo samples and lunar meteorite SaU 169 [7,8] are likely inherited from target rocks and are not primary zircons grown in impact melts [9]. Thus, such grains should be interpreted with caution when investigating impact chronologies for terrestrial and extraterrestrial samples.

Furthermore, modeled crystallization temperature spectrum results for impacts on early Earth suggest formation temperatures significantly higher [12] than reported for the Hadean population [15]. Thus, we conclude that impacts were not a dominant source for the Hadean zircons and their age distribution does not provide a constraint for impacts on early Earth [7].

Conclusion: Given fewer inherent complications than commonly used ^{40}Ar-^{39}Ar method, U-Pb dating of zircon may become an important new tool to probe planetary impact histories. However, a better understanding of zircon crystallization in response to impact shock and heating is required. Specifically, being able to discriminate inherited zircons grown in endogenic environments as opposed to impact melts is important for their use in establishing impact histories. Only in the case of small parent bodies without the thermal capacity for prolonged endogenic magmatism can zircon age and geochemistry currently be used to conclusively identify an impact. Lastly, the terrestrial Hadean zircon population is quite inconsistent with formation in impact environments.

References:

[1] G. Turner, P. H. Cadogan, and C. J. Yonge, (1973) *Lunar Planet. Sci. Conf. Proc.* 4, 1889–1914. [2] F. Tera, D. A. Papanastassiou, and G. J. Wasserburg, (1974) *Apollo Int. Mag. Art Antiq.* 22, 1–21. [3] G. B. Dalrymple and G. Ryder, (1993) *J. Geophys. Res.* 98, 13,085–13,095. [4] B. A. Cohen, T. D. Swindle, and D. A. Kring, (2000) *Science* 290, 1754–1756. [5] T. M. Harrison and O. M. Lovera, (2013) *Geol. Soc. London, Spec. Publ.* 378, 1–36. [6] E. Gnos, B. a Hofmann, A. Al-Kathiri, S. Lorenzetti, O. Eugster, M. J. Whitehouse, I. M. Villa, A J. T. Jull, J. Eikenberg, B. Spettel, U. Krähenbühl, I. A Franchi, and R. C. Greenwood, (2004) *Science* 305, 657–659. [7] D. Liu, B. L. Jolliff, R. A. Zeigler, R. L. Korotev, Y. Wan, H. Xie, Y. Zhang, C. Dong, and W. Wang, (2012) *Earth Planet. Sci. Lett.* 319–320, 277–286. [8] M. L. Grange, R. T. Pidgeon, A. A. Nemchin, N. E. Timms, and C. Meyer, (2013) *Geochim. Cosmochim. Acta*. 101, 112–132. [9] J. S. Scoates and K. R. Chamberlain, (1995) *Am. Mineral.* 80, 1317–1327. [10] S. Marchi, W. F. Bottke, L. T. Elkins-Tanton, M. Bierhaus, K. Wuennemann, A. Morbidelli, and D. A. Kring, (2014) *Nature* 511, 578–582. [11] P. Boehnke, E. B. Watson, D. Trail, T. M. Harrison, and A. K. Schmitt, (2013) *Chem. Geol.* 351, 324–334. [12] M. M. Wielicki, T. M. Harrison, and A. K. Schmitt, (2012) *Earth Planet. Sci. Lett.* 321–322, 20–31. [13] D. J. Taylor, K. D. McKeegan, and T. M. Harrison, (2009) *Earth Planet. Sci. Lett.* 279, 157–164. [14] J. W. Valley, M. J. Spicuzza, and T. Ushikubo, (2013) *Contrib. to Mineral. Petrol.* 167, 956. [15] E. B. Watson and T. M. Harrison, (2005) *Science* 308, 841–844. [16] E. Gnos, B. A Hofmann, A. Al-Kathiri, S. Lorenzetti, O. Eugster, M. J. Whitehouse, I. M. Villa, a J. T. Jull, J. Eikenberg, B. Spettel, U. Krähenbühl, I. A Franchi, and R. C. Greenwood,(2004) *Science* 305, 657–659. [17] T. M. Harrison and E. B. Watson, (1983) *Contrib. to Mineral. Petrol.* 84, 66–72. [18] E. B. Watson and T. M. Harrison,(1983) *Earth Planet. Sci. Lett.* 64, 295–304. [19] E. B. Watson, (2011) *Trans. R. Soc. Edinb. Earth Sci.* 87, 43–56. [20] A. A. Nemchin, R. T. Pidgeon, M. J. Whitehouse, J. P. Vaughan, and C. Meyer,(2008) *Geochim. Cosmochim. Acta* 72, 668–689.

RELATIONSHIPS AMONG CHEMICAL COMPOSITION, SIZE, AND SHAPE WHEN EVALUATING ^{40}AR/^{39}AR AGES OF LUNAR IMPACT GLASSES N. E. B. Zellner[1] and J. W. Delano[2], [1]Department of Physics, Albion College, Albion, MI 49224 USA (nzellner@albion.edu), [2]New York Center for Astrobiology, Department of Atmospheric and Environmental Sciences, University at Albany (SUNY), Albany, NY 12222 USA

Introduction: Using size, shape, and chemical composition of impact glasses from Apollo 12, 14, 16, and 17 [1-4], we have developed criteria for assessing whether (or not) the ^{40}Ar/^{39}Ar ages of those individual glasses are reliable values for the age of the impact event in which they formed. Of the >100 samples investigated, ~49% of them are likely to report an actual age. Of these, ~75% (shards and spheres) have formation ages of ≤2000 Ma. A remnant population of impact glasses with ages >3500 Ma survived from the tail end of the late heavy bombardment, and these old samples are more likely to be shards (and not spheres).

Investigation: Gombosi *et al*. [5] studied ^{40}Ar/^{39}Ar systematics in three large (~1.6 mm diameter) glass spherules having chemical compositions similar to that of Apollo 16 regolith and suggested that significant loss of radiogenic ^{40}Ar could occur in those glasses during diurnal temperature-cycling in the upper ~20 cm of the lunar regolith. Gombosi *et al.* [5] further proposed that melt structure, which is closely related to chemical composition, and diffusivity of radiogenic ^{40}Ar could be described using the fraction of non-bridging oxygens, X(NBO) [6,7]. Using the criteria that shape, size, and composition together [1,2,4] can best characterize any impact glass, >100 lunar impact glasses from all data sets [1-4] were assessed to determine if shape, size, and/or major-element compostion might affect how well the lunar impact glass could retain argon.

Results: With the suggestion that diurnal heating of the regolith may be important [5], the assumption of all previous investigators [1-4,8,9] that the glass retains radiogenic ^{40}Ar during extended residence of the glass in the shallow regolith was questioned [10]. Since diffusive loss of radiogenic ^{40}Ar in glass would also be related to the size of the glass sphere/shard, Zellner and Delano [10] revisited ^{40}Ar/^{39}Ar results on dust-free and inclusion-free lunar impact glasses where sizes, shapes, and chemical compositions were known.

We have reported [10] on the relationship between argon diffusion and composition (as described by the fraction of non-bridging oxygen atoms in a specific major element, X(NBO) [6,7]), and report here that the retention of radiogenic ^{40}Ar is also a strong function of temperature and sample size. By assuming that thermal diffusion during cosmic ray exposure (CRE) in the shallow lunar regolith was the main process for causing Ar loss in lunar glasses, the fraction of total ^{40}Ar retained in the sphere can provide an estimate for the distance below the exterior surface of the glass sphere from which ^{40}Ar has been lost. A model for the temperature,time-integrated-Ar-diffusion-size dependence was developed.

Discussion: Previously, we found that glasses with the lowest values of X(NBO) (e.g., <0.21; felsic compositions) would be most susceptible to diffusive loss of radiogenic ^{40}Ar, while glasses with X(NBO) >0.21 have a distinctly older distribution of ^{40}Ar/^{39}Ar ages [10]. We now show that to report an actual ^{40}Ar/^{39}Ar age, where the sample is virtually unaffected by argon diffusion, a lunar glass with X(NBO) = 0.30 would require a minimum dimension of ~90 μm for a CRE age of 750 Ma. However, its size would need to be just 55 μm if it experienced a CRE age of 250 Ma. Thus, samples with high X(NBO) values (i.e., more mafic compositions), larger size, and shorter CRE ages are more likely to record actual ^{40}Ar/^{39}Ar ages of the impact melting event, instead of a minimum value (i.e., apparent age) caused by diffusive-loss of radiogenic ^{40}Ar [5]. This conclusion is independent of the shape of the sample [Figure 1].

Shape does appear to matter, however, in the case of old samples. Figure 2 shows the age-distribution of 50 lunar impact glass spheres (and dumbbells) and shards that met the criteria of being likely to report an actual ^{40}Ar/^{39}Ar formation age. These samples come from the Apollo 14, 16, and 17 landing sites and range in size from ~115 μm to ~575 μm. The age distribtution shows that

ages >3500 Ma are dominated by shards. These shards have a large compositional range (X(NBO) = 0.22-0.38; Figure 1), suggesting that they are products of multiple impact melting events into compositionally diverse regions. We suggest that these impact glasses could represent the lingering remnants of an initially large population of impact glasses generated during the tail end of the late heavy bombardment.

Shape also appears to matter in the case of young samples. We suggest that the pronounced enhancement of $^{40}Ar/^{39}Ar$ ages <1000 My seen in lunar impact glass spherules [e.g., 3,8,9] is a product of limited lifespans prior to being broken into angular shards. The age-distribution of young samples appears to be not controlled by chemical composition (Figure 1), and spherules dominate the ≤500-Ma age bin (Figure 2). There is also a scarcity of impact glass spheres with reliable $^{40}Ar/^{39}Ar$ ages ≥2000 Ma (Figure 2).

As a result of the observations of Figures 1 and 2, we suggest that $^{40}Ar/^{39}Ar$ dating of feldspathic lunar impact glasses is not likely to provide much information about very old episodes of lunar bombardment. We also continue to speculate that impact-produced glass spheres become broken into shards over time during gardening of the lunar regolith.

Conclusion: If a true assessment of the lunar impact flux is to be obtained, many characteristics of the sample need to be considered when evaluating the reliability of the reported $^{40}Ar/^{39}Ar$ age. In particular, the retention of radiogenic ^{40}Ar in lunar impact glasses [5], and hence the reliability of $^{40}Ar/^{39}Ar$ ages, increases with physical size and increasing X(NBO) values of the glass samples [10,11]. Additionally, shards may be the preferred sample shape, since it is suggested that glass spheres have short lifetimes (≤1000 Ma) before being broken into shards.

References: [1] Zellner N. E. B. *et al.* (2009) *GCA*, **73**, 4590-4597. [2] Delano J. W. *et al.* (2007) *MAPS*, **42**, 6, 993-1004. [3] Levine J. *et al.* (2005) *GRL*, **32**, L15201. [4] Zellner N. E. B. *et al.* (2009) *MAPS*, **44**, 839-852. [5] Gombosi D. *et al.*, *GCA*, in review. [6] Lee S. K. (2011) *PNAS*, **108**, 6847-6852. [7] Mysen B. O. and Richet P. (2005) Silicate Glasses and Melts: Properties and Structure. Elsevier, Amsterdam. 560pp. [8] Hui S. *et al.* (2010) *Proc. 9th Aust. Space Sci. Conf.* p. 43-54. [9] Culler T. *et al.* (2000) Science, 287, 1785-1788. [10] Zellner N. E. B. and Delano J. W. (2014), 45th LPSC, 1069.pdf. [11] Zellner N. E. B. and Delano J. W., *GCA*, in review.

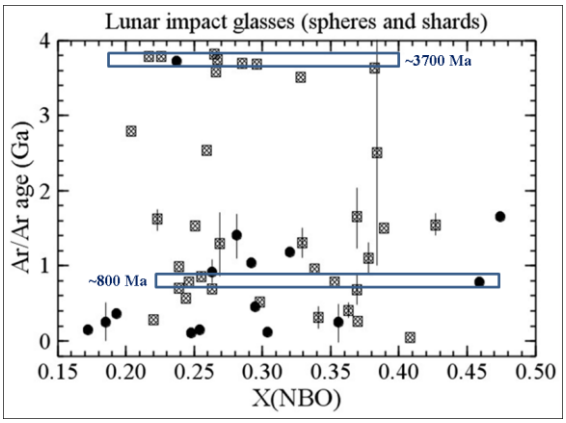

Figure 1. Diagram of ~50 lunar impact glasses [1,2,4,11] showing the distribution of ages compared to chemical composition, as represented by the fraction of non-bridging oxygen atoms, X(NBO). These impact glasses would have likely retained at least 90% of their radiogenic ^{40}Ar during 750 Ma of residence at a time-integrated temperature of ~290K. The circles represent spheres and the squares represent shards. Uncertainties in age that are larger than the size of the symbols are shown.

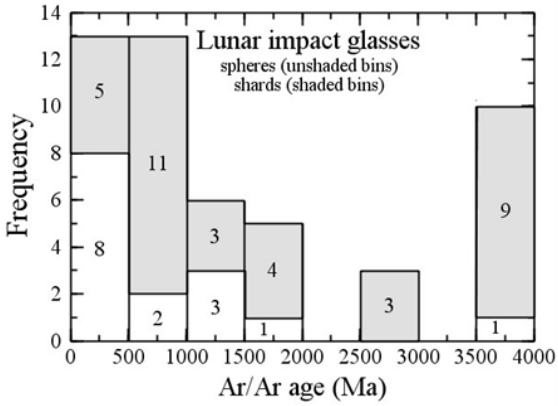

Figure 2. Age-frequency distribution of lunar impact glass spheres (unshaded bins) and lunar impact glass shards (shaded bins) that exceed the minimum sizes required to have retained at least 90% of their radiogenic ^{40}Ar during 750 Ma and are likely to have yielded accurate ages of the impact events that generated the melts [11]. The number of impact glasses within each bin is shown.

NOTES

NOTES